63-3-4

AFCRL 63-102

FINAL REPORT M58-4
CONTRACT No. AF 19(604)-4983
PROJECT No. 4600
TASK No. 460002

NEW TECHNIQUES OF PATTERN SHAPING FOR LOW SILHOUETTE ANTENNAS

by

A S. THOMAS

for

Electronics Research Directorate
AIR FORCE CAMBRIDGE RESEARCH LABORATORIES
Office of Aerospace Research
United States Air Force
Bedford, Massachusetts

January, 1963

NEW TECHNIQUES OF PATTERN SHAPING FOR LOW SILHOUETTE ANTENNAS

Abdelnour S. Thomas

A. S. THOMAS, INC.
355 Providence Highway
Westwood, Massachusetts

FINAL REPORT

January 1963

Contract No. AF19(604)-4983
Project No. 4600
Task No. 460002

Prepared for

ELECTRONICS RESEARCH DIRECTORATE
AIR FORCE CAMBRIDGE RESEARCH LABORATORIES
OFFICE OF AEROSPACE RESEARCH
UNITED STATES AIR FORCE
BEDFORD, MASSACHUSETTS

Requests for additional copies by Agencies of the Department of Defense, their contractors, and other Government agencies should be directed to the:

ARMED SERVICES TECHNICAL INFORMATION AGENCY
ARLINGTON HALL STATION
ARLINGTON 12, VIRGINIA

Department of Defense contractors must be established for ASTIA services or have their "need-to-know" certified by the cognizant military agency of their project or contract.

All other persons and organizations should apply to the:

U.S. DEPARTMENT OF COMMERCE
OFFICE OF TECHNICAL SERVICES
WASHINGTON 25, D.C.

ACKNOWLEDGMENT

The author wishes to acknowledge with gratitude the encouragement and suggestions extended throughout the course of this investigation by Francis J. Zucker of the Air Force Cambridge Research Laboratories.

TECHNICAL PERSONNEL

A. S. Thomas

W. F. Reynolds

S. Rubin

R. Moran

E. M. Thomas

ABSTRACT

The infinite modulated reactance sheet is studied with the phase and amplitude contours of the near field presented. It is shown that the infinite reactance sheet is an excellent description of the modulated Yagi. Experimental radiation patterns of low sidelobe endfire arrays are given together with radiation patterns of Yagi arrays giving cosecant type radiations, flat top flared beams, and beams at an arbitrary angle. The beams at an arbitrary angle are obtained from a cosine to the even power modulation of the relative wave number.

TABLE OF CONTENTS

LIST OF FIGURES

I. INTRODUCTION

Under Contract No. AF19(604)-1714 [1,2], spatial phase modulation along a linear array was studied under the assumption of constant amplitude along the array to show the feasibility of spatial modulations. In that work no attempt was made to correlate with actual structures.

TM fields in general have been studied and then specialized to an infinite reactive surface.

W. F. Reynolds, of this firm, and independently and for different purposes, Hessel and Oliner [3,4], studied a modulated reactive sheet. The latter used the transmission line approach, while the approach at A. S. Thomas, Inc. was the field approach, both, however, as can be expected, yielding identical solutions.

It was demonstrated, as had been anticipated, that, associated with a phase modulation, there occurs an amplitude modulation and a complex relative wave number. It will be demonstrated that the impedance sheet is a good approximation to the modulated linear array. The near field was computed for the three field components and constant phase and amplitude

contours drawn.

Based on the study of phase modulation assuming constant amplitude and the study of the modulated reactance sheet, endfire arrays were designed that gave radiation patterns with 20 db sidelobes and relatively narrow beam widths in both planes. Although relatively frequency sensitive, arrays have been designed and tested giving cosecant, modified cosecant and flared flat top beams. It was demonstrated that a class of distributions of the relative wave number where the modulation is either a cosine or cosine and sine terms raised to an even power, give a beam at an arbitrary angle from endfire to beyond broadside with the position of the beam depending on the amplitude of modulation, the frequency of modulation, and the power to which the sine or cosine term is raised.

II. REACTIVE SURFACE

A. GENERAL

In order to design a phase-modulated slow wave antenna, it is desirable to know not only the spectrum of relative wave numbers that results from the spacial modulation but also the relative amplitude and phase of the fundamental and each of the side bands, together with the attenuation along the array. Since for physical structures, no exact or near exact solutions exist, an infinite reactive surface occupying the xz plane with a normalized surface reactance given by the non-negative real function

$$X(z) = j\sqrt{\frac{\epsilon}{\mu}}\ \frac{E_z}{H_x}, \tag{1}$$

and supporting TM electromagnetic fields with H_x, E_y, and E_z defined for $y \geq 0$, where ϵ and μ are the permittivity and permeability of free space, was studied to obtain insight. From the field equations, it is readily

seen that for TM waves

$$E_y = \frac{1}{j\omega\epsilon} \frac{\partial H_x}{\partial z} \tag{2}$$

$$E_z = -\frac{1}{j\omega\epsilon} \frac{\partial H_x}{\partial y} \tag{3}$$

$$H_x = -\frac{1}{j\omega\mu} \left(\frac{\partial E_z}{\partial y} - \frac{\partial E_y}{\partial z} \right) \tag{4}$$

$$S_x = 0,\ S_y = \tfrac{1}{2} \mathrm{Re}\,(E_z H_x^*),\ S_z = \tfrac{1}{2} \mathrm{Re}\,(-E_y H_x^*) \tag{5}$$

where S_x, S_y, and S_z are the time-averages of the energy flux.

Now let

$$H_x = |H|_x \, e^{j\Psi(y,z)} \tag{6}$$

where $\Psi(y,z)$ is real and represents the phase of H_x in radians. It is convenient to consider the logarithm of H_x and differentiate with respect to y and z giving

$$\frac{\partial(\ell n H_x)}{\partial z} = \frac{\partial(\ell n |H|_x)}{\partial z} + j \frac{\partial \Psi}{\partial z} = \frac{\partial H_x}{H_x \partial z} = j\omega\epsilon \frac{E_y}{H_x} \tag{7}$$

$$\frac{\partial(\ell n H_x)}{\partial y} = \frac{\partial(\ell n|H|_x)}{\partial y} + j\frac{\partial \Psi}{\partial y} = \frac{\partial H_x}{H_x \partial y} = -j\omega\epsilon \frac{E_z}{H_x} \tag{8}$$

Equating real and imaginary parts of equations (8) and (9) we have

$$\frac{\partial(\ell n|H|_x)}{\partial z} = \omega\epsilon \, \mathrm{Im} \frac{E_y}{H_x} \tag{9}$$

$$\frac{\partial \Psi}{\partial z} = -\omega\epsilon \, \mathrm{Re} \frac{E_y}{H_x} = -\omega\epsilon \frac{S_z}{|H|_x^2} \tag{10}$$

$$\frac{\partial(\ell n|H|_x)}{\partial y} = \omega\epsilon \, \mathrm{Im} \frac{E_z}{H_x} \tag{11}$$

$$\frac{\partial \Psi}{\partial y} = \omega\epsilon \, \mathrm{Re} \frac{E_z}{H_x} = \omega\epsilon \frac{S_y}{|H|_x^2} \tag{12}$$

Since by definition of the reactive surface $\frac{E_z}{H_x}$ is pure imaginary, then $\frac{\partial \Psi}{\partial y} = 0$ and $S_y = 0$. Hence, the lines of constant phase are normal to the reactive surface and there is no energy flow on the time average through an

infinite reactive plane in either direction. From equation (10), it is seen that

$$|H|_x = \sqrt{\omega\epsilon}\sqrt{\frac{S_z}{-\partial\Psi/\partial z}} \,. \tag{13}$$

On the surface y = 0,

$$\frac{1}{2\pi}\frac{\partial\Psi}{\partial z} = \delta(z). \tag{14}$$

This is the instantaneous relative wave number $\delta = \beta/k$ where β is the wave number along the surface and k is the free space wave number.

Again consider the following solutions of the field equations:

$$H_x = e^{-\alpha y - j\beta z} \tag{15}$$

$$E_y = \frac{-\beta}{\omega\epsilon} e^{-\alpha y - j\beta z} \tag{16}$$

$$E_z = \frac{-j\alpha}{\omega\epsilon} e^{-\alpha y - j\beta z} \tag{17}$$

where

$$\beta^2 = a^2 + k^2$$

$$k^2 = \omega^2 \mu\epsilon$$

$$\omega = 2\pi f$$

f = the frequency

From (17) and (18), it is readily seen that a reactive surface along the xy plane can support the field since

$$X(z) = j\sqrt{\frac{\epsilon}{\mu}}\ \frac{E_z}{H_x} = \frac{a}{k} \tag{18}$$

hence

$$\delta = \frac{\beta}{k} = \pm\sqrt{X^2(z)+1} = \frac{1}{2\pi}\ \frac{d\Psi}{dz} \tag{19}$$

Placing this result in (13), we have

$$|H_x| = \omega\epsilon\sqrt{\frac{S_z}{\sqrt{X^2(z)+1}}}\,. \tag{20}$$

This result should be compared with the following expression suggested by F. H. Zucker

$$H_x = C \sqrt{\frac{X(z)}{\sqrt{X^2(z)+1}}}\, e^{-k\int\sqrt{X^2(z)+1}\,dz} \tag{21}$$

which would represent an excellent approximation if S_z were proportional to X(z), however this would mean no energy flow for X(z) = 0. Nevertheless, other than the fact that this gives for the modulated impedance sheet a real δ with no attenuation in the z direction, it will be shown that the numerical results agree quite closely with those obtained from the exact formulation for real amplitude and δ.

It is of interest to consider for TM waves, the case of constant amplitude and modulated phase $\Psi(0, z)$ such that

$$H_x = C\, e^{-j\Psi(0, z)}, \tag{22}$$

then from (2) and (3)

$$E_y = -\frac{C}{\omega\epsilon}\frac{\partial\Psi(0, z)}{\partial z}\, e^{-j\Psi(0, z)} = -\frac{1}{f\epsilon}\,\delta(z)H_x \tag{23}$$

and

$$E_z = 0. \tag{24}$$

This result implies that for phase modulated surface wave structures such as Yagis, discs on rod, etc., there will be an inherent amplitude modulation.

B. RIGOROUS SOLUTION OF MODULATED REACTANCE SHEET

Let $X(z)$ be periodic such that

$$X(z+a) = X(z) \tag{25}$$

and that the field satisfies the Floquet condition

$$H_x(y,z) = e^{-jk\delta_o z}\hat{H}_x(y,z) \tag{26}$$

where

δ_o is a complex constant, and

$$\hat{H}_x(y,z+a) \equiv \hat{H}_x(y,z). \tag{27}$$

This implies the corresponding relations for E_y and E_z.

The Fourier theorem shows that we have an expansions of the form

$$H_x(y,z) = \sum_{n=-\infty}^{\infty} (A_n e^{-k\gamma_n y} + B_n e^{k\gamma_n y}) e^{-jk\delta_n z} \tag{28}$$

where

$$\delta_n = \delta_o + n\,p,$$

$$p = \frac{\lambda}{a}, \text{ and}$$

$$\gamma_n^2 = \delta_n^2 - 1;$$

the presence of both A_n and B_n terms is due to the existence of two complex square roots of $\delta_n^2 - 1$.

If this is restricted, for physical reasons, to fields whose components are surface waves attenuated as they travel in either z direction, and radiated waves traveling outward from the surface and possibly attenuating as z increases, the B_n term in (28) can be omitted and the square

roots of $\delta_n^2 - 1$ chosen so that

$$\mathrm{Im}\gamma_n \leq 0 \text{ for } \mathrm{Re}\delta_n < 1, \text{ and} \tag{29}$$

$$\mathrm{Im}\gamma_n \geq 0 \text{ for } \mathrm{Re}\delta_n > 1 \tag{30}$$

then H_x, E_y, and E_z are as follows

$$H_x = \sum A_n e^{-k\gamma_n y - jk\delta_n z} \tag{31}$$

$$E_y = -\frac{k}{\omega\epsilon} \sum \delta_n A_n e^{-k\gamma_n y - jk\delta_n z} \tag{32}$$

$$E_z = -\frac{jk}{\omega\epsilon} \sum \gamma_n A_n e^{-k\gamma_n y - jk\delta_n z} \tag{33}$$

giving the following expressions for X(z):

$$X(z) = \frac{\sum \gamma_n A_n e^{-jnpz}}{\sum A_n e^{-jnpz}} \tag{34}$$

the periodic function X(z) has a complex Fourier series:

$$X(z) = \sum C_n e^{-jnpz} \tag{35}$$

From (34) and (35) by substituting, multiplying, and equating coefficients, the following expression is

obtained:

$$\gamma_n A_n = \sum_{n_1+n_2=n} C_{n_1} A_{n_2}. \tag{36}$$

Now let

$$X(z) = X_o(1+M\cos kpz),$$

$$X_o > 0, \tag{37}$$

$$M \leq 1$$

and write equation (35) as follows:

$$X(z) = X_o\left(1+ \frac{M}{2} \left(e^{jkpz} + e^{-jkpz}\right)\right) = \sum C_n e^{-jnkpz} \tag{38}$$

giving

$$C_o = X_o,\ C_1 = \frac{M}{2},\ \text{and}\ C_{-1} = \frac{M}{2}. \tag{39}$$

which when substituted in equation (37) gives the basic difference equation

$$\gamma_n A_n = \frac{M}{2} X_o A_{n-1} + X_o A_n + \frac{M}{2} X_o A_{n+1} \tag{40}$$

which may be written as follows:

$$A_{n-1} + W_n A_n + A_{n+1} = 0 \tag{41}$$

where

$$W_n = \frac{2}{M}\left(1 - \frac{\gamma_n}{X_o}\right).$$

This is identical to the result obtained by Oliner and Hessel by an alternate method. The coefficients of the difference equation (41), given X_o, M, and p, depend on the constant δ_o. The basic condition on δ_o is that (41) should have a non-zero solution for which $\sum_{n=-\infty}^{\infty} |A_n|^2$ is finite. It can be demonstrated that for

$$\left(W_1 - \cfrac{1}{W_2 - \cfrac{1}{W_3 - \cdots}}\right)\left(W_o - \cfrac{1}{W_{-1} - \cfrac{1}{W_{-2} - \cdots}}\right) = 1 \tag{42}$$

(41) has the continued fraction solutions

$$\frac{A_n}{A_{n+1}} = -\cfrac{1}{W_n - \cfrac{1}{W_{n-1} - \cfrac{1}{W_{n-2} - \cdots}}} \quad \text{for } n = -1, -2, -3\ldots \tag{43}$$

$$\frac{A_n}{A_{n+1}} = - \frac{1}{W_{n+1} - \frac{1}{W_{n+2} - \frac{1}{W_{n+3} - \ldots}}} \quad \text{for } n=0,\ 1,\ 2\ldots \tag{44}$$

C. COMPUTATION OF THE NEAR FIELD

The phase and amplitude of the near field for H_x, E_y, and E_z may be obtained from equations (31), (32), and (33) provided δ_o and A_n are known. The coefficients A_n may be readily obtained from (43) and (44) if the relationship (42) is satisfied. Hence the first step is to obtain the required δ_o.

1. Computation of δ_o

The "zero-th" order approximation of δ_o is given by

$$\delta_o^{(o)} = \sqrt{X_o^2 + 1} \tag{45}$$

and the first order approximation is given by

$$\delta_o^{(1)} = \delta_o^{(o)} - \frac{X_o^2 M^2}{4\delta_o^{(o)}} \left(\frac{1}{1 - \frac{\gamma_{-1}^{(o)}}{X_o}} + \frac{1}{1 - \frac{\gamma_1^{(o)}}{X_o}} \right) \tag{46}$$

the accuracy of the approximation may be determined from the ratio

$$\phi^{(m)} = \frac{D_+^{(m)}}{D_-^{(m)}} \tag{47}$$

where $$D_+^{(m)} = W_1^{(m)} - \cfrac{1}{W_2^{(m)} - \cfrac{1}{W_3^{(m)} - \ldots}}$$

$$D_-^{(m)} = \cfrac{1}{W_0^{(m)} - \cfrac{1}{W_{-1}^{(m)} - \cfrac{1}{W_{-2}^{(m)} - \ldots}}}$$

m is the order of the approximation.

If, $\phi^{(m)} = 1.0$, the value of $\delta^{(m)}$ obtained is exact, hence the closeness of $\phi^{(m)}$ to 1.00 determines the accuracy of the approximation. If neither $\delta_o^{(0)}$ or $\delta_o^{(1)}$ are sufficiently close approximations, then higher order approximations may be obtained from the following relationship:

$$\delta_o^{(m)} = \delta_o^{(m-1)} + \frac{(1-\phi^{(m-1)})\,(\delta_o^{(m-2)} - \delta_o^{(m-1)})}{\phi^{(m-2)} - \phi^{(m-1)}} \tag{48}$$

2. Computed Fields

Assuming X(z) as follows:

$$X(z) = (1+0.4\cos\frac{\pi}{\lambda_o} z) \tag{49}$$

the spectrum, amplitude, phase, and Poynting vector were computed. However, before the detailed computations from the rigorous solution are presented, it is interesting to compare the results from the approximation given in equation (21) with the rigorous solution. Table I compares the spectrum obtained from the approximation with that from the exact method which shows attenuation (complex δ_n's). The A_n's are the amplitude and phase of the δ_n's. Here the A_n's from the exact method are, with the exception of A_o, complex while those from the approximation are all real. The agreement is best for the slow wave side bands (negative n). The relative amplitude for H_x from the exact solution and the approximation is given in Figure 1. The relative wave number $\delta(z)$ from the approximation and the exact method seem to agree quite well in this case as is seen by Figure 2 with the major difference being at the extremes of the excursions in $\delta(z)$.

	EXACT METHOD		APPROXIMATION	
n	δ_n	A_n	δ_n	A_n
3	-0.0650 - j0.0086	0.0013 - j0.0037	-0.0858	0.0026
2	0.4350 - j0.0086	0.0123 + j0.0249	0.4142	0.0089
1	0.9350 - j0.0086	-0.1751 - j0.0657	0.9142	-0.2384
0	1.4350 - j0.0086	1.0000	1.4142	1.0000
-1	1.9350 - j0.0086	0.3209 + j0.0051	1.9142	0.3480
-2	2.4350 - j0.0086	0.0536 + j0.0013	2.4142	0.0551
-3	2.9350 - j0.0086	0.0062 + j0.0002	2.9142	0.0061

TABLE 1. Comparison of spectrum by approximation and exact method for $X_o = 1$, $M = 0.4$ and $a = 2\lambda_o$.

The amplitude and phase of H_x computed by the exact method are given in Figures 3 and 4. These illustrate that the lines of constant phase are normal to the surface as is readily seen from equation (12) where $\frac{\partial \Psi}{\partial y} = 0$ for y=0 and $\frac{E_z}{H_x}$ is pure imaginary.

Since $H_x(y, z/\lambda_o+2) = e^{-j\beta(2\lambda_o)}H_x(y, z/\lambda_o)$, where β is a complex constant and the field is not periodic in z/λ_o, a shift from z/λ_o to z/λ_o+2 gives a phase shift of 5.740π and a decrease in the amplitude due to attenuation by a factor of 0.897. In Figure 3 the amplitude contours, drawn in broken line, illustrate this effect. For example, the contour 0.25, when translated $2\lambda_o$ to the right, retains its shape but becomes the contour 0.224. Again, the contour 0.20, when translated $2\lambda_o$ to the right, retains its exact shape but becomes the contour 0.174.

The constant phase contours of Figure 4 were calculated for phase differences of $\pi/4$. Since in every $2\lambda_o$ there is a phase difference of 5.740π, the contour $3\pi/2$ at the left, which starts at $y/\lambda_o=0$ and $z/\lambda_o = -1.938$, repeats as the contour 1.74π at $y/\lambda_o=0$ and $z/\lambda_o=0.062$. However, in Figure 4

the contour $7\pi/4$ is drawn which leads this contour by 0.01π and is $0.0035\lambda_o$ to the right. In the neighborhood of the intersection of a set of phase contours, there is a circling of very low level power and a null in the amplitude of H_x which occurs every $2\lambda_o$.

The constant phase and amplitude contours for E_y and E_z are given in Figures 5, 6, 7, and 8. These are similar in form to the corresponding contours for H_x. Note, in Figures 3 through 8, the direction of radiation is orthogonal to the constant phase contours with the direction of maximum radiation in the neighborhood of 25^o.

The relative wave numbers $\delta_{H_x}(z)$, $\delta_{E_y}(z)$, and $\delta_{E_z}(z)$ (the relative wave numbers associated with the three phase components) for y=0 are such that

$$\delta_{H_x}(z) = \delta_{E_z}(z) \neq \delta_{E_y}(z).$$

Although this is not readily discernible from Figures 4, 6, and 8, these are apparent in the plots of δ versus z given in Figure 9, the major difference being at the extremes of

the excursion in δ. The normalized amplitudes of H_x, E_y, and E_z are not equal as is readily seen from Figure 10.

These plots clearly show that care must be exercised in measuring the amplitude of the field since if a probe is at a given distance from a modulated array, the measured amplitude will differ significantly from that along the array. This is seen from the sketch (Figure 11) of the amplitude of E_y for the modulated reactive surface showing that the positions of the maxima and minima shift with distance from the array. If the probe were at y=0, the maxima of the amplitude would coincide with the maxima of δ and the minima with the minima of δ. However, as the probe is moved away from the array, the relative excursion in amplitude decreases with the maxima and minima shifting until at a distance of approximately 0.12λ from the array, the amplitude becomes constant and with increased distance, the amplitude modulation reappears, however, with the maxima of the amplitude occuring where the minima of δ occur.

Figures 12 and 13 give the calculated plots of the amplitude and orientation of the Poynting Vector. At the

surface the orientation is parallel, and in the direction of the positive Z-axis. The neighborhood of the point $y=0.33\lambda_o$ and $z=0.10\lambda_o$ is interesting in that there is a whirlpool of very low level energy with the Poynting Vector circling about this point. This repeats periodically every $2\lambda_o$. Slightly above this point, $y=0.45\lambda_o$, all of the energy is flowing out at an oblique angle from the surface. However, below $y=0.45\lambda_o$ and to the left of this whirlpool, the flow is toward the surface and to the right of this point away from the surface.

D. EXPERIMENTAL VERIFICATION

In order to determine how closely the postulated modulated reactance sheet approximates an actual physical structure, a 9λ modulated Yagi type structure was designed and tested. The Yagi elements consisted of solid alumnium rods 0.1875 inches in diameter, equally spaced 0.836 inches apart, and supported in a styrofoam column with a dielectric constant of 1.05. The modulation was obtained by means of varying the element length. The δ, as a function of element length, diameter, and spacing was based on the published results of Ehrenspeck and Poehler [5] and also those of Senacchioli and Levis [6].

1. Feed

Since a high efficiency of excitation is necessary in order to obtain reasonable agreement between the theoretical and experimental results, a highly efficient feed was developed experimentally. The feed geometry is essentially a dipole with flared arms bent so that

if they were extended, they would form a 45° - Vee. This Rabbit Ear Feed, Figure 14, is broadband with an essentially omnidirectional radiation pattern with a 2db ripple. The configuration is an outgrowth of experimenting with the relatively long wire Vee originally used by Reynolds [7]. The Rabbit Ears are fed by two equal lengths coaxial lines from the colinear arms of an E-plane tee; hence, giving a very broadband feed. For a design frequency of 2850 mcs, the feed is placed at a distance of between 1/18 and 1/16 inch from the first element of the array, with the relative wave number of the array tapered from $1.5 \leq \delta \leq 2$ over a distance greater than one-half wave length. This feed was found to give an efficiency of excitation greater than 95%. If no reflector is used with the feed, the efficiency of excitation is evidenced from the level of energy radiated in the rear quadrant.

2. Relative Wave Number and Amplitude

Having devised a high efficiency feed to minimize the perturbation of the near field by the feed radiation, the near field was studied at various distances from the modulated Yagi. It was found that the modulated Yagi is described for the field components E_y and H_x by the modulated reactance sheet. The agreement between the theoretical and experimental is evidence by the plots of $\delta(z)$ and $|E_y|$ taken at $y=0.2\lambda$ given in Figures 15 and 16. The superimposed oscillations in the amplitude are due to the elements.

3. Radiation Pattern

The radiation pattern computed on the basis of the approximation (21) is compared with the experimental radiation pattern of the modulated Yagi in Figure 17. Since equation (21) gives all real δ_n's and A_n's, the rigorous

solution of the reactance sheet as per Table 1 shows that the δ_n's are complex and, with the exception of A_o, the A_n's are complex. It is readily seen that if the attenuation were taken into account that the minima in the radiation pattern would be shallower.

E. INDEPENDENT PHASE AND AMPLITUDE CONTROL

Since independent phase and amplitude control would provide the designer with a powerful means of controlling the radiation pattern, it was decided, in spite of the result given by equations (22) and (23), namely, that an amplitude modulation is inherent to modulated surface wave structures, to study a co-planar system of Yagis. The system may be described as follows: In the XYZ coordinate system, let the central Yagi be along the Z-axis with the elements in the YZ-plane. Then each of the other parallel Yagis will be displaced equal distances to either side of the XZ-plane. The central Yagi only is fed and the side Yagis are parasitic. The hope here was that since the maxima and minima of the amplitude shift at a distance greater than 0.12λ from the driven array with the maxima of the amplitude occuring where the minimum δ of the side array occurs, that this system of modulated coplanar

Yagis could conceivably result in constant amplitude. Unfortunately, this did not happen and the amplitude modulations were but slightly altered.

III. EXPERIMENTAL RESULTS

Although the modulated reactance sheet is an excellent description of a modulated Yagi, unfortunately the rigorous formulation can take into account only one term in the modulation, whereas radiation patterns of interest require considerably more complicated modulations. Since the mathematics seemed prohibitive for more complex modulations, an experimental approach based on the results of the previous work was undertaken to obtain low-side lobe endfire arrays, shaped beams, and beams at arbitrary angles.

A. ENDFIRE

The idealized case of phase modulation with constant amplitude gave optimum theoretical end-fire radiation patterns for distributions of relative wave number, δ, having maxima at the input, center and end of the array. An example of this is given in Figure 18. This distribution for constant amplitude may be expected to give a radiation pattern with less

than 20db sidelobes and half-power angle of 23 degrees for an 8λ array. The high δ at the input is advantageous for the launching of the surface wave since it has been found that a relatively large δ is required in order to achieve a high efficiency of excitation. However, a large δ at the end of the array is not desirable, in that it would introduce a mismatch and produce a standing wave along the structure due to the reflected wave from the end. Recognizing that the amplitude modulation produced by the phase modulation results in a degradation of the radiation pattern, a careful experimental study of the radiation pattern from 3.0 to 2.6 kmcs was undertaken. The array designed according to the solid line of Figure 18 exhibited 10db first sidelobes and a beamwidth of 17 degrees. Here the beamwidth was improved; however, the sidelobes were raised considerably. The effect of the mismatch to free space was evidenced by a beam in the backward direction whose amplitude varied with frequency due to interference with the feed radiation in that direction. The addition of a taper at

the end of the array eliminated the backward beam; however, with additional degradation of the radiation pattern. It became clear from this that the phase modulated arrays with large δ at the end required modification. The buildup at the end was arbitrarily eliminated as shown by the broken line of Figure 18. This modification gave the radiation patterns of Figures 19 to 26 with the results tabulated below:

Frequency in kmcs	H.P. Angle in degrees	First Sidelobe in db down
3.00	22.0	12.0
2.95	22.0	13.0
2.90	22.5	14.0
2.85	22.5	14.5
2.80	22.0	16.0
2.75	22.5	15.5
2.70	23.0	16.0
2.65	24.5	17.0

These results warranted additional experimental

work, especially in connection with varying the excursions in δ at the center and near the ends.

A serious experimental effort led to the array design given in Figure 27, showing an initial taper in δ from 1.7 to 1.03 at the center of the array and continuing with constant δ of 1.03 to the end of the array. This array gives the radiation patterns of Figures 28 to 45, for both horizontal and vertical polarizations, with sidelobe levels 20 db down and half power angles of 20° at the design frequency. This design is not considered optimum, but merely one that gives a low sidelobe end-fire array.

B. COSECANT TYPE

Designing according to Figure 46, giving δ vs element length in inches, for element spacing of 0.49 inches center to center, the distribution of δ vs distance along the array of Figure 47 gave the $\csc^2\theta$ type pattern from 16° to 56° given in

Figure 48 at 2770 mcs, whereas the δ vs distance along the array given in Figure 49 gave a radiation pattern, Figure 50, that followed $\csc^2\theta \sqrt{\cot\theta}$ from approximately 16° to 60°. In essence, this requires a δ that is approximately 1.8 at the input, dropping to approximately 1.0, rising to a maximum of 1.92 at center and dropping again to 1.0 at the end of the array. Although these arrays are frequency sensitive, they nevertheless demonstrate that shaped beams may be obtained by varying the relative wave number along slow wave structures.

The distributions for the endfire case and shaped beam case differ from those computed on the basis of constant amplitude in that they are not symmetric or nearly symmetric about the center of the array. Nevertheless, the distributions obtained on the basis of constant amplitude did provide a first coarse approximation to those that gave the more satisfactory radiation patterns when the array was tapered at the end and the second order oscillations were suppressed.

C. BEAM AT ARBITRARY ANGLE

The following four parameter distribution of the relative wave number was studied in order to obtain beams at an arbitrary angle:

$$\delta = 1.0 + m_1 \cos^{2n} 2\pi pz + m_2 \sin^{2n} 2\pi pz \qquad (50)$$

where

n	a positive integer
m_1, m_2	arbitrary constants
p	frequency of modulation
z	distance along the array from the input in wavelength.

It has been found for $m_2 = 0.0$ and varying m_1, that for increasing m_1, the beam is moved towards endfire; while for constant m_1 increasing n, the beam is moved away from endfire towards broadside and increasing p the beam is moved in the direction of broadside. In effect, increasing m_1, is increasing δ_o and keeping the frequency of modulation constant, while increasing n is in effect an increasing of the

frequency of modulation causing the beam to swing away from endfire toward broadside, and of course, increasing p swings the beam in the direction of broadside. However, in every case, it has been found that the beam moves with increasing frequency of operation in the direction of endfire. With increased frequency of operation, there is an effective increase of m and a decrease in p, which, of course, will tend to shift the beams in the direction of endfire.

The second term in equation (50) helps in reducing the sidelobes. A 10λ array designed according to the distribution

$$\delta = 1+0.7\cos^4 0.9\pi z + 0.1\sin^4 0.9\pi z \qquad (51)$$

plotted in Figure 51 gives the radiation patterns given in Figures 52 to 54. At the higher frequency the radiation pattern is endfire and as the frequency is decreased, the beam broadens forming a square

beam, Figure 53 and finally splitting giving a well defined beam, Figure 54; with a maximum at 24° and 19db first sidelobe. An array, therefore, designed according to Figure 51 based on the δ vs length of element of Figure 46 gives an endfire radiation pattern at 3000 mcs, a square beam at 2950 mcs and a beam at 24° at 2925 mcs. Now if the number of oscillations is increased, the main beam can be made to occur at any desired angle. For example, an array designed with

$$\delta = 1+0.54 \cos^{8} 2.5\pi z \qquad (52)$$

as given in Figure 55 has radiation patterns as given in Figures 56 to 61 with the main lobe occuring at 86° at 3200 mcs and shifting progressively with frequency to 102° at 2950 mcs. This array seems to support a relative wave number changing from δ=1.0 to δ=1.54 in three tenths of a free space wave length.

IV. CONCLUSIONS

Endfire slow wave Yagi type antennas with beamwidth approximately 56 $\sqrt{\frac{\lambda}{L}}$ and sidelobes 20 db down have been designed. These require a taper from $\delta = 1.7$ at the input to approximately $1 + \frac{1}{4\frac{L}{\lambda}}$ at the center, then either remaining constant to the end of the array or with but a slight taper to $\delta = 1$ at the end of the array. These antennas are relatively broadband.

Distributions of δ have been found that give, although frequency sensitive,

1.) Cosecant squared beams from 16° to 56°.

2.) Modified cosecant beams from 16° to 60°.

3.) Flared flat top beams suitable, if arrayed, for antennas with flared beam in one plane and a sharp beam in the orthogonal plane, or as feeds to parabolic reflectors. By decreasing

or increasing the length of the array and appropriately changing the distribution of the relative wave number, the beam width of the flat top beam may be altered.

4.) Beam at arbitrary angle. It has been demonstrated that distributions of

$$\delta = 1.0 + m \cos^{2n} 2\pi pz$$

can give beams at any desired angle from endfire to well beyond broadside. These exhibit a limited frequency scan. The beam near endfire, at approximately 24°, has sidelobes of approximately 20 db, while those near broadside have sidelobes of approximately 10 db. It is expected that by modifying the modulation, the sidelobe level can be improved.

Considerable insight has been obtained from the study of the modulated reactive sheet. It has been found to give an excellent description of the finite Yagi. Unfortunately, the rigorous

formulation seems to be mathematically prohibitive for the modulations necessary to produce desirable radiation patterns. Hence additional theoretical and experimental work is needed to obtain a mathematical model that will permit resynthesis. A first approximation in this direction is that of equation (21).

LIST OF REFERENCES

1) Thomas, A. S., "Study of Gain Limitations and Pattern Synthesis of Traveling Wave Antennas", for Air Force Cambridge Research Center, Contract No. AF19(604)-1714, Final Report M56-1, 30 November 1958.

2) Thomas, A. S. and F. J. Zucker, "Radiation from Modulated Surface Wave Structures - I", 1957 IRE National Convention Record, Pt. 1, pp. 153-160.

3) Hessel, Alexander, "Guiding and Scattering by Sinusoidally-Modulated Reactance Surfaces", for Air Force Cambridge Research Laboratories, Contract No. AF19(604)-2031, Research Report PIBMRI-825-60, June, 1960.

4) Oliner, A. A. and A. Hessel, "Guided Waves on Sinusoidally-Modulated Reactance Surfaces", Transactions of the IRE, Vol. AP-7, 1959, pp. S201-S208.

5) Ehrenspeck H. W. and H. Poehler, "A New Method for Obtaining Maximum Gain from Yagi Antennas", Transactions of the IRE, Vol. AP-7, No. 4, October 1959, pp. 379-386.

6) Serracchioli, F. and C. A. Levis, "The Calculated Phase Velocity of Long Endfire Uniform Dipole Arrays", Transactions of the IRE, Vol. AP-7, December 1959, pp. S424-S434.

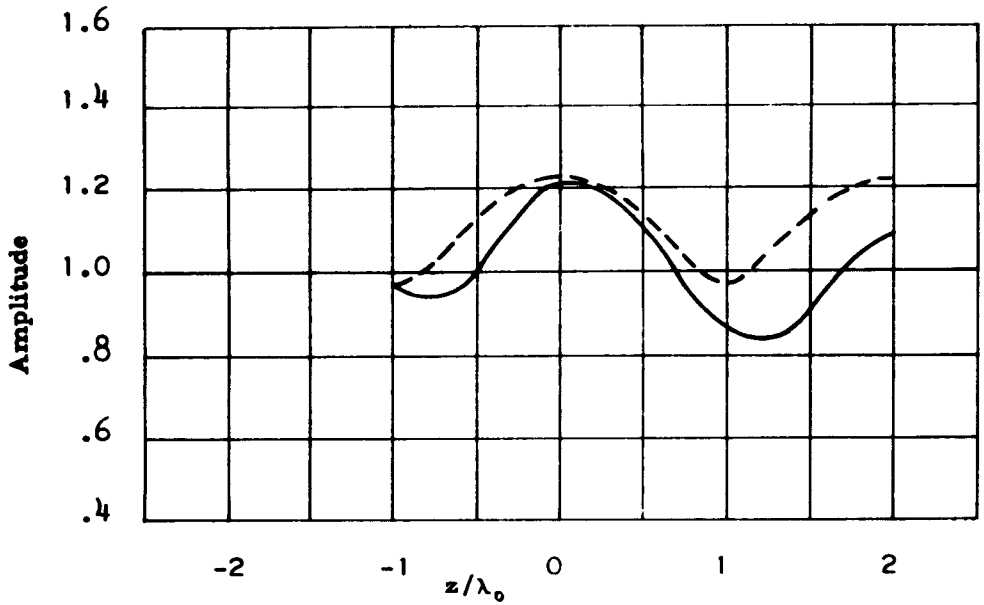

FIGURE 1. Relative Amplitude.

——— H_x

------- Approx.

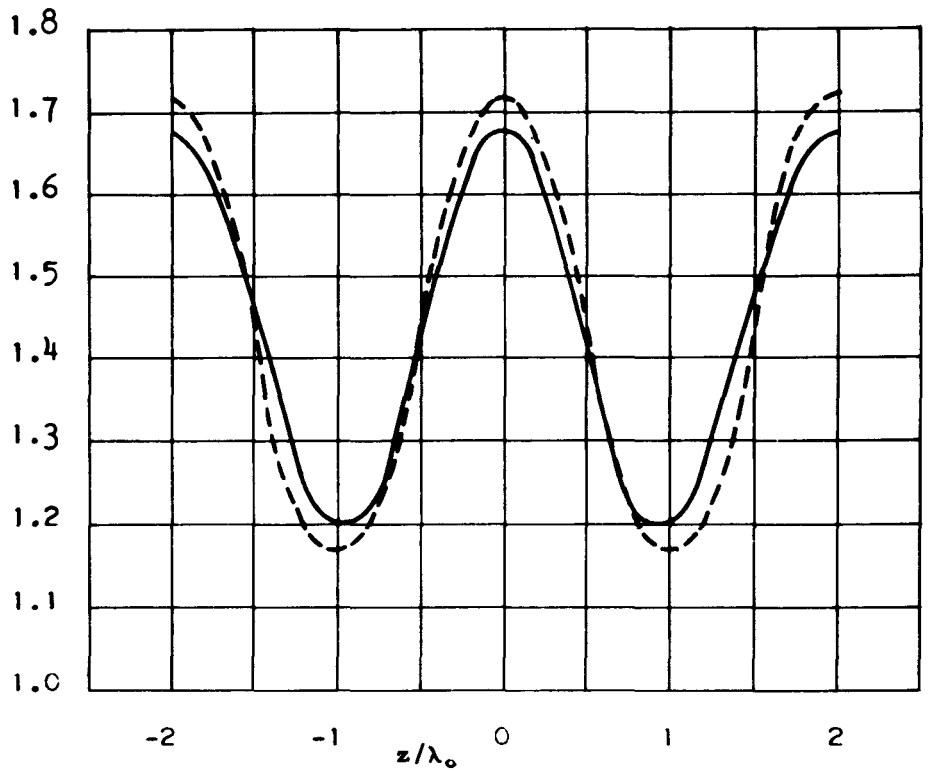

FIGURE 2. δ(z) - Relative Wave Number. ——— δ(z) for H_x
-------- Approx.

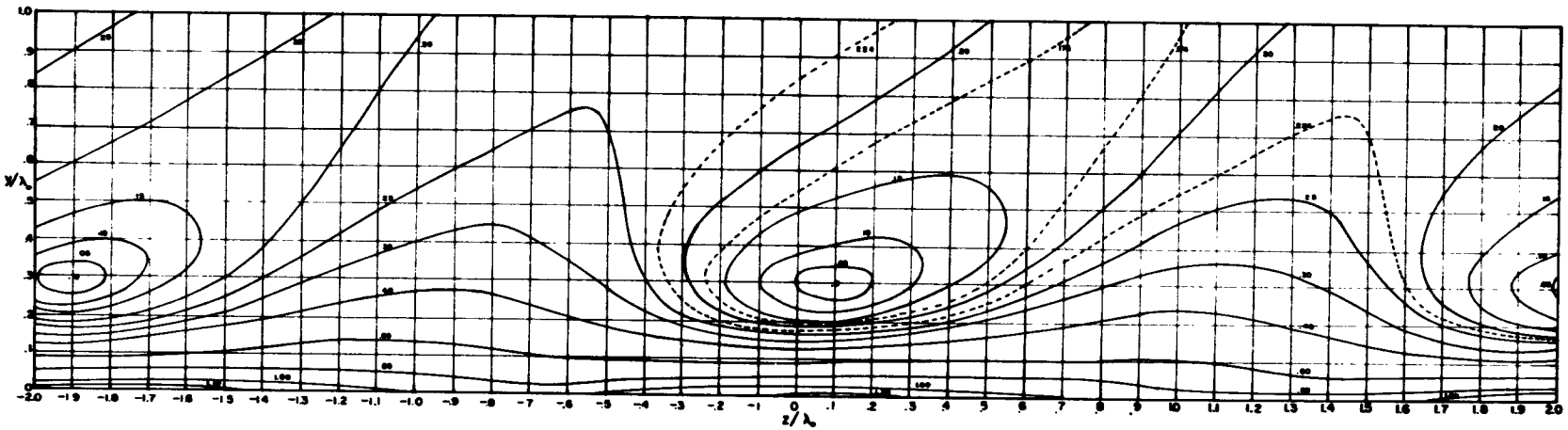

FIGURE 3 — $|E_\phi|$ in Near Field.

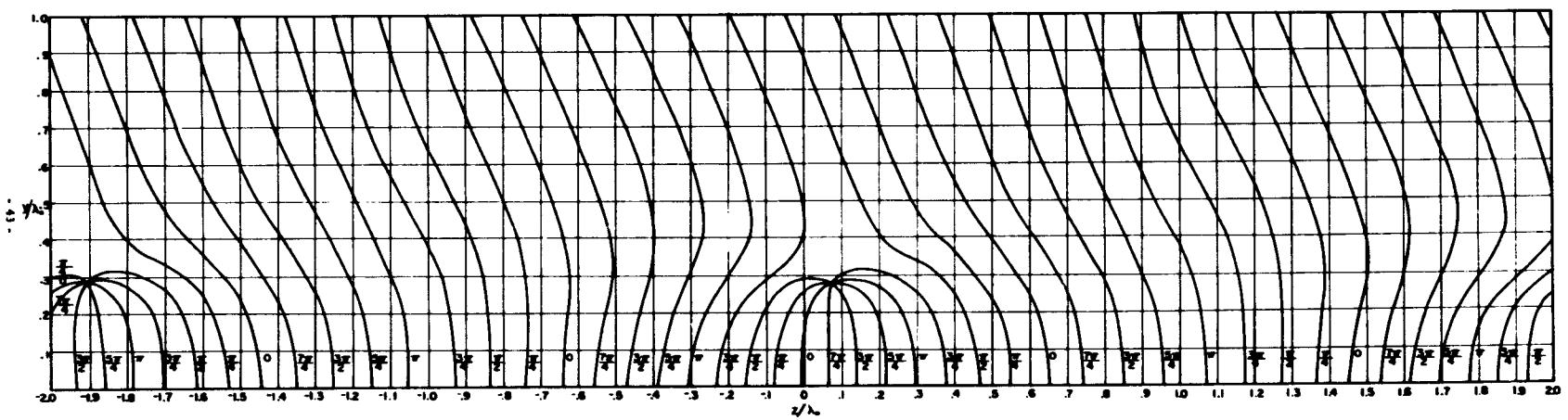

FIGURE 4 —Phase of H_y in Near Field

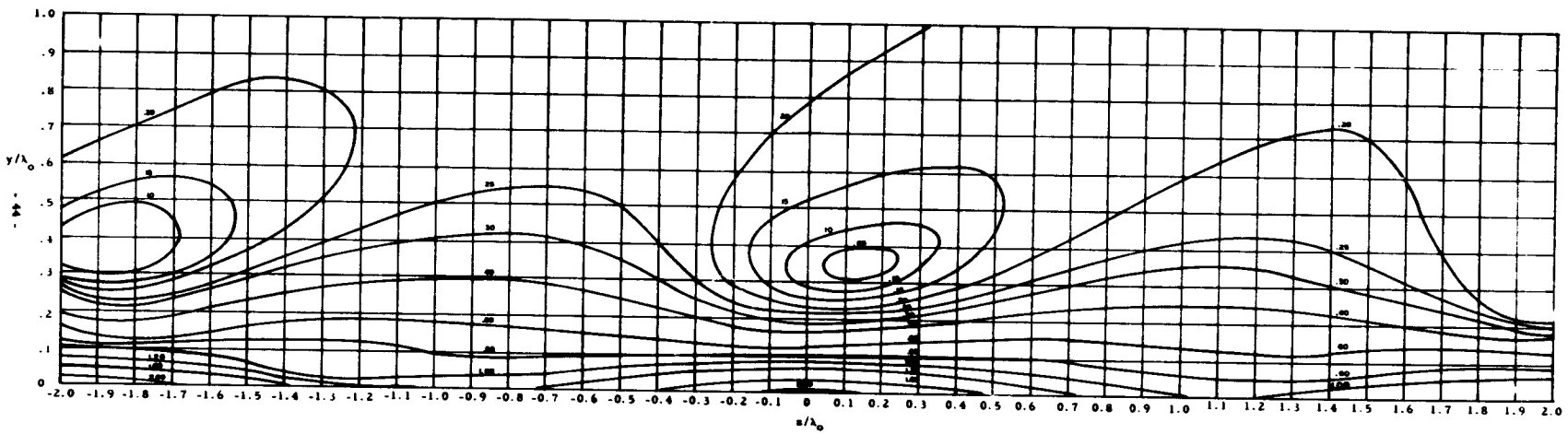

FIGURE 5. Amplitude of E_y in Near Field

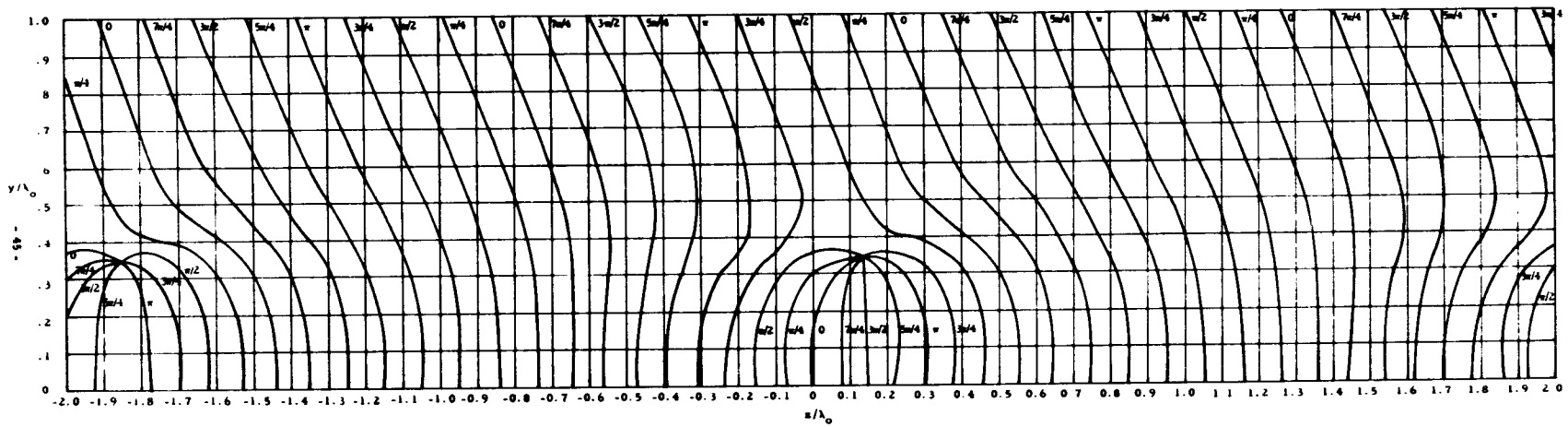

FIGURE 6. Phase of E_y in Near Field

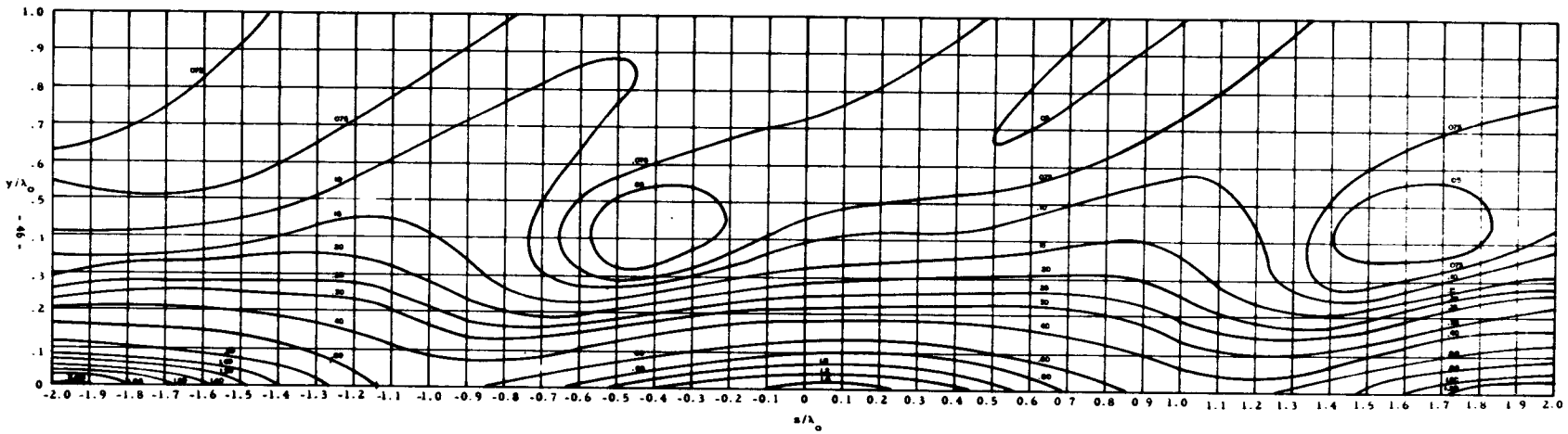

FIGURE 7. Amplitude of E_z in the Near Field

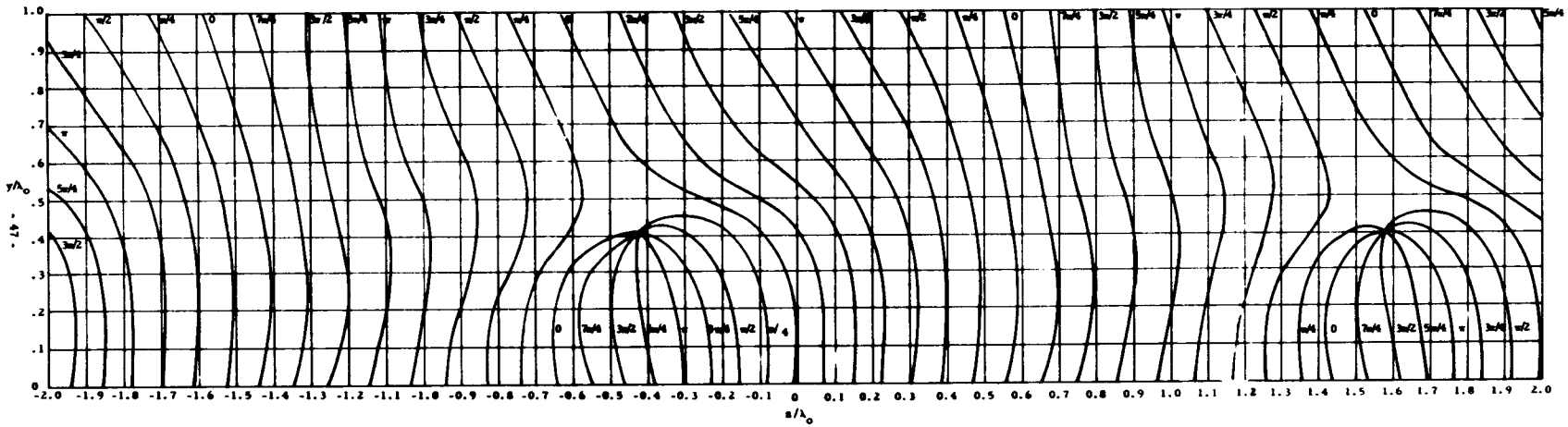

FIGURE 8. Phase of E_z in Near Field

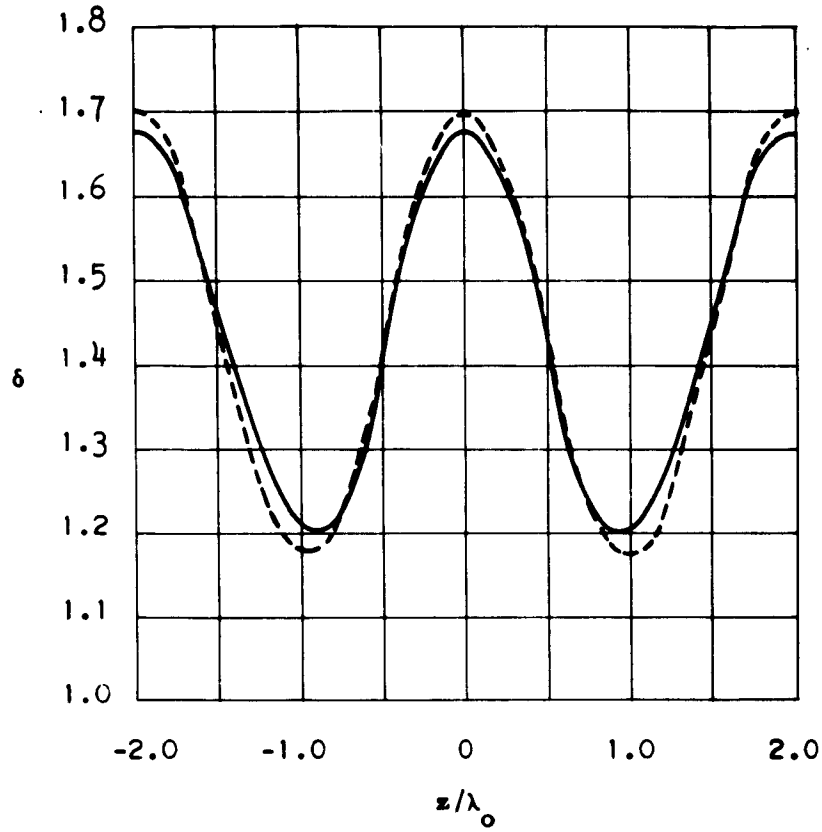

FIGURE 9. Relative Wave Number versus z/λ_o for H_x, E_y, and E_z.

---------- δ_{E_y}

———— $\delta_{E_z} = \delta_{H_x}$

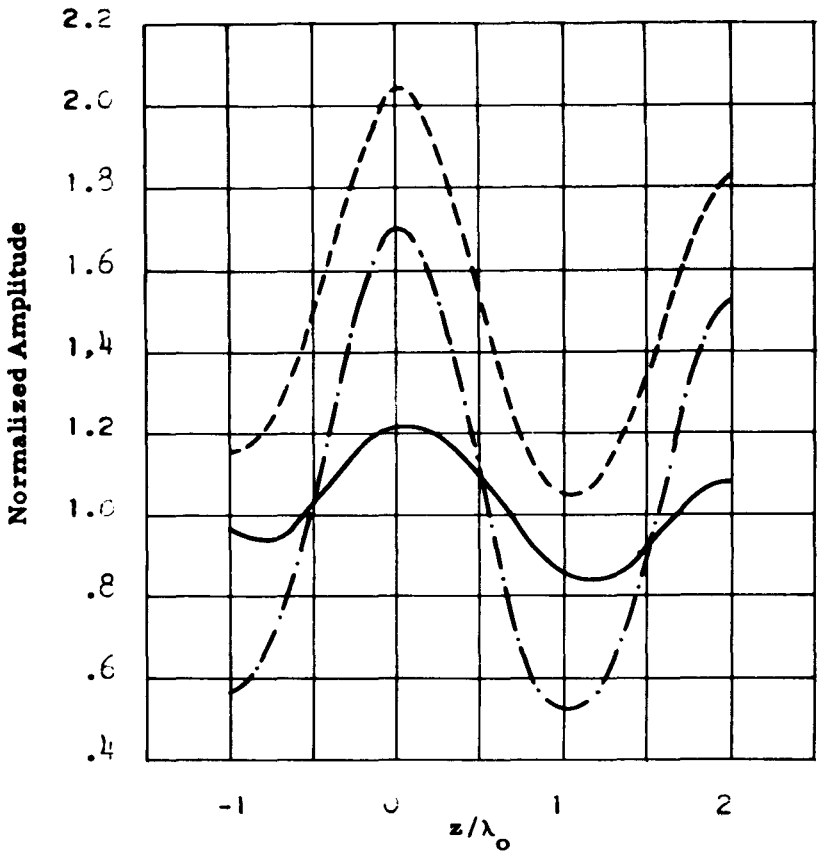

FIGURE 10. Amplitude vs z/λ_o.

———— H_x

---------- $\frac{\omega\epsilon}{k} E_y$

—·—·— $\frac{\omega\epsilon}{k} E_z$

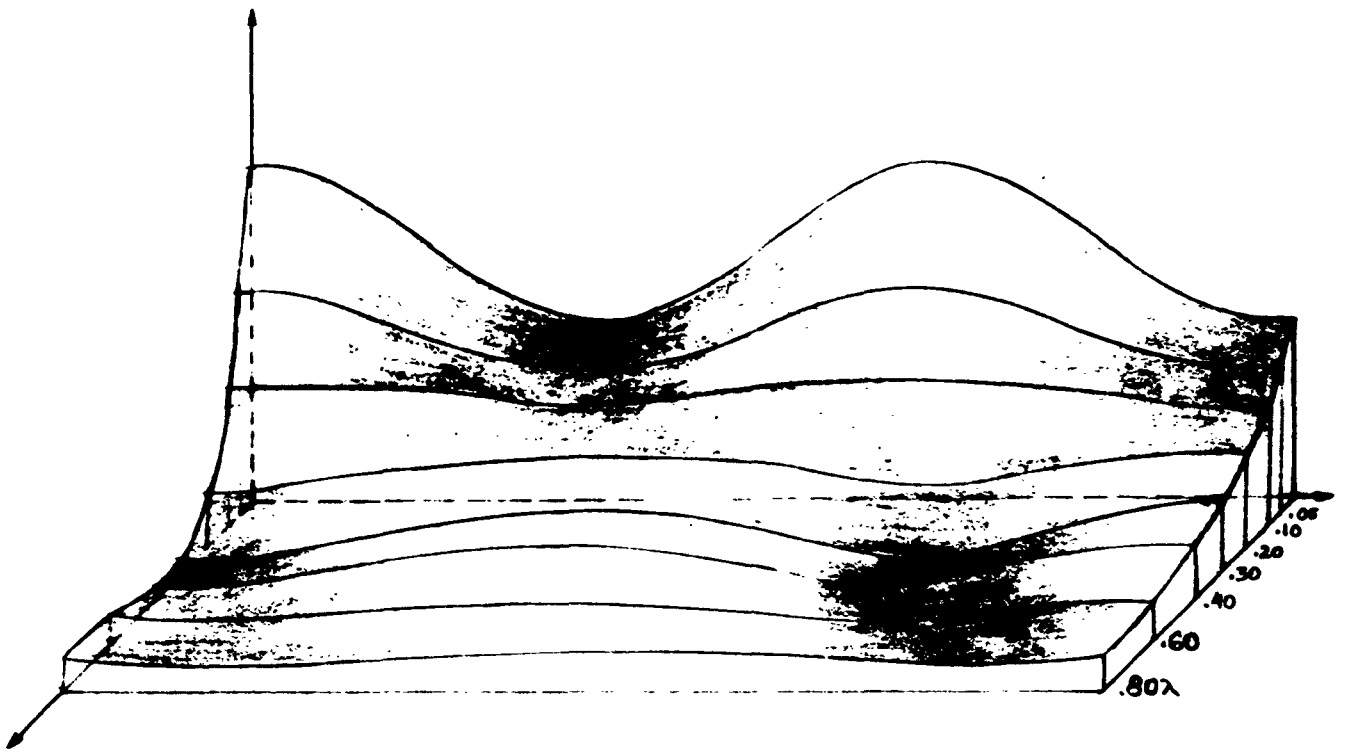

FIGURE 11. Sketch of Amplitude of E_y.

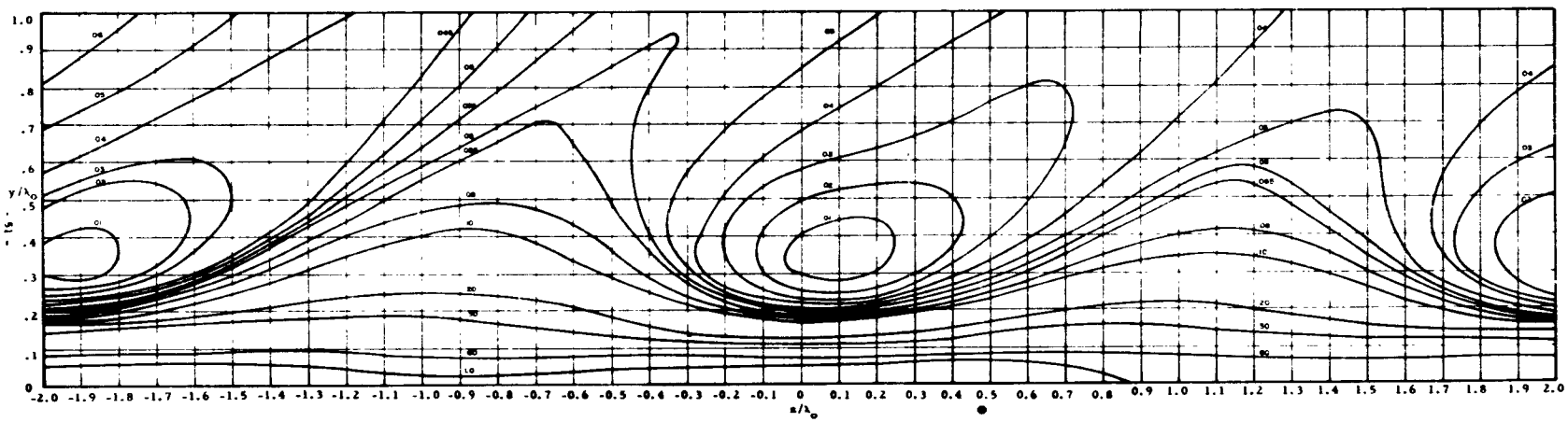

FIGURE 12. Amplitude of the Poynting Vector

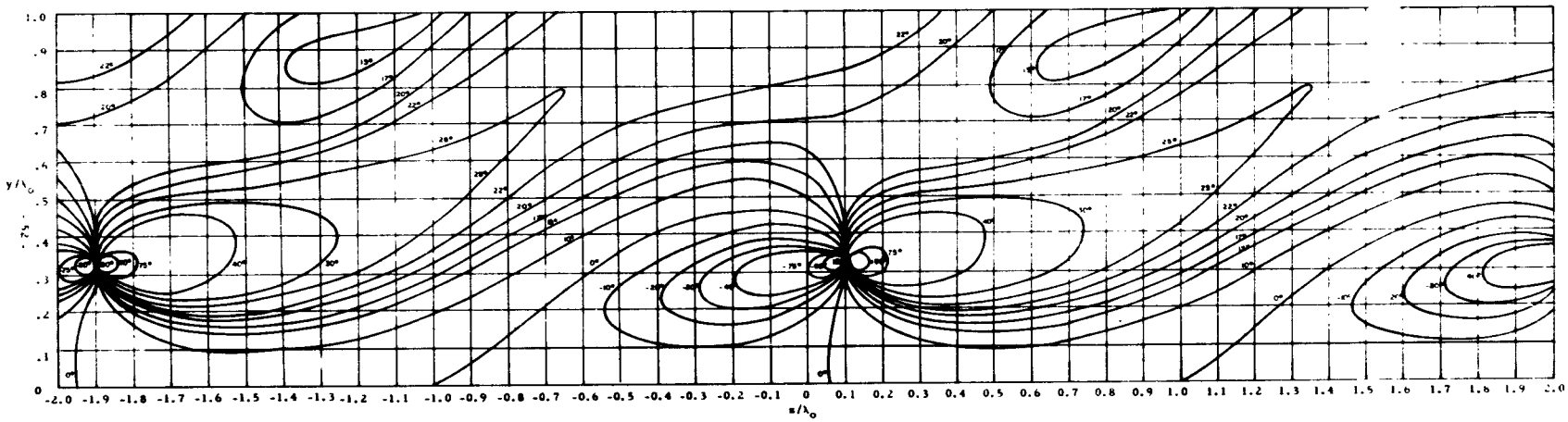

FIGURE 13. Orientation of the Poynting Vector in Degrees with the Positive Direction of the Z-Axis Taken as Reference (0^{o})

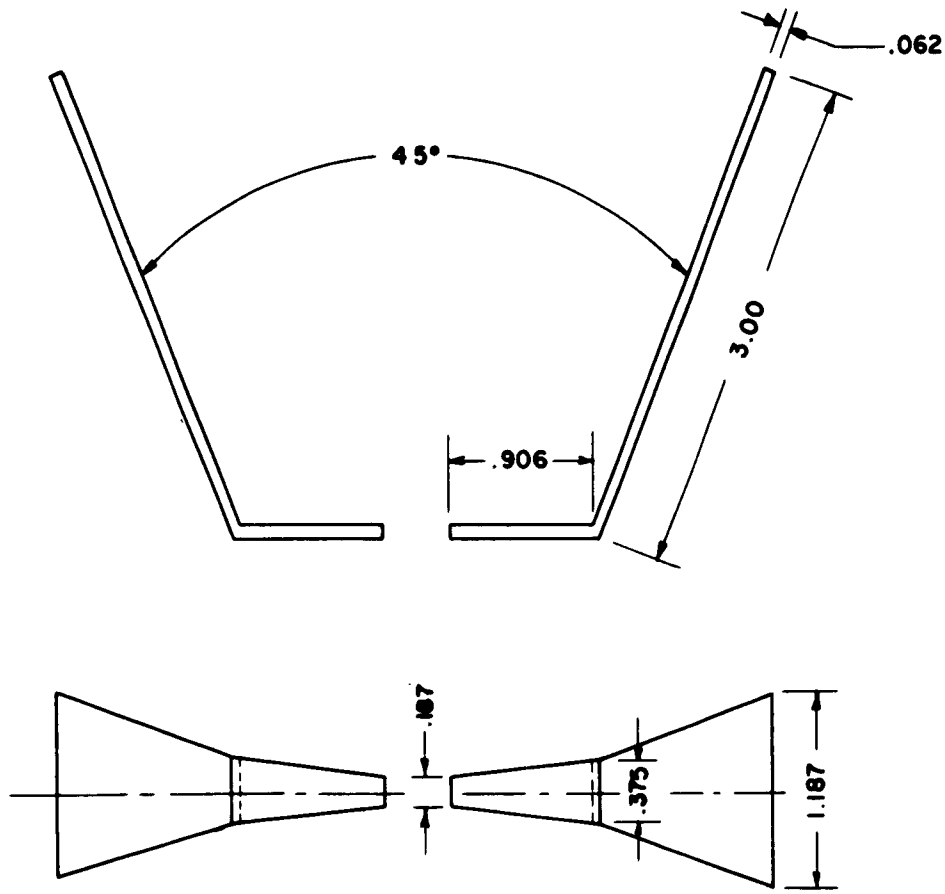

FIGURE 14. Rabbit Ear Feed.

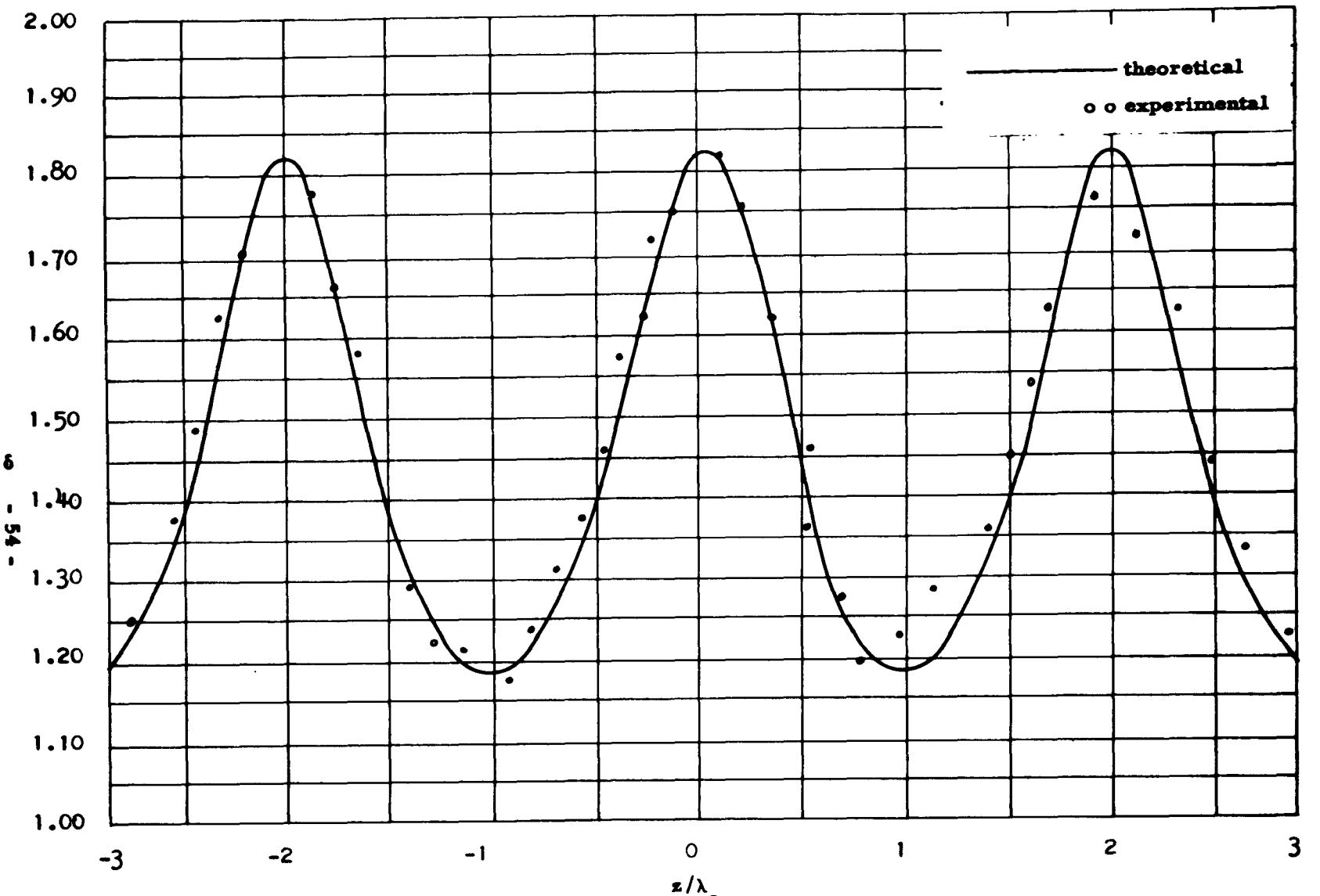

FIGURE 15. Theoretical and experimental δ vs z/λ_o of modulated Yagi at y=0.2λ.

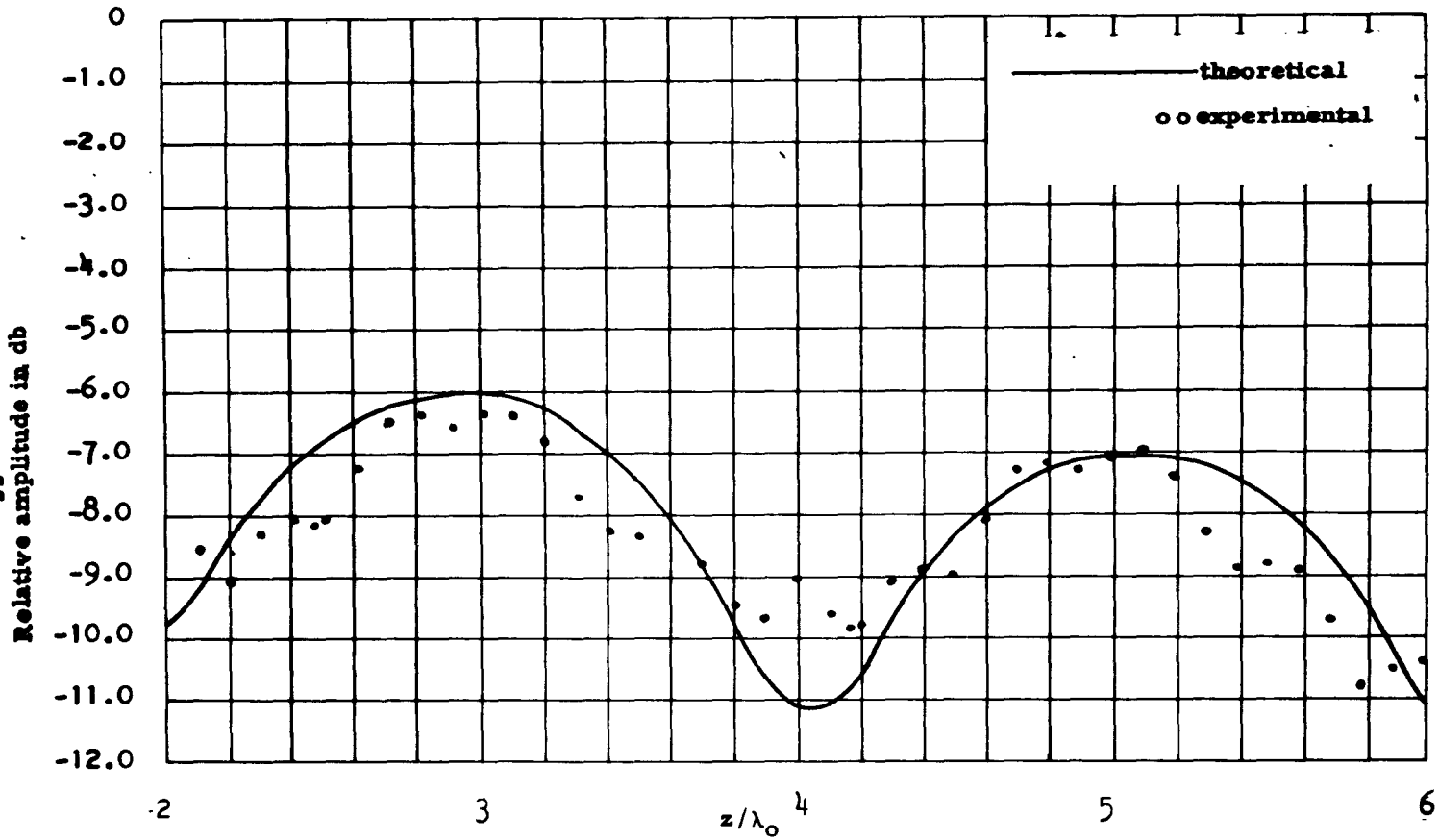

FIGURE 16. Theoretical and experimental relative amplitude of E_y vs z/λ_o for $y = 0.2\lambda$.

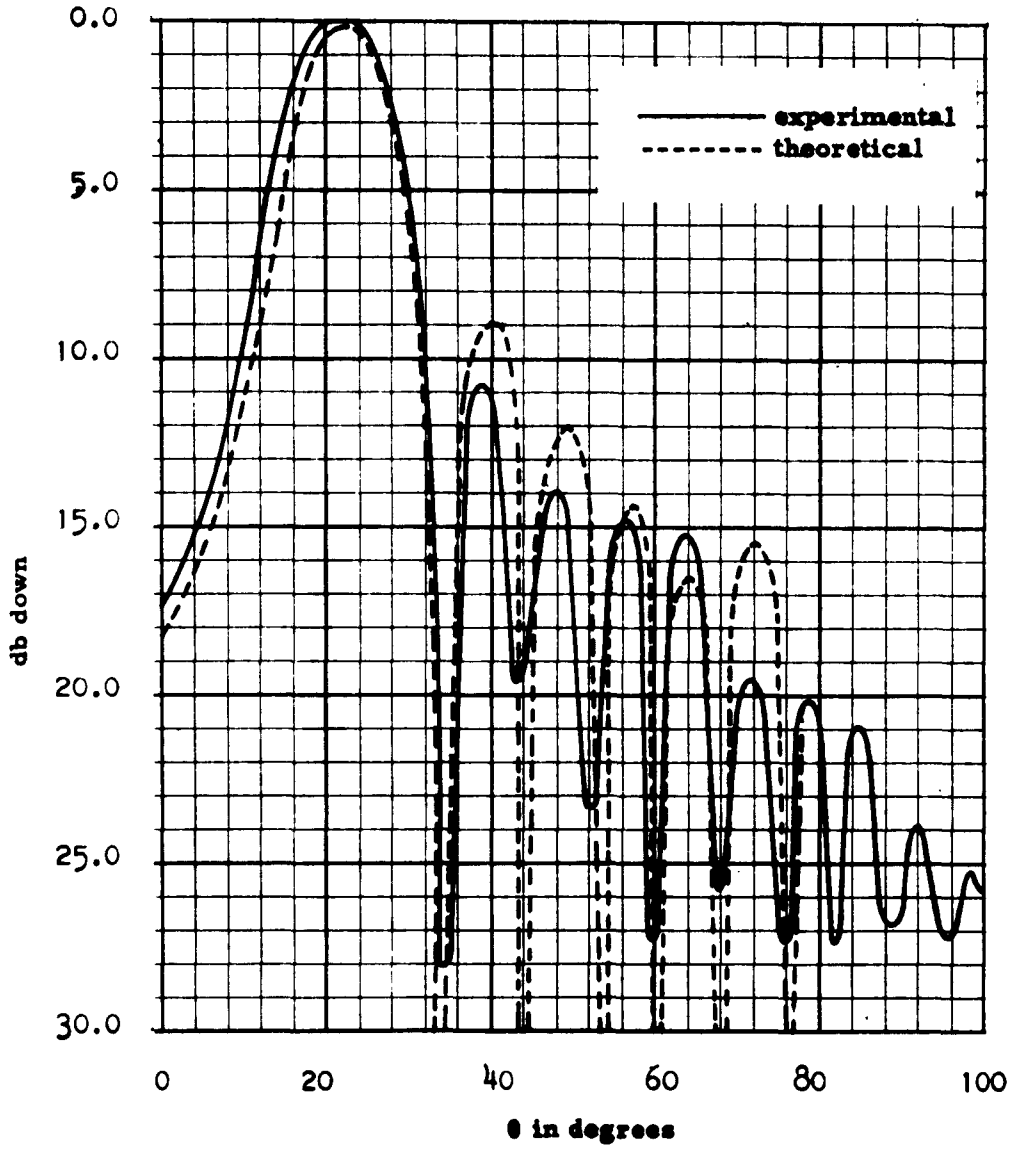

FIGURE 17. **Approximation Theoretical pattern vs Experimental Radiation pattern of modulated 9λ Yagi.**

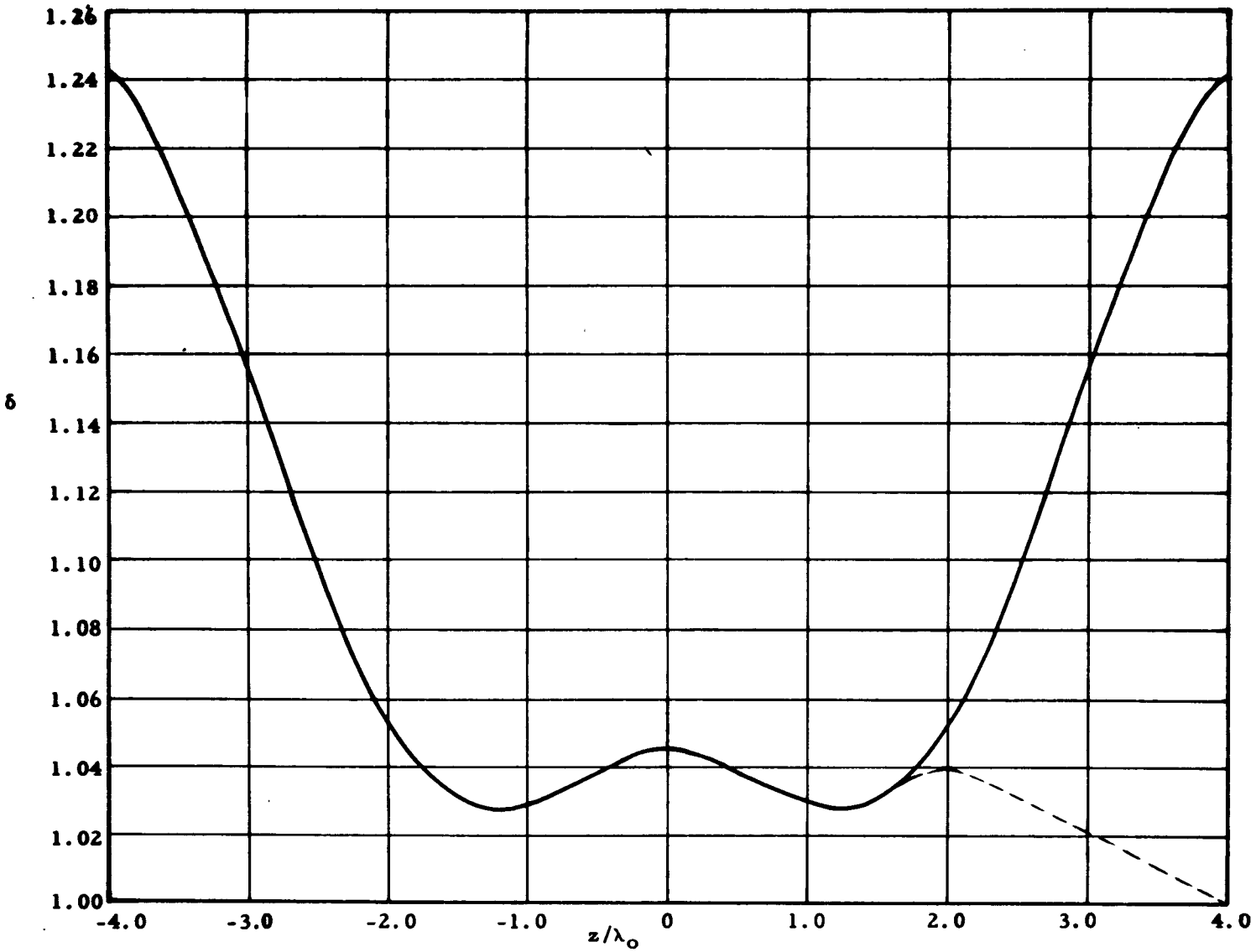

Figure 18. Relative Wave number versus Distance for an 8λ Array.

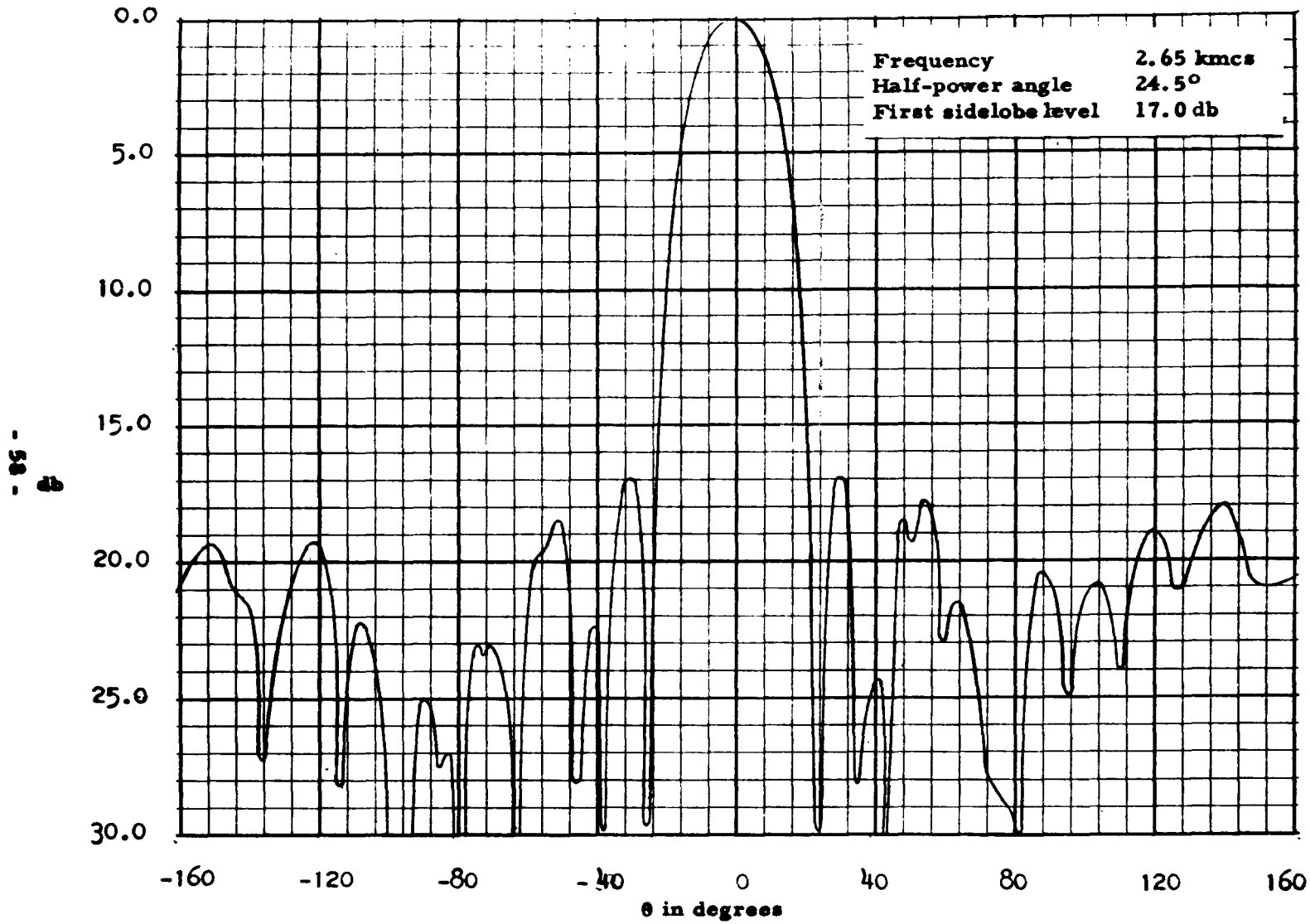

FIGURE 19. Re plotted Radiation patterns of 8λ Yagi as per distribution of Figure 18 with dotted line.

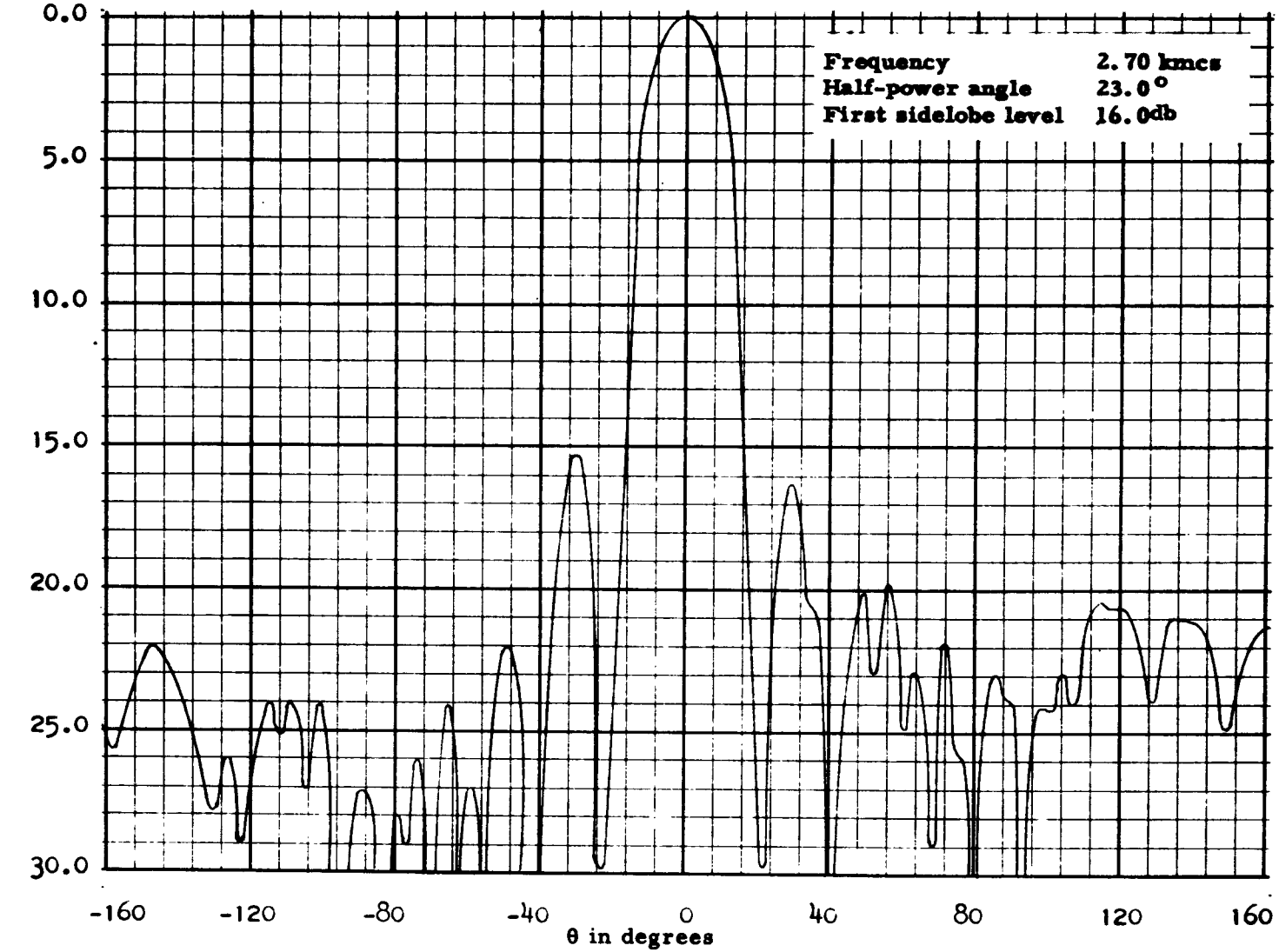

FIGURE 20. Re plotted Radiation patterns of 8λ Yagi as per distribution of Figure 18 with dotted line.

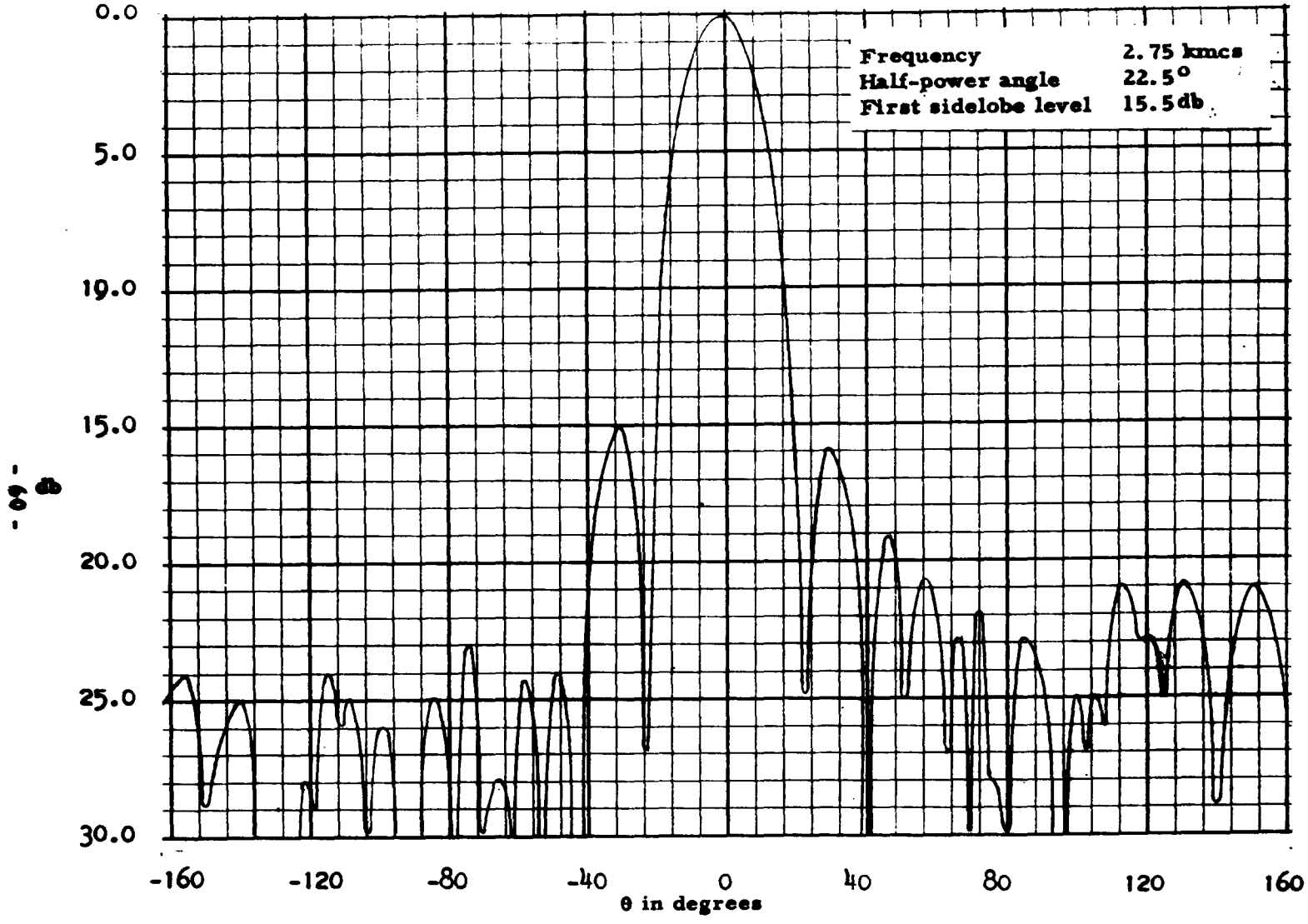

FIGURE 21. Replotted Radiation patterns of 8λ Yagi as per distribution of Figure 18 with dotted line.

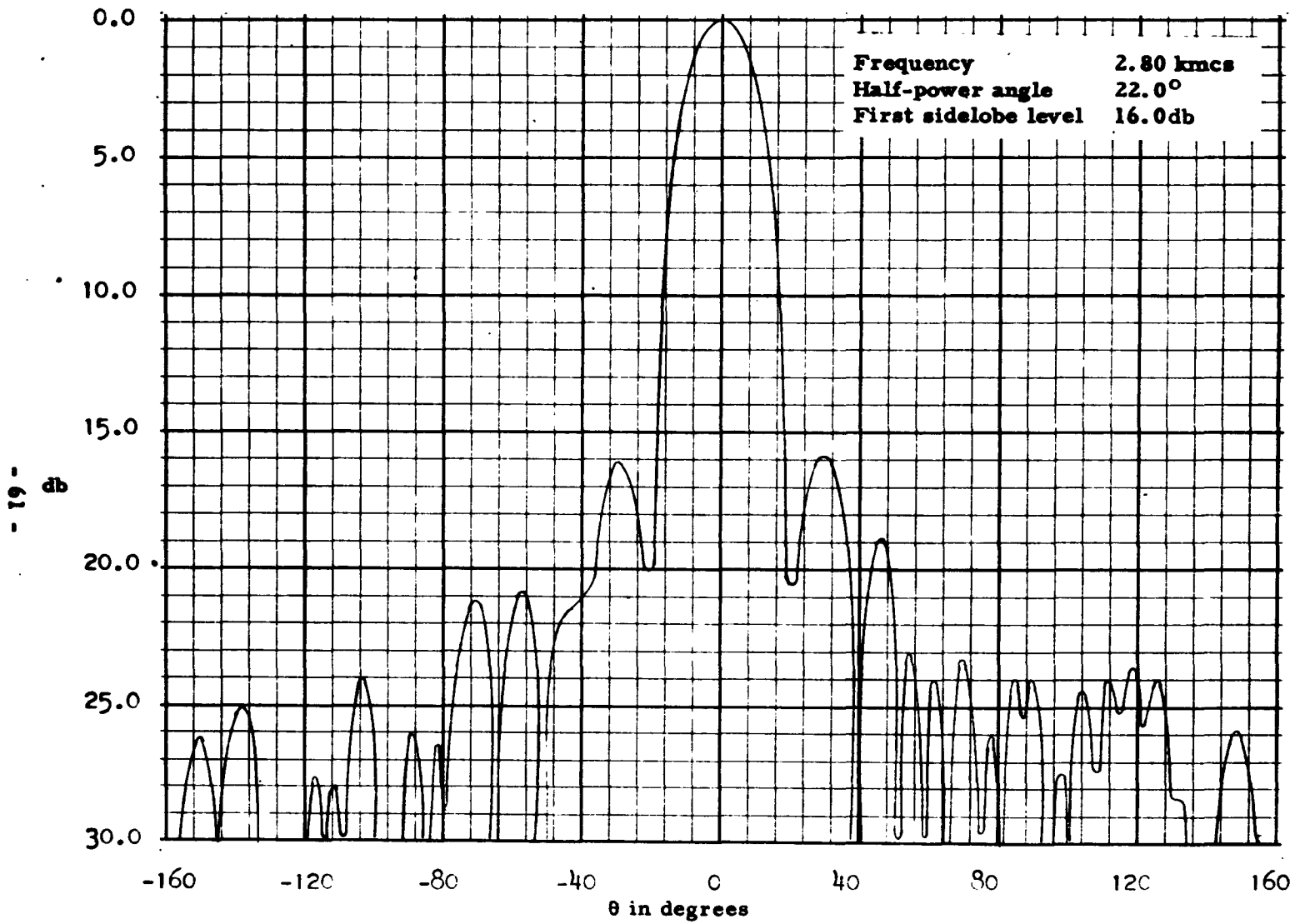

FIGURE 22. Replotted Radiation patterns of 8λ Yagi as per distribution of Figure 18 with dotted line.

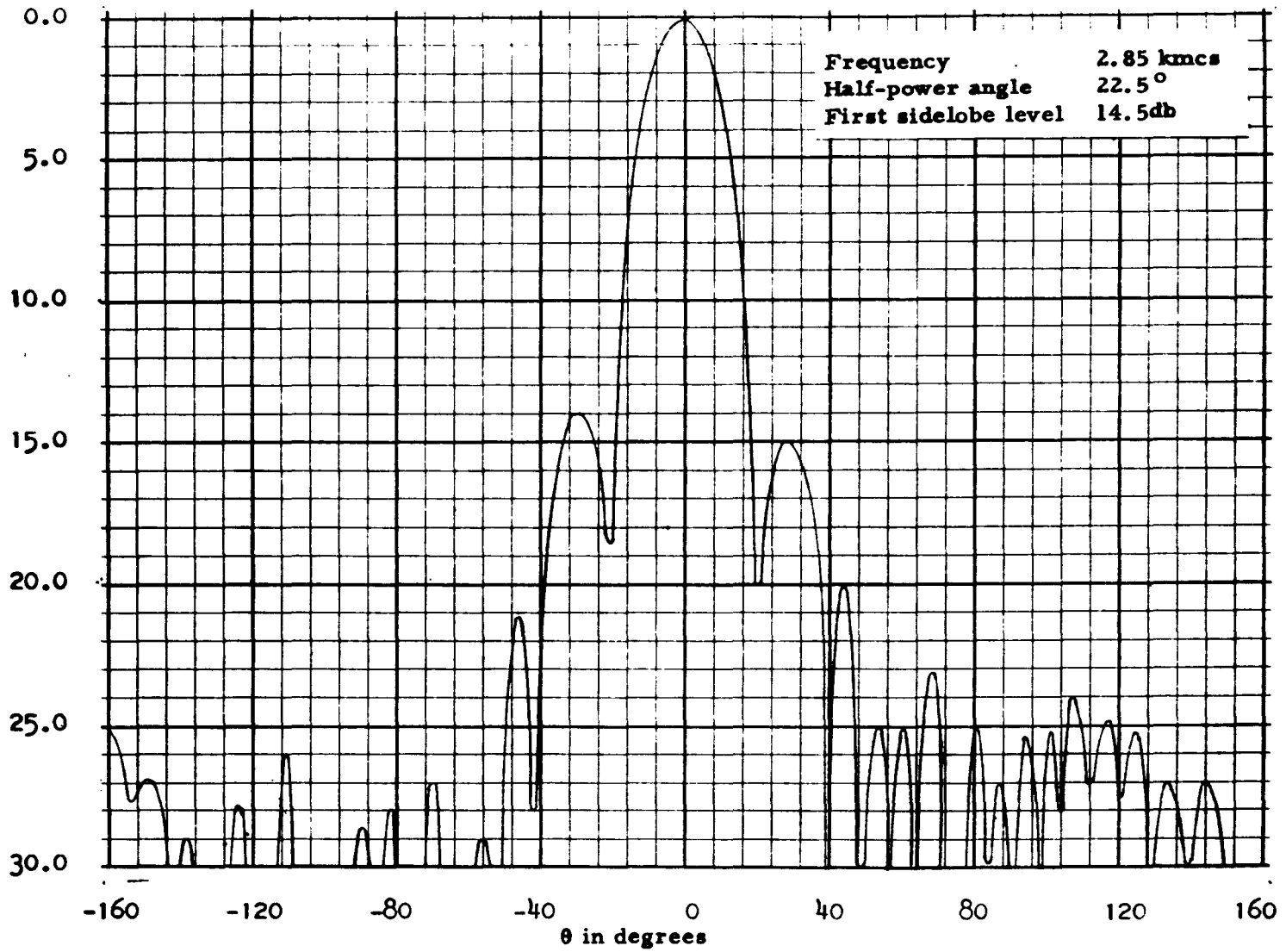

FIGURE 23. Replotted Radiation patterns of 8λ Yagi as per distribution of Figure 18 with dotted line.

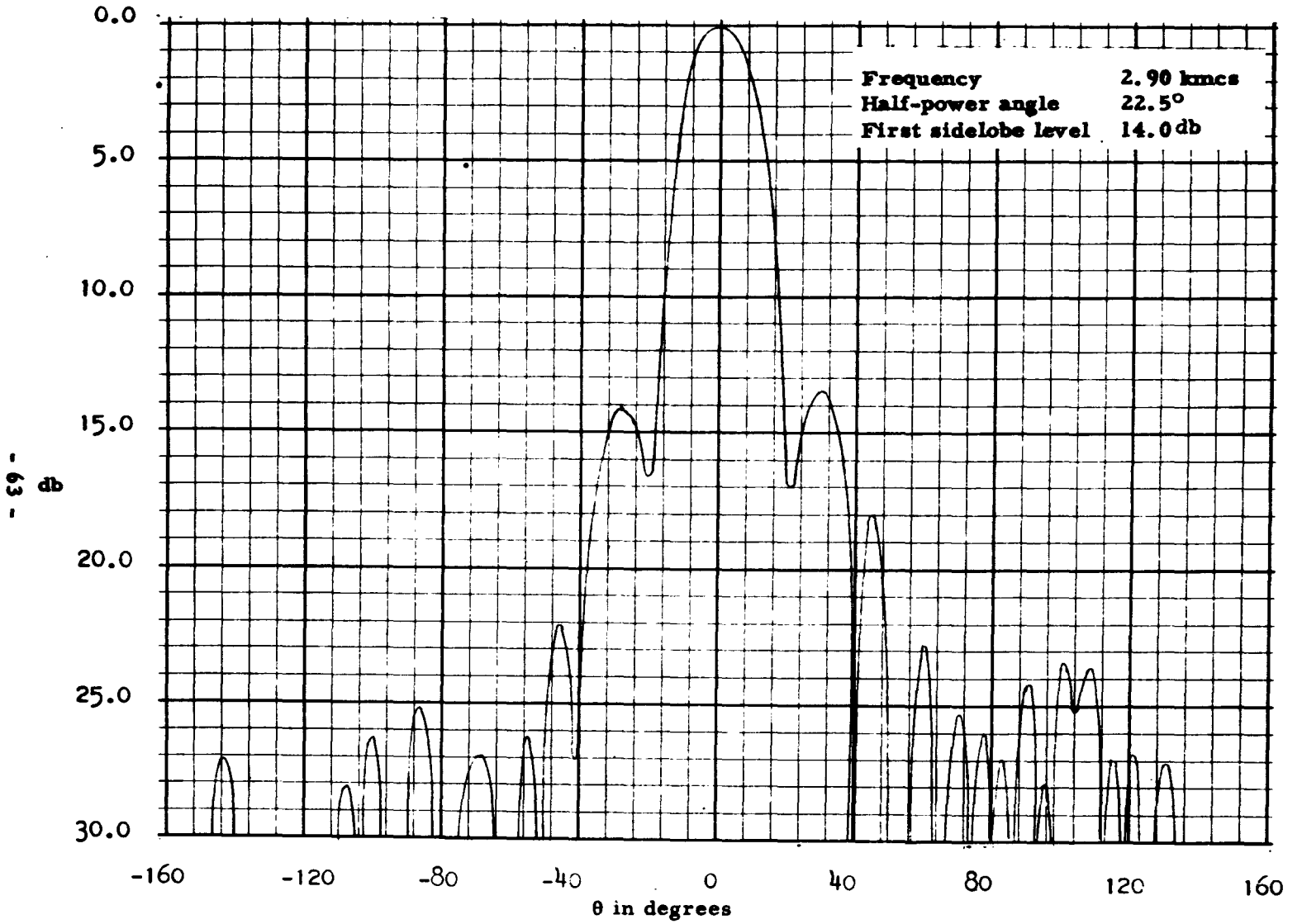

FIGURE 24. Replotted Radiation patterns of 8λ Yagi as per distribution of Figure 18 with dotted line.

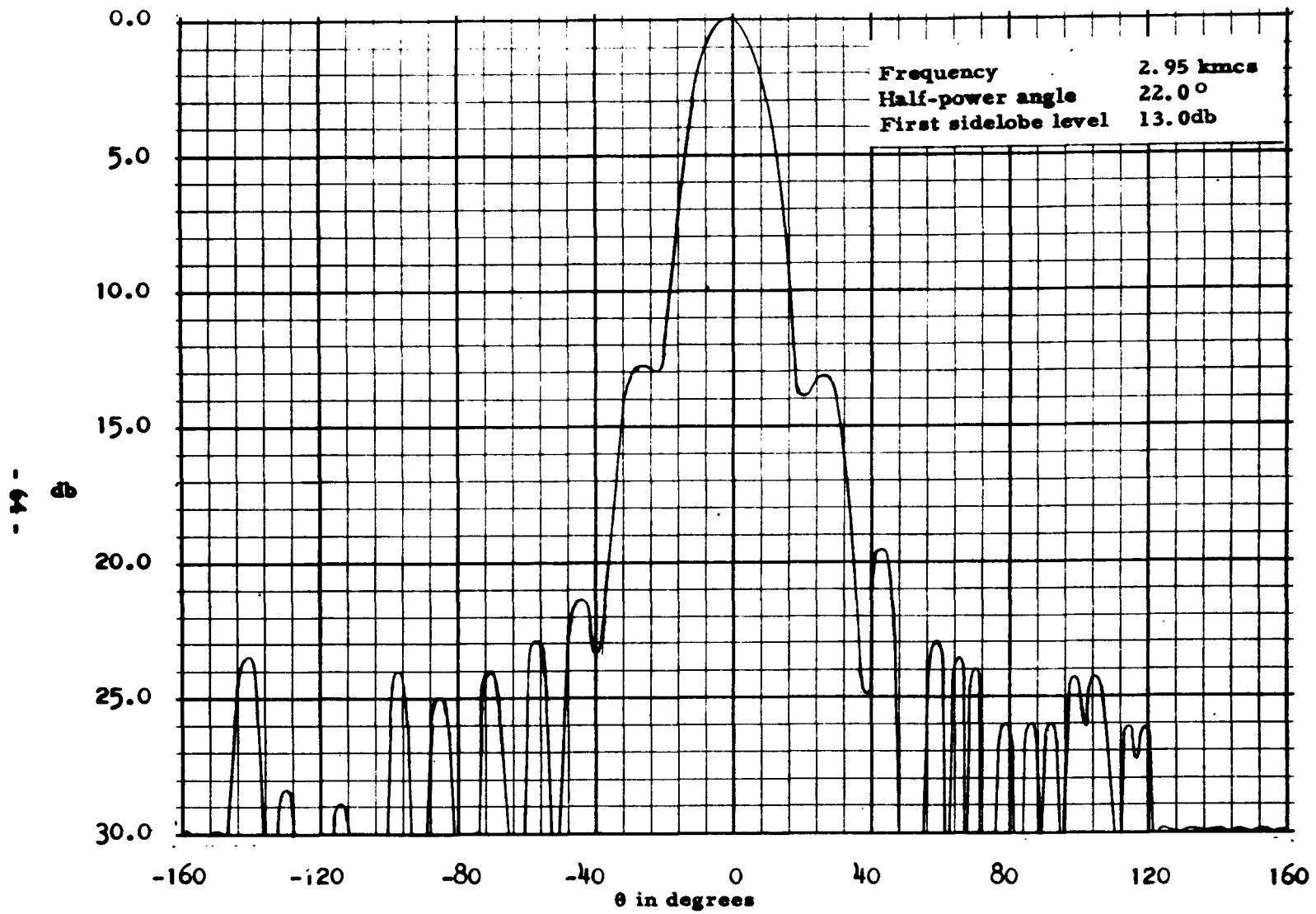

FIGURE 25. Replotted Radiation patterns of 8λ Yagi as per distribution of Figure 18 with dotted line.

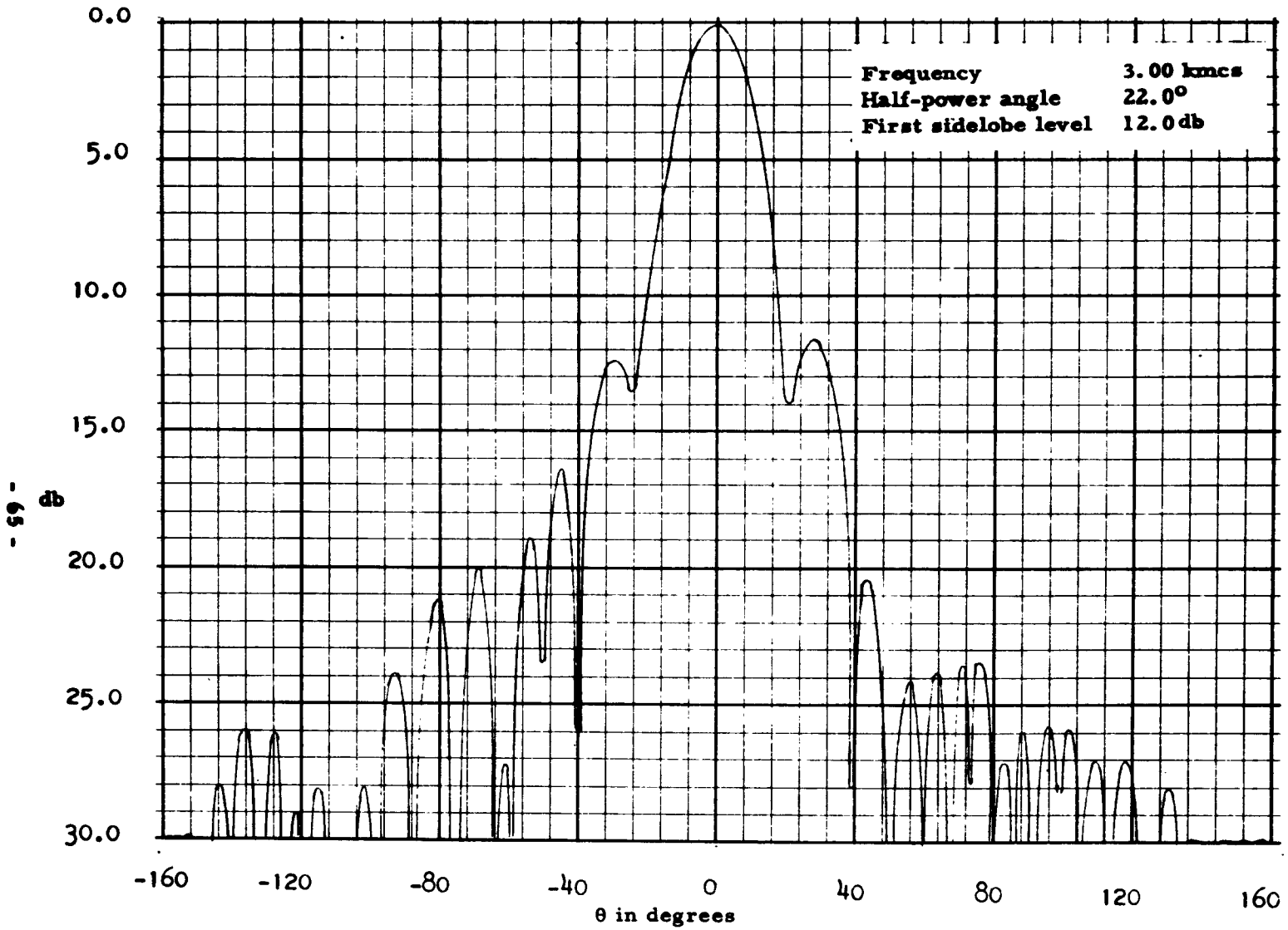

FIGURE 26. Replotted Radiation patterns of 8λ Yagi as per distribution of Figure 18 with dotted line.

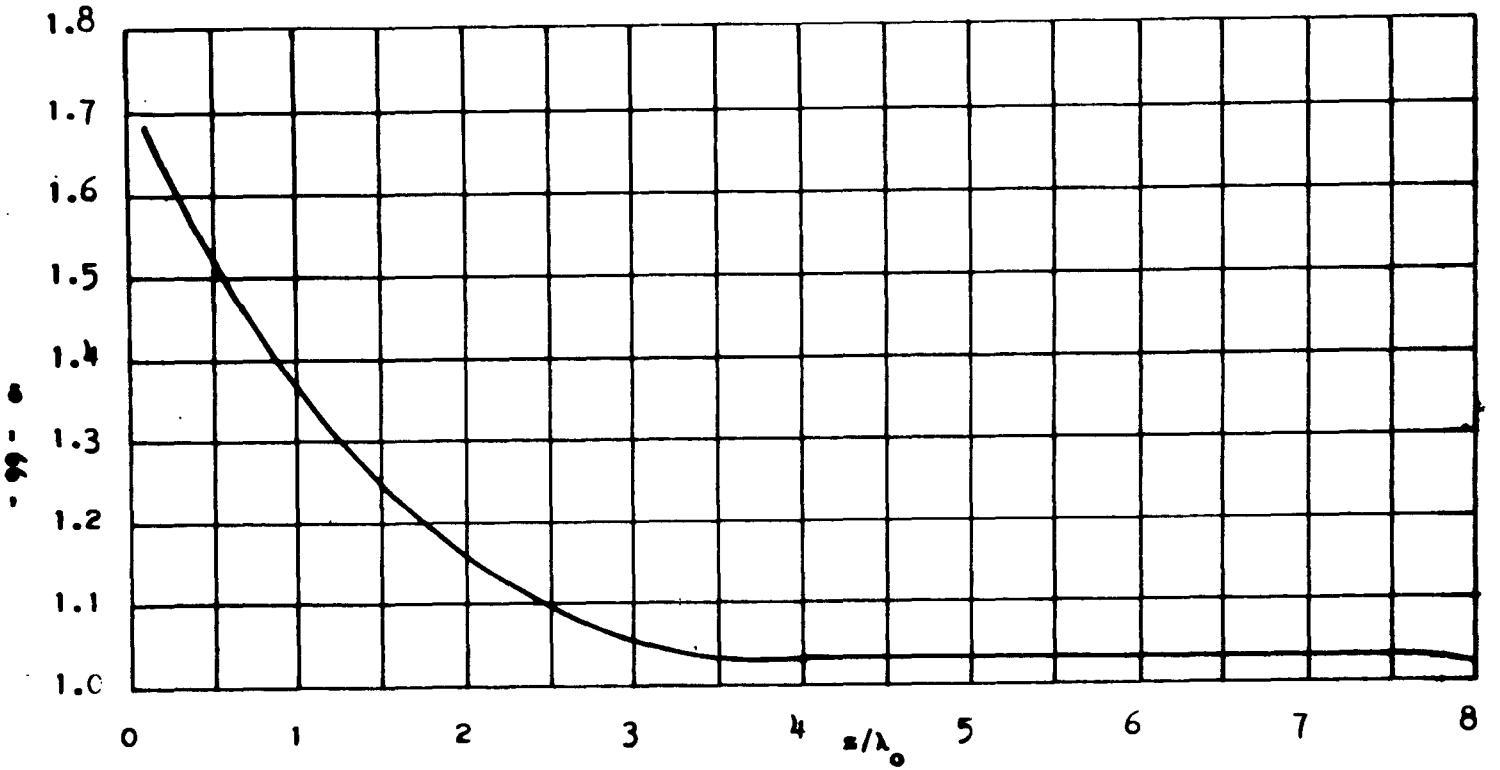

FIGURE 27. Relative wave number vs distance for 8λ endfire array.

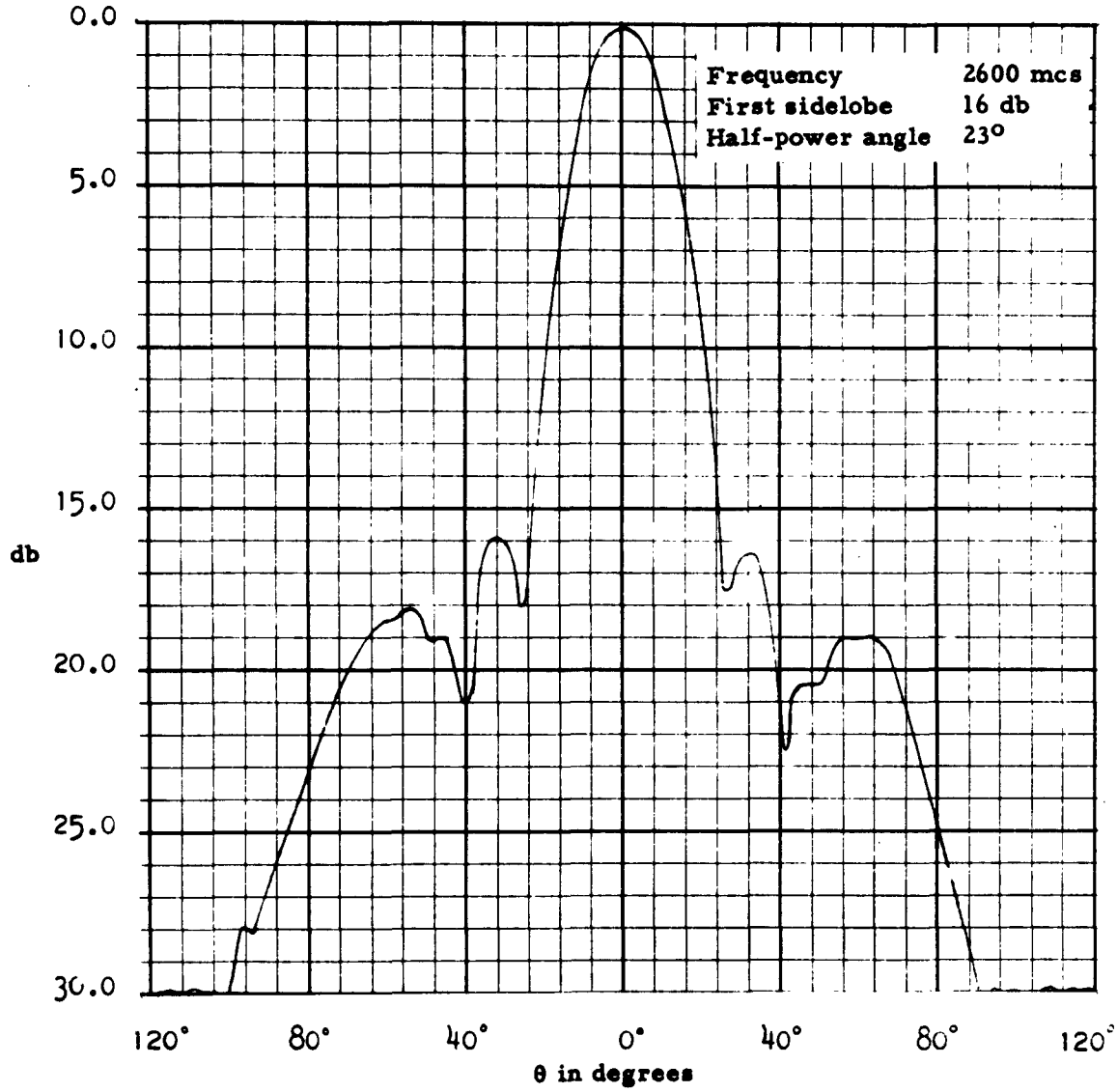

FIGURE 28. Replotted radiation pattern for δ of array given in Figure 27.

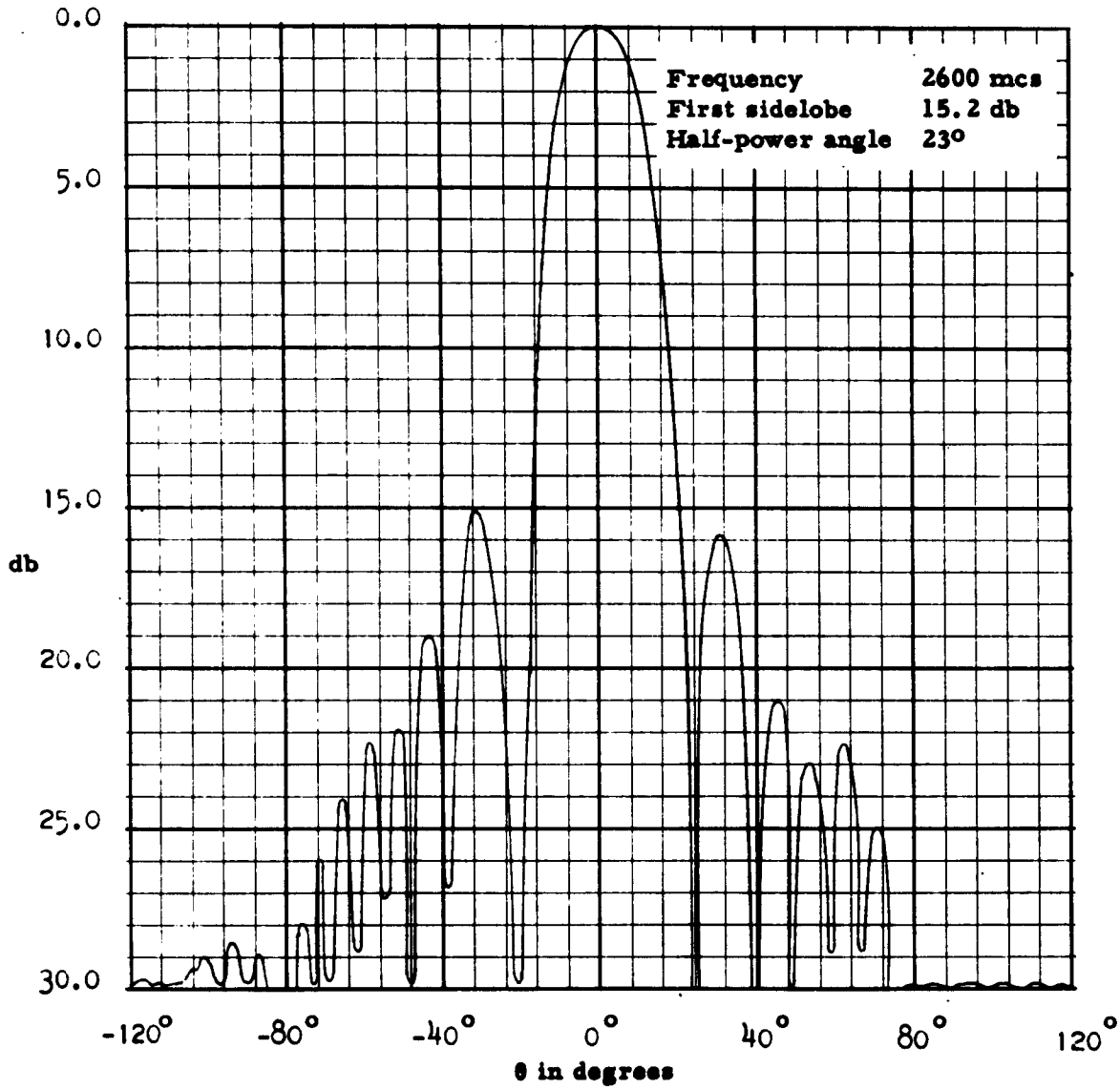

FIGURE 29. Replotted radiation pattern for δ of array given in Figure 27.

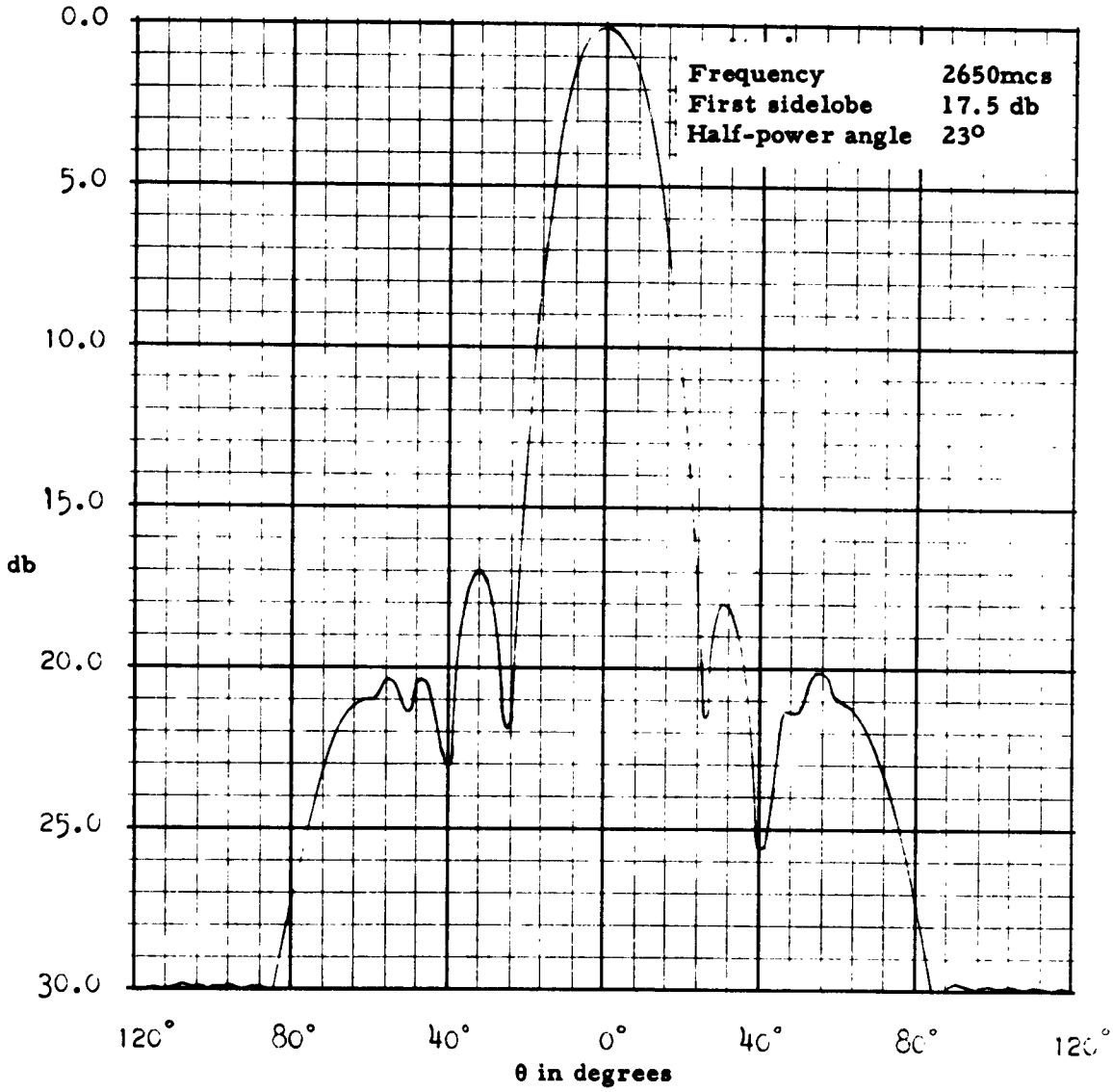

FIGURE 30. Replotted radiation pattern for δ of array given in Figure 27.

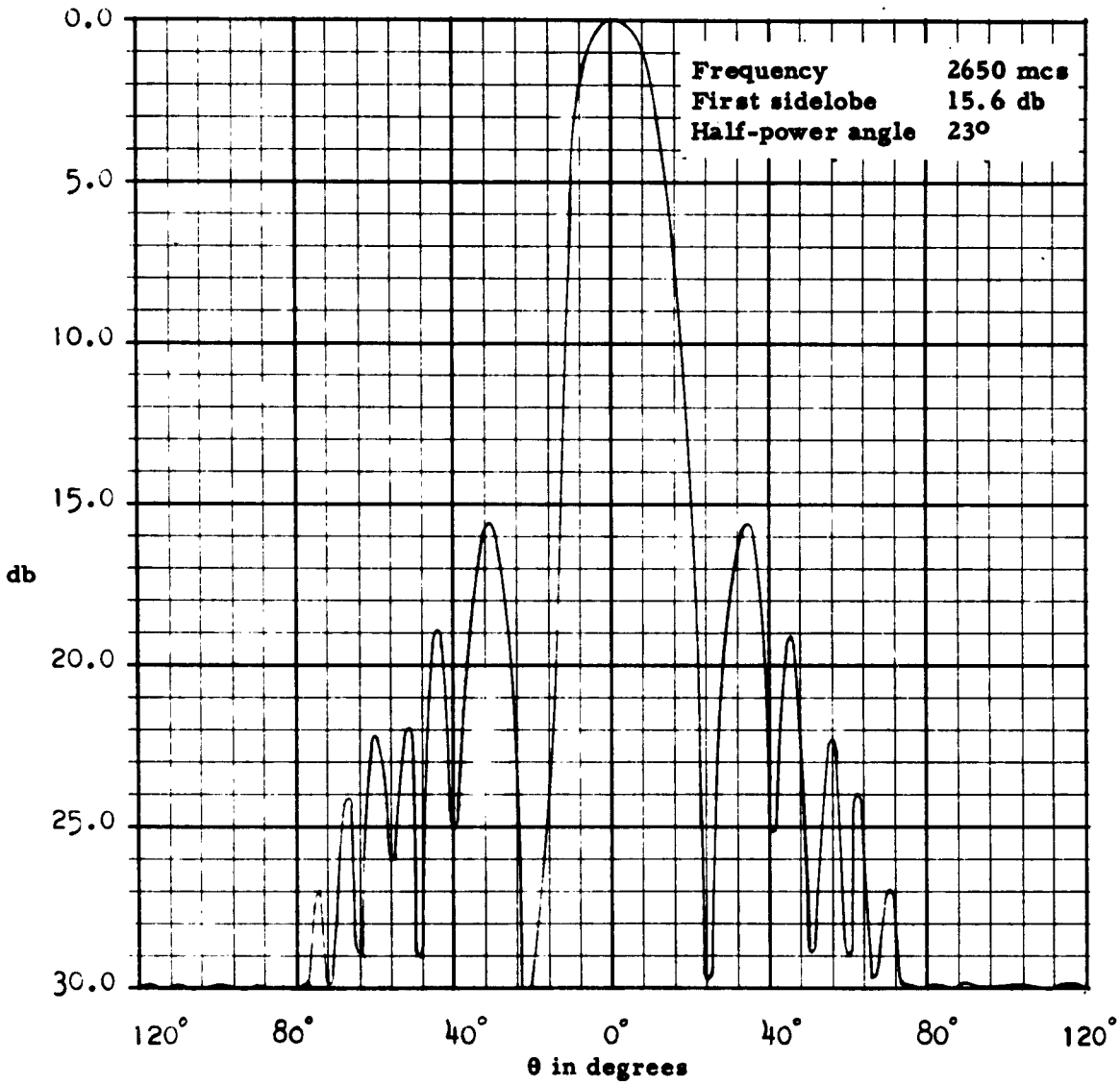

FIGURE 31. **Replotted radiation pattern for δ of array given in Figure 27.**

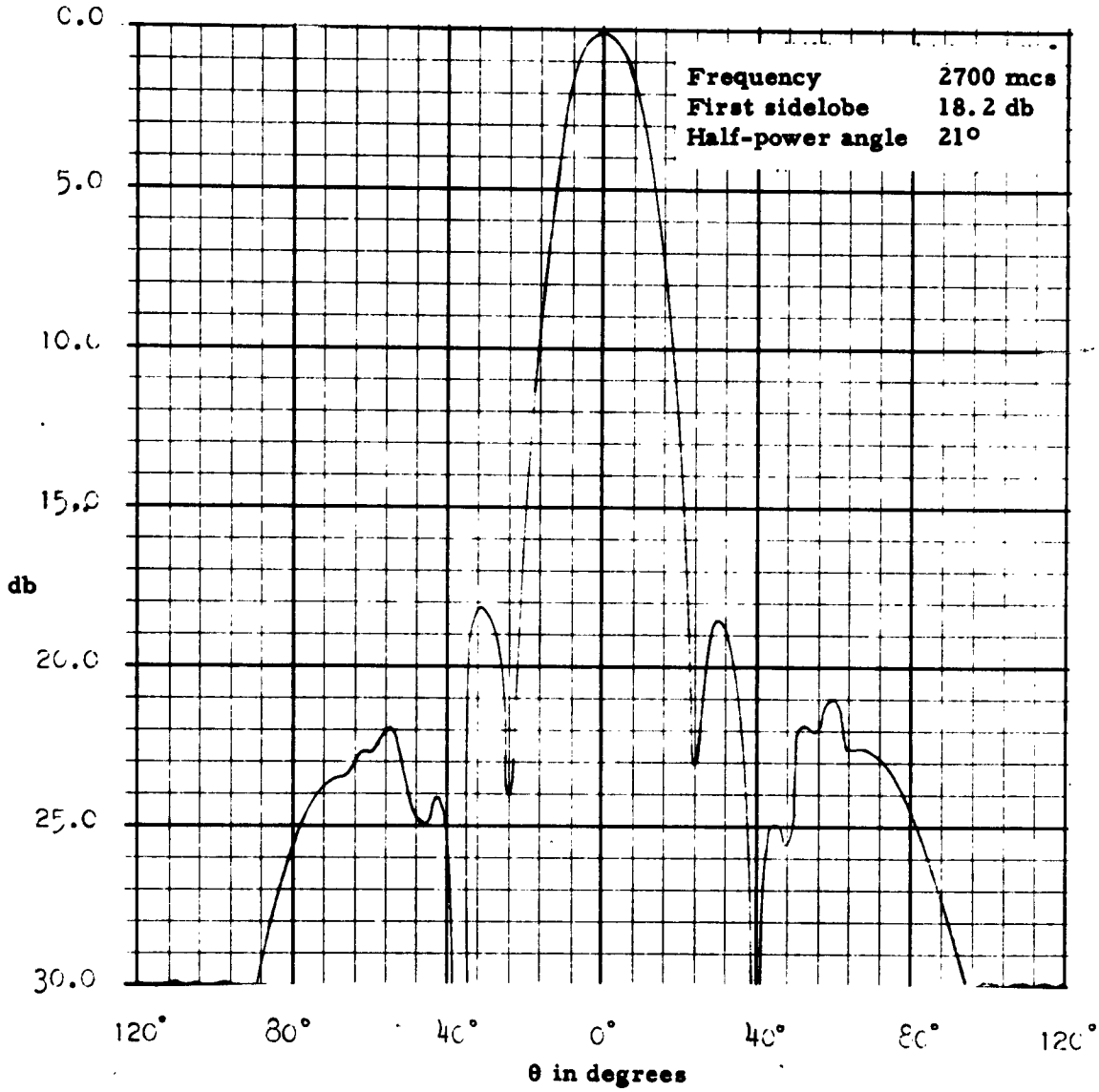

FIGURE 32. Replotted radiation pattern for δ of array given in Figure 27.

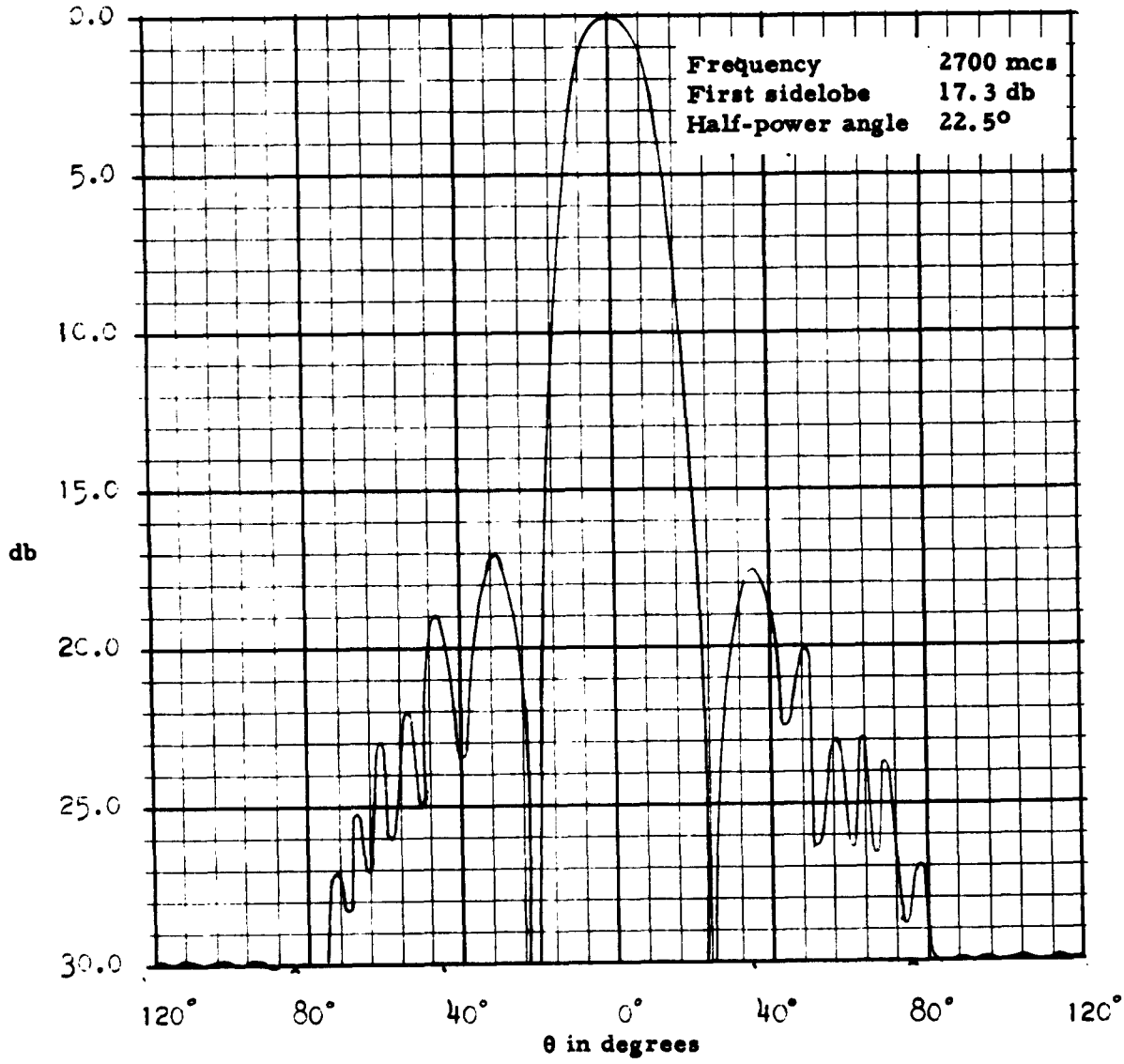

FIGURE 33. **Replotted radiation pattern for δ of array given in Figure 27.**

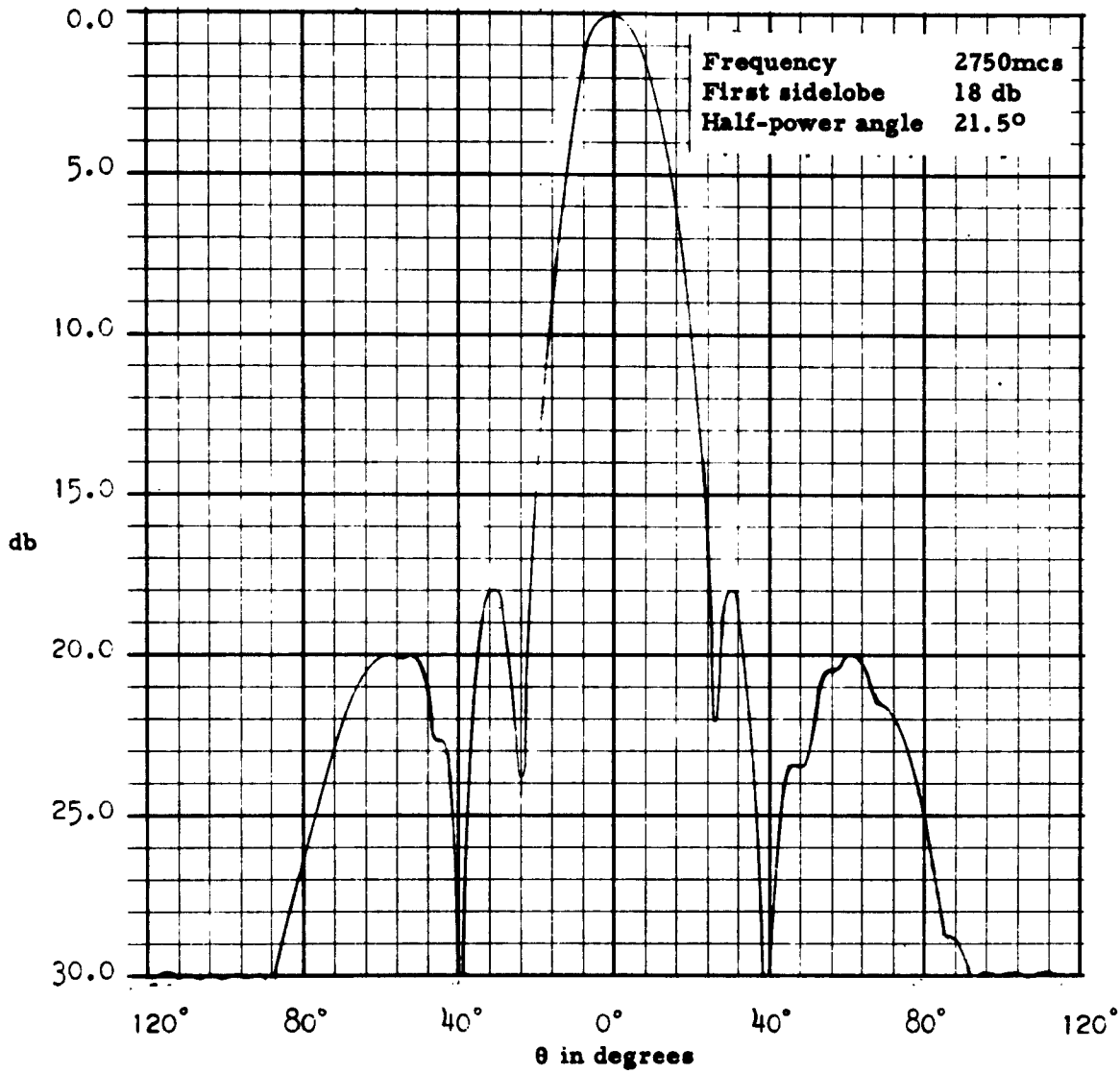

FIGURE 34. **Replotted radiation pattern for δ of array given in Figure 27.**

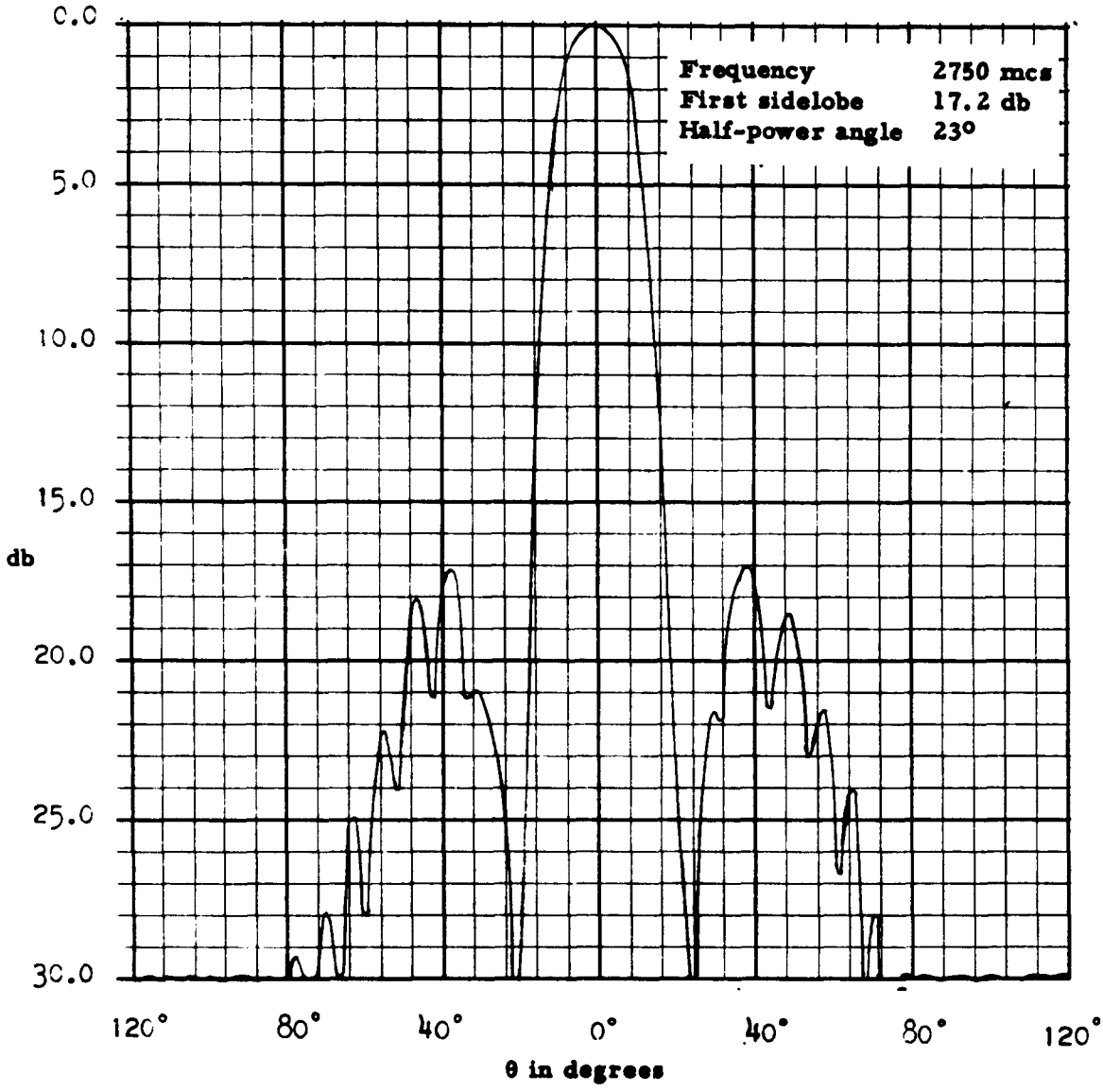

FIGURE 35. Replotted radiation pattern for δ of array given in Figure 27.

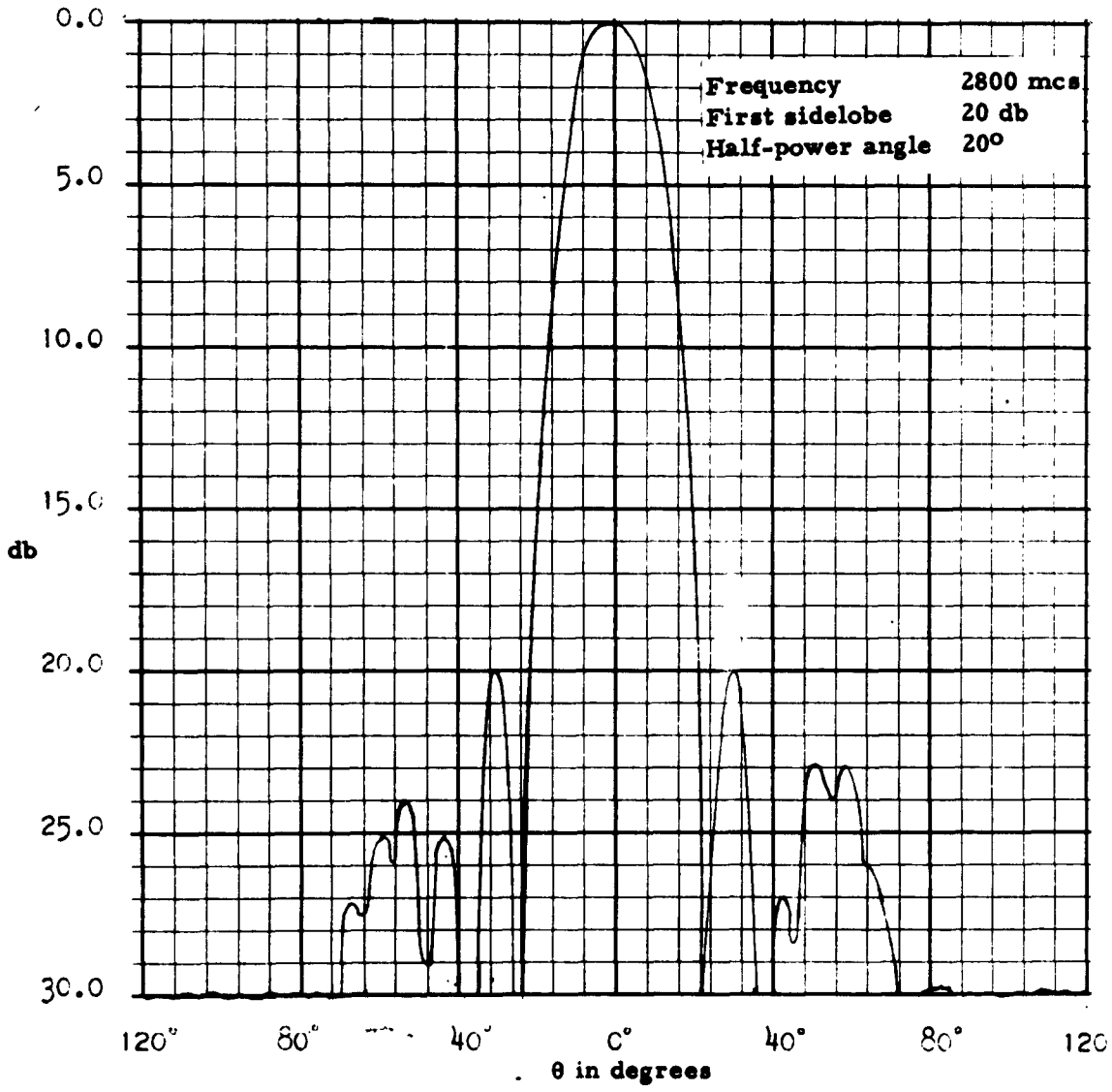

FIGURE 36. Replotted radiation pattern for δ of array given in Figure 27.

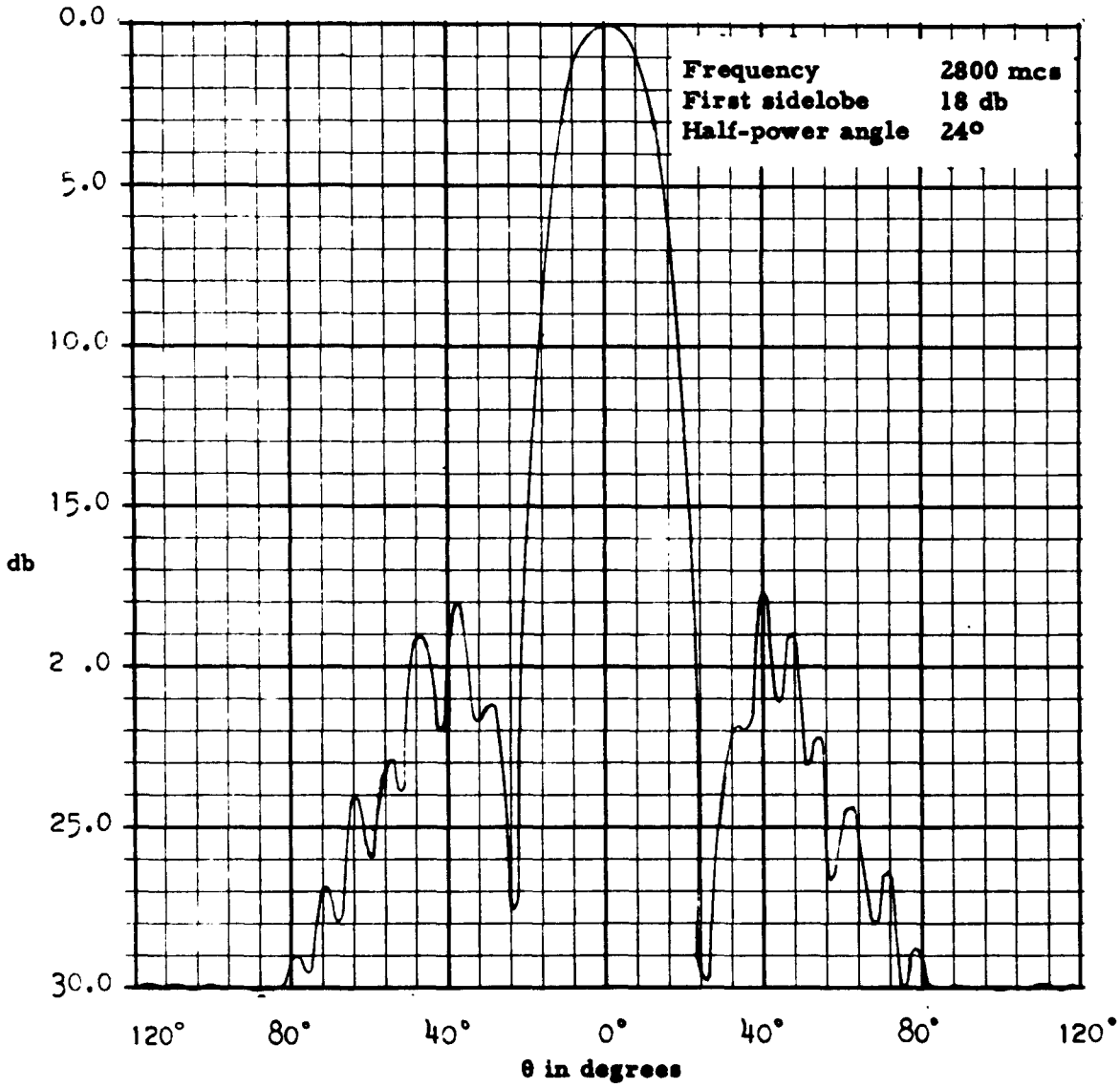

FIGURE 37. **Replotted radiation pattern for δ of array given in Figure 27.**

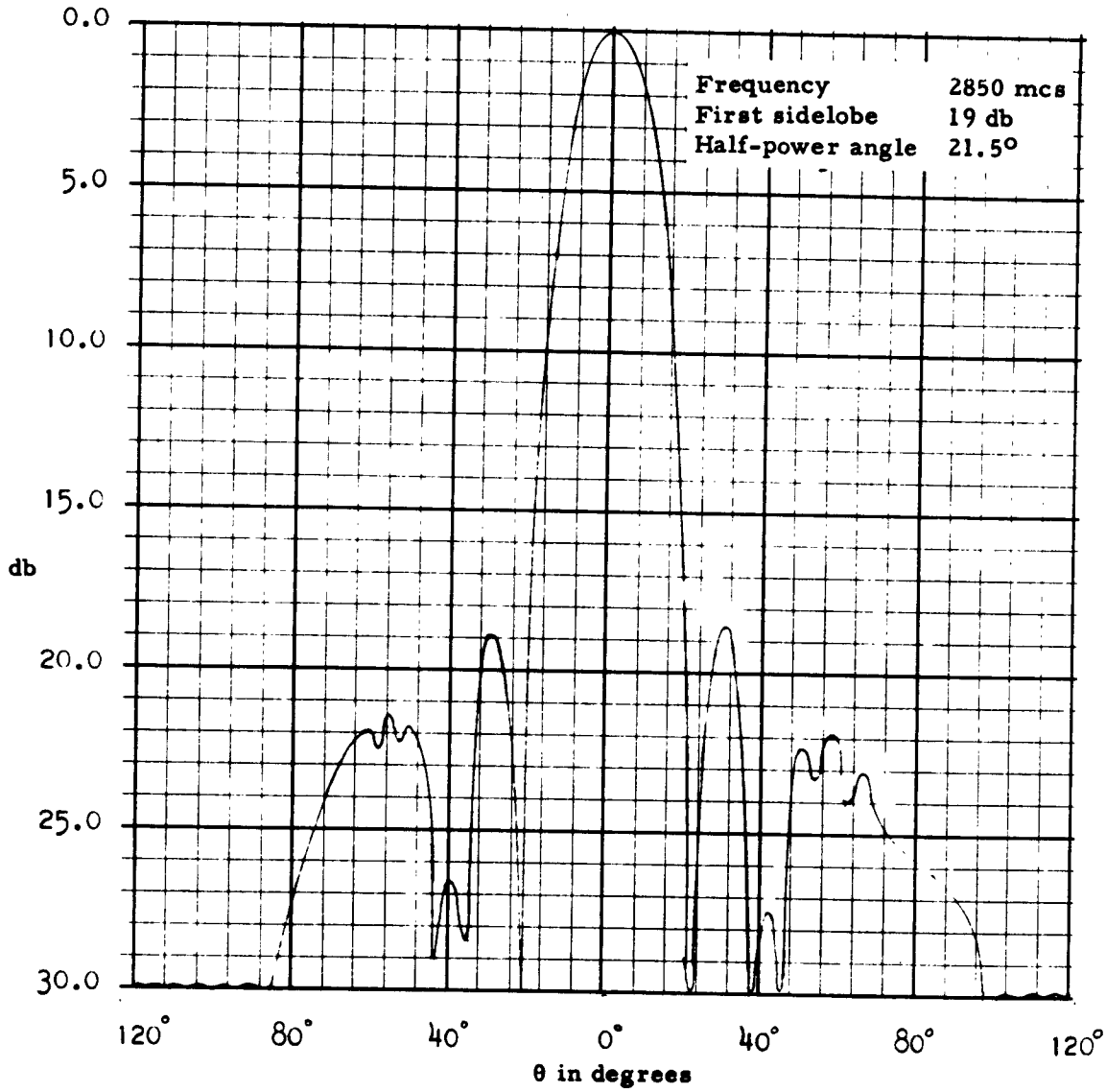

FIGURE 38. Replotted radiation pattern for δ of array given in Figure 27.

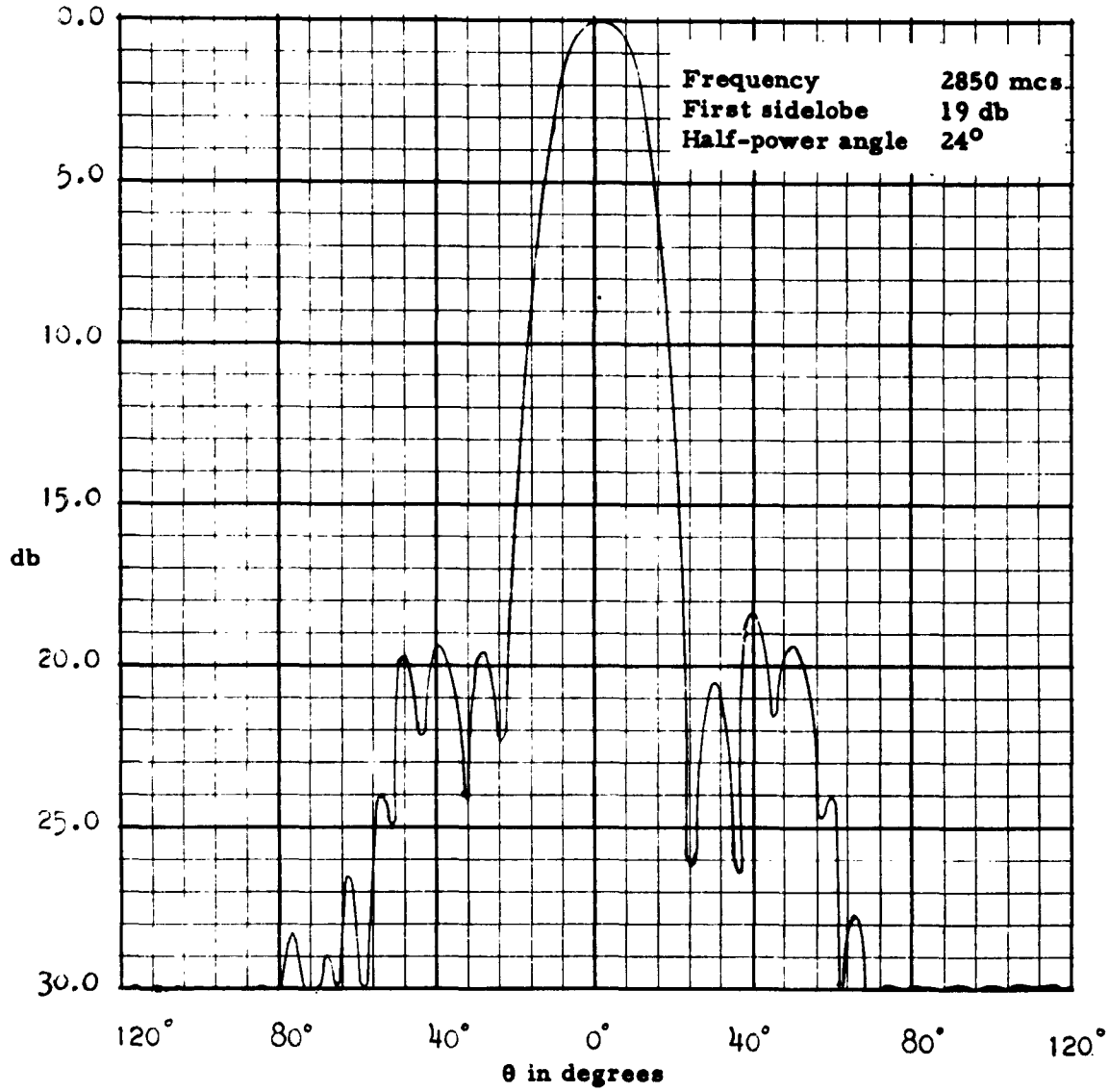

FIGURE 39. Replotted radiation pattern for δ of array given in Figure 27.

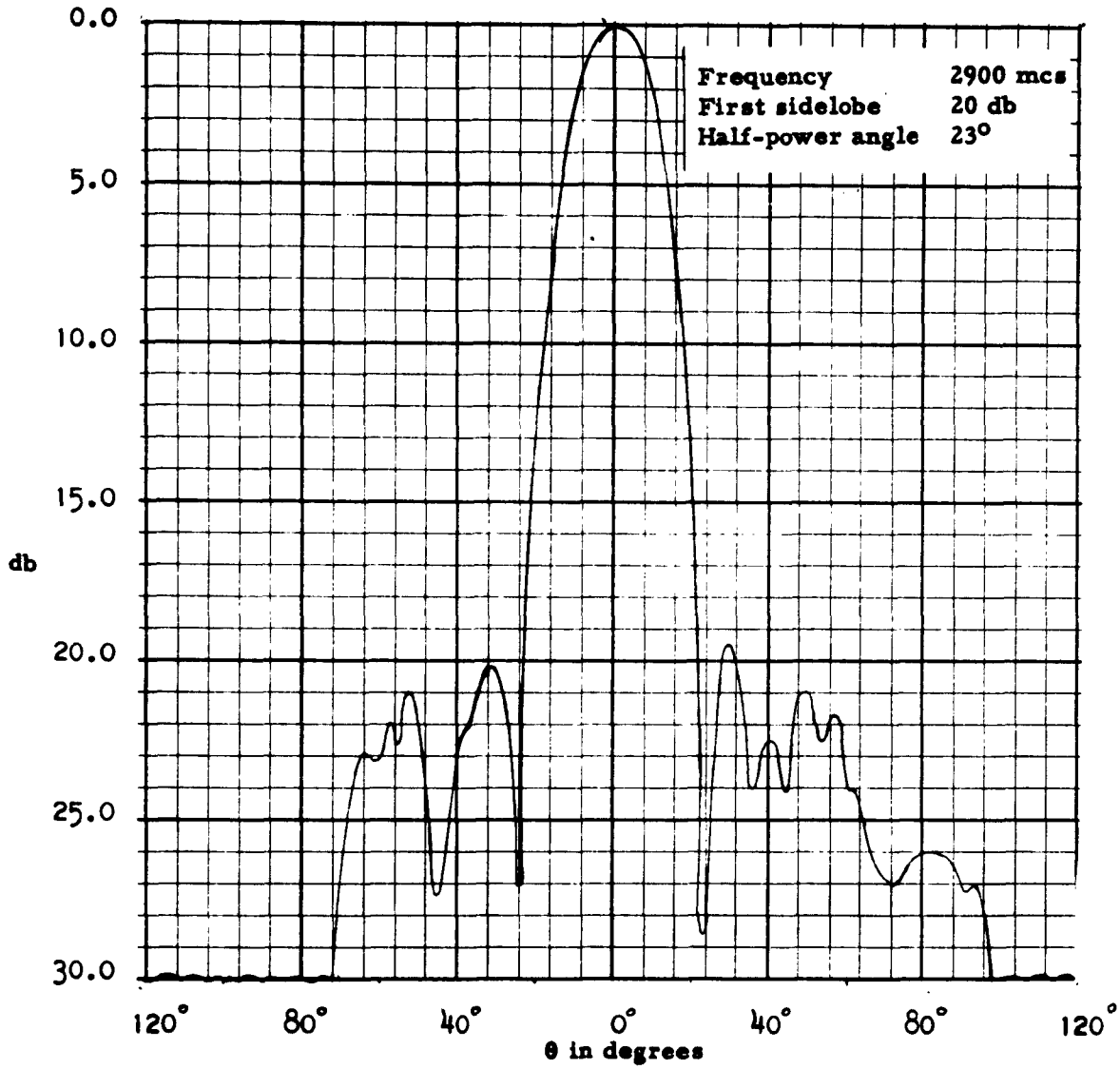

FIGURE 40. Replotted radiation pattern for δ of array given in Figure 27.

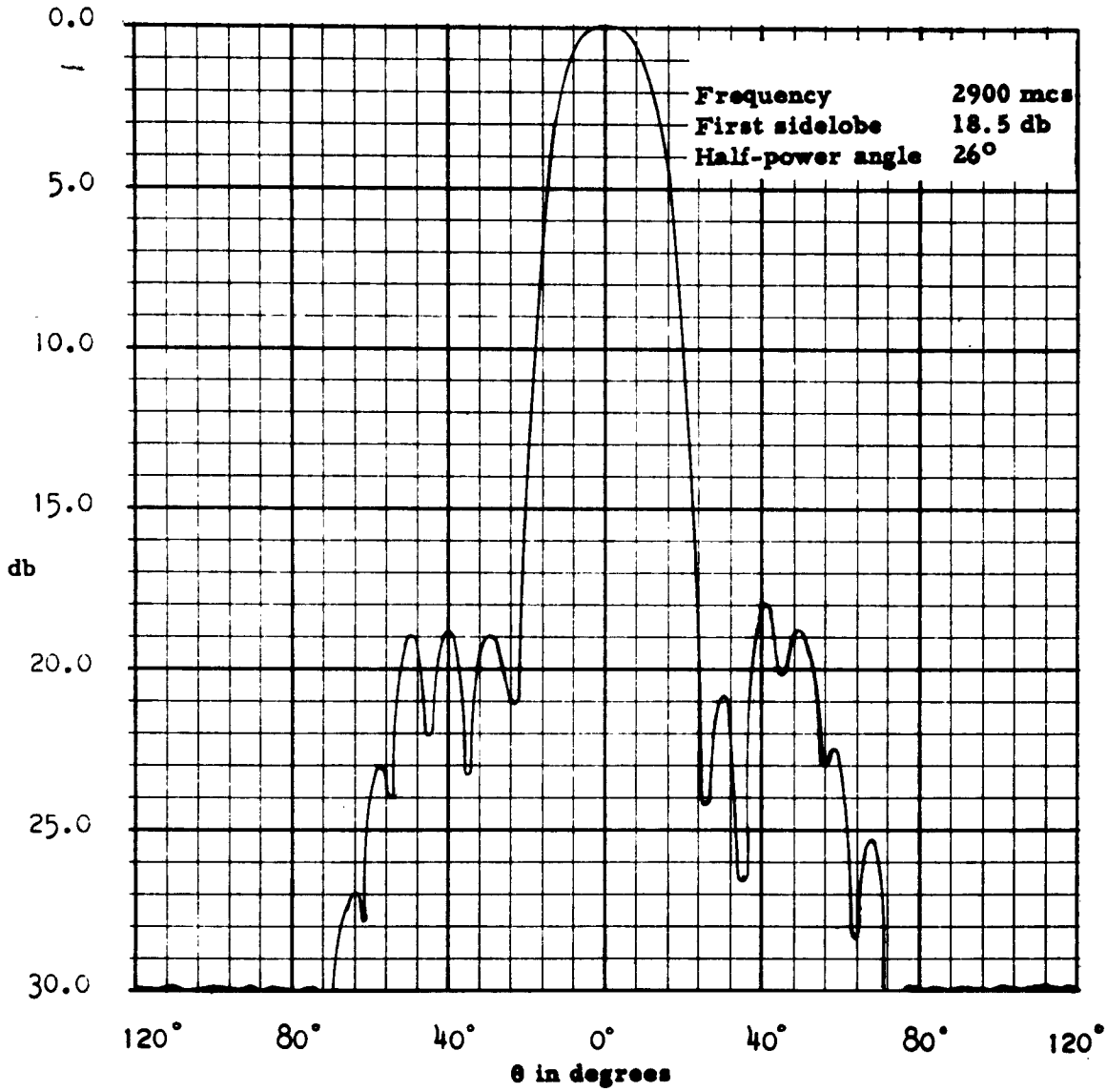

FIGURE 41. Replotted radiation pattern for 6 of array given in Figure 27.

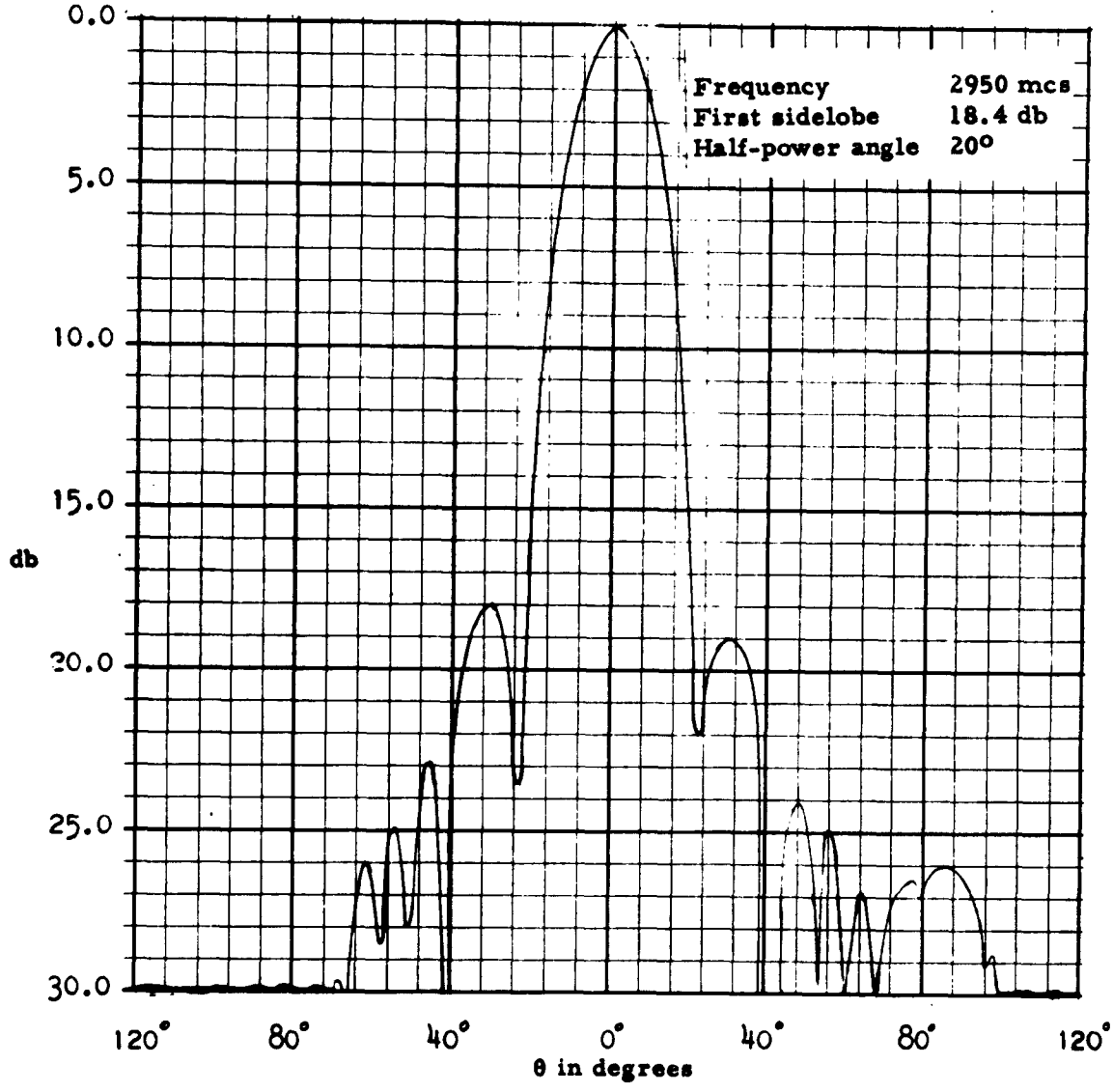

FIGURE 42. Replotted radiation pattern for δ of array given in Figure 27.

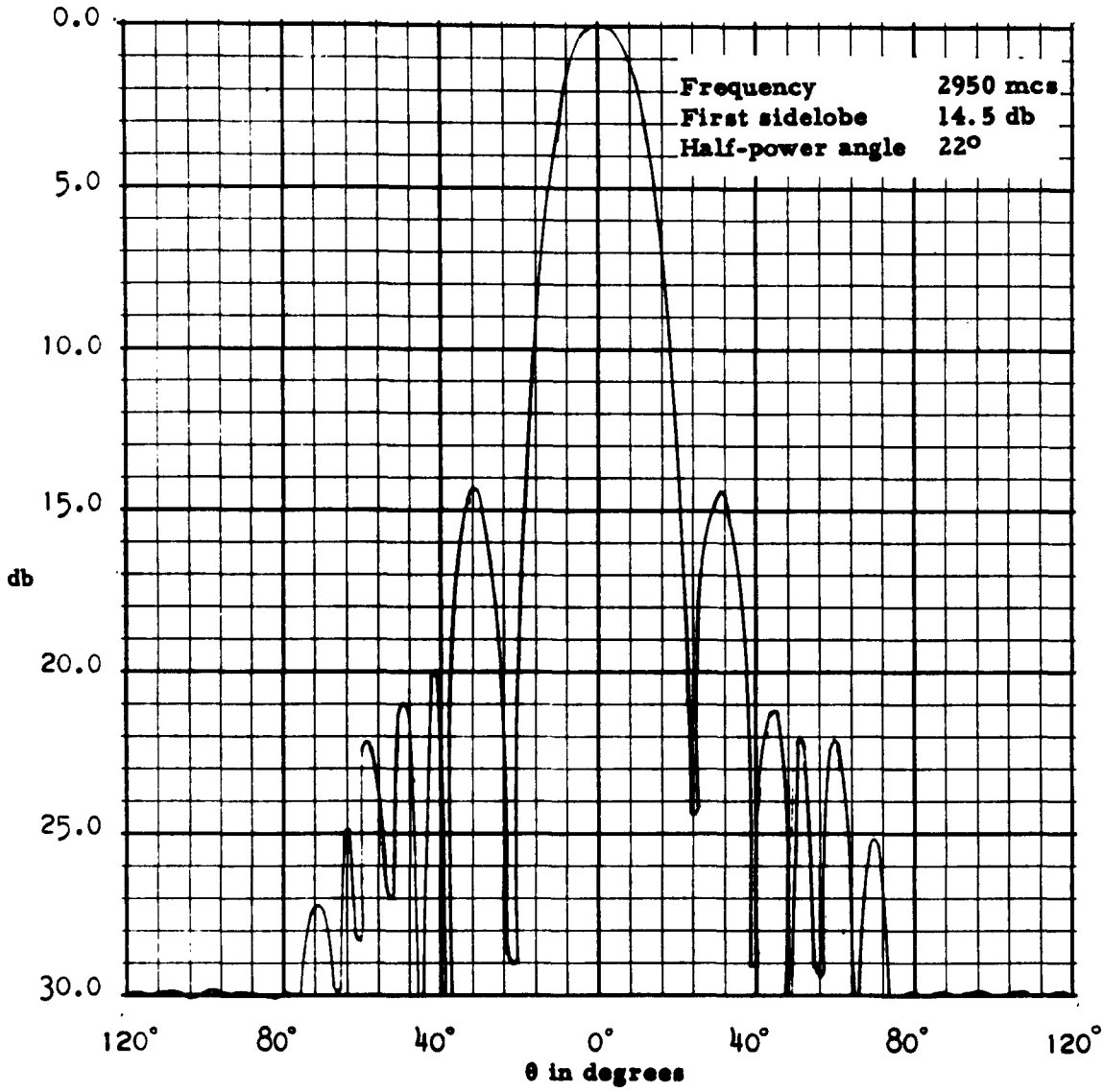

FIGURE 43. **Replotted radiation pattern for δ of array given in Figure 27.**

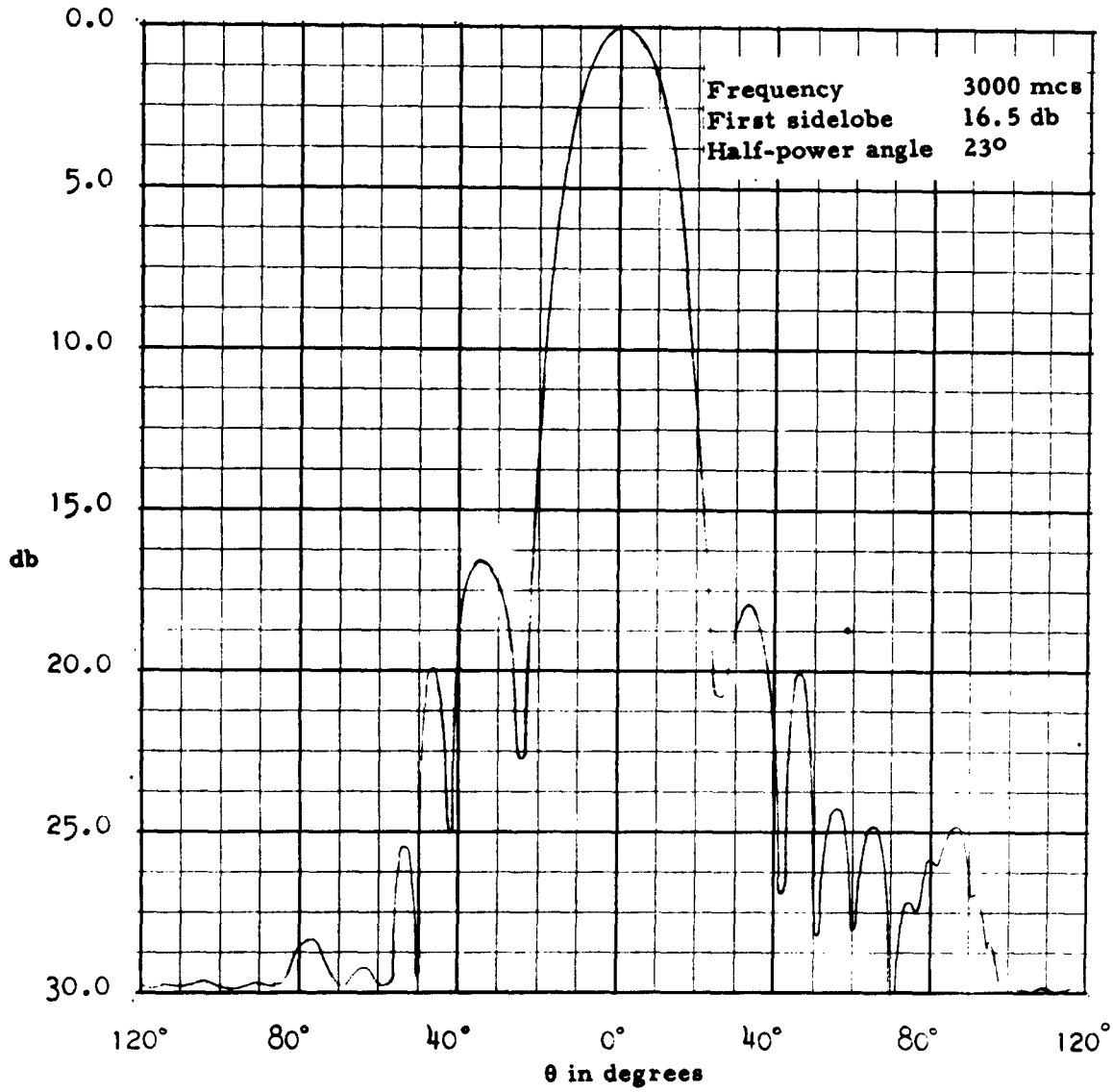

FIGURE 44. Replotted radiation pattern for δ of array given in Figure 27.

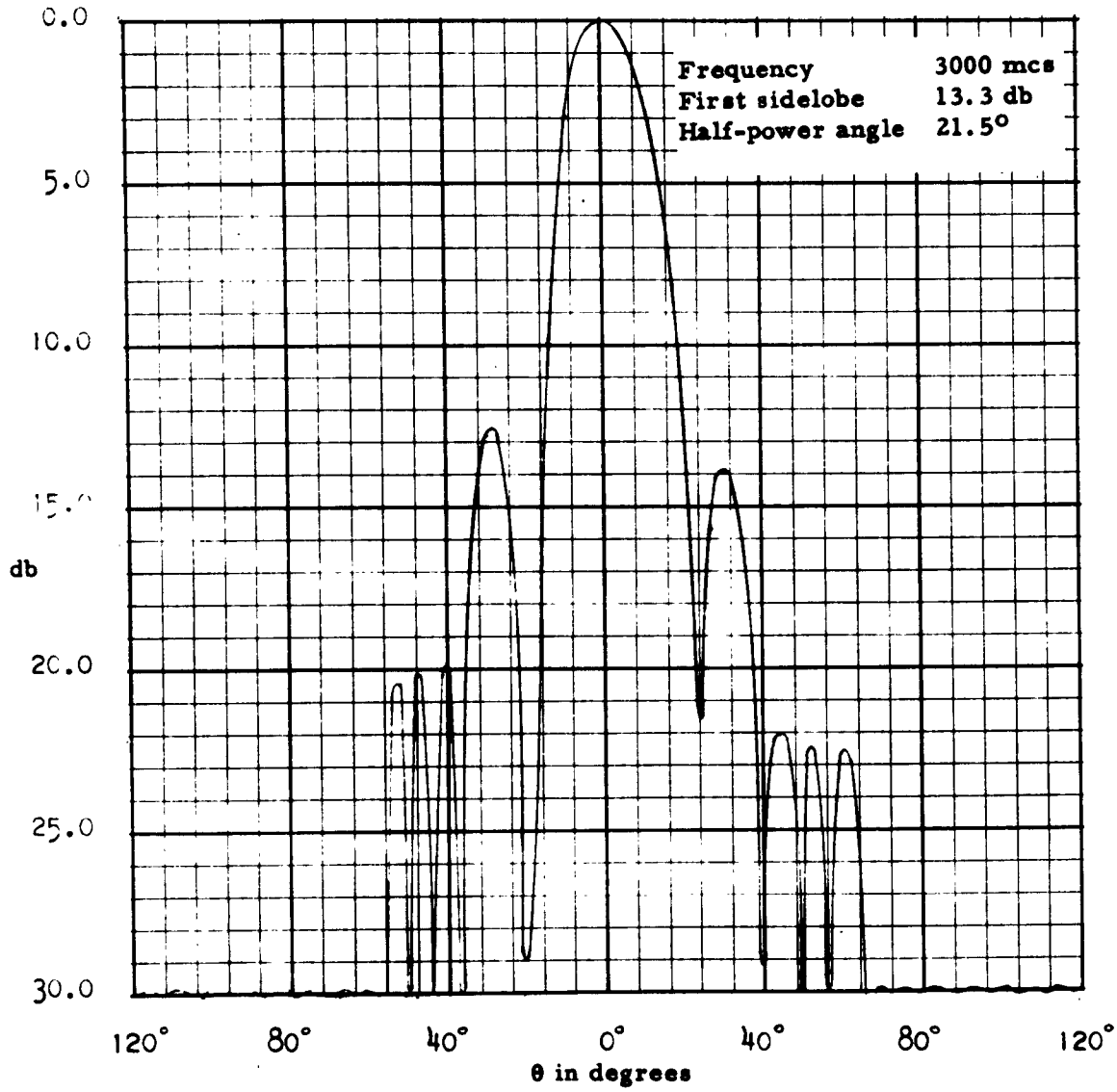

FIGURE 45. **Replotted radiation pattern for δ of array given in Figure 27.**

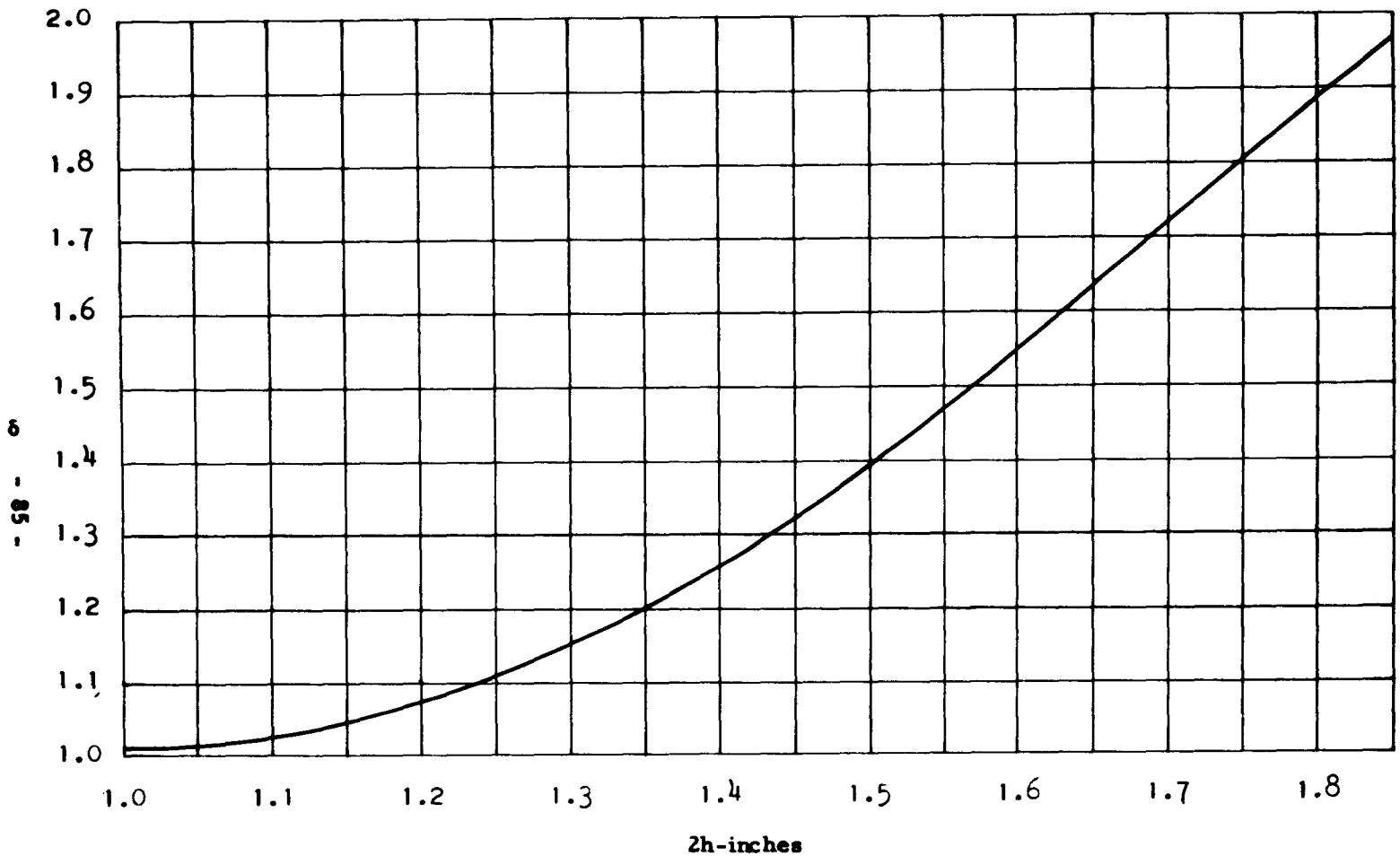

FIGURE 46. δ vs element length in inches, for spacing of 0.49 inches center to center.

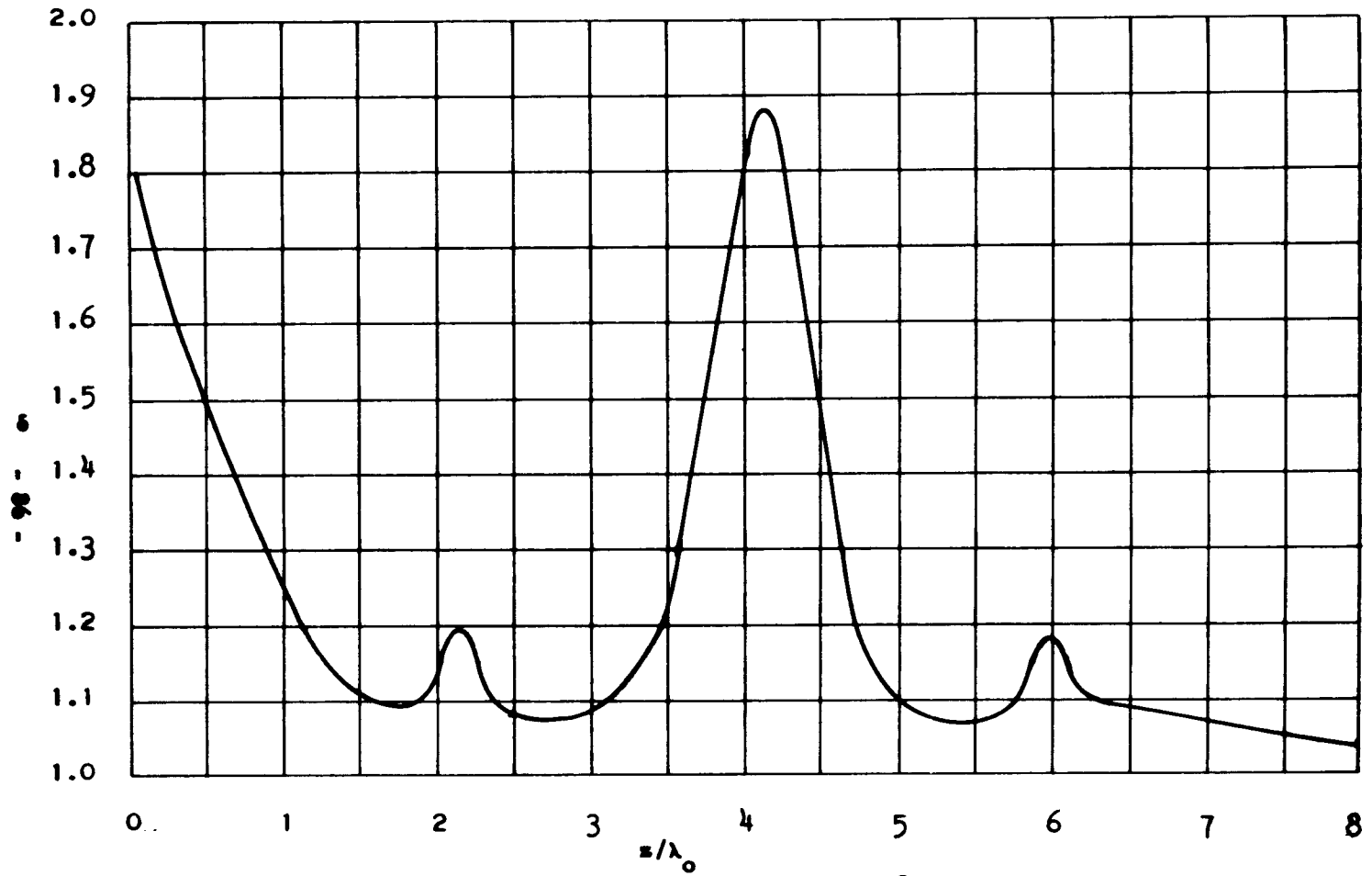

FIGURE 47. Relative wave number vs distance for 8λ csc^{2}θ array.

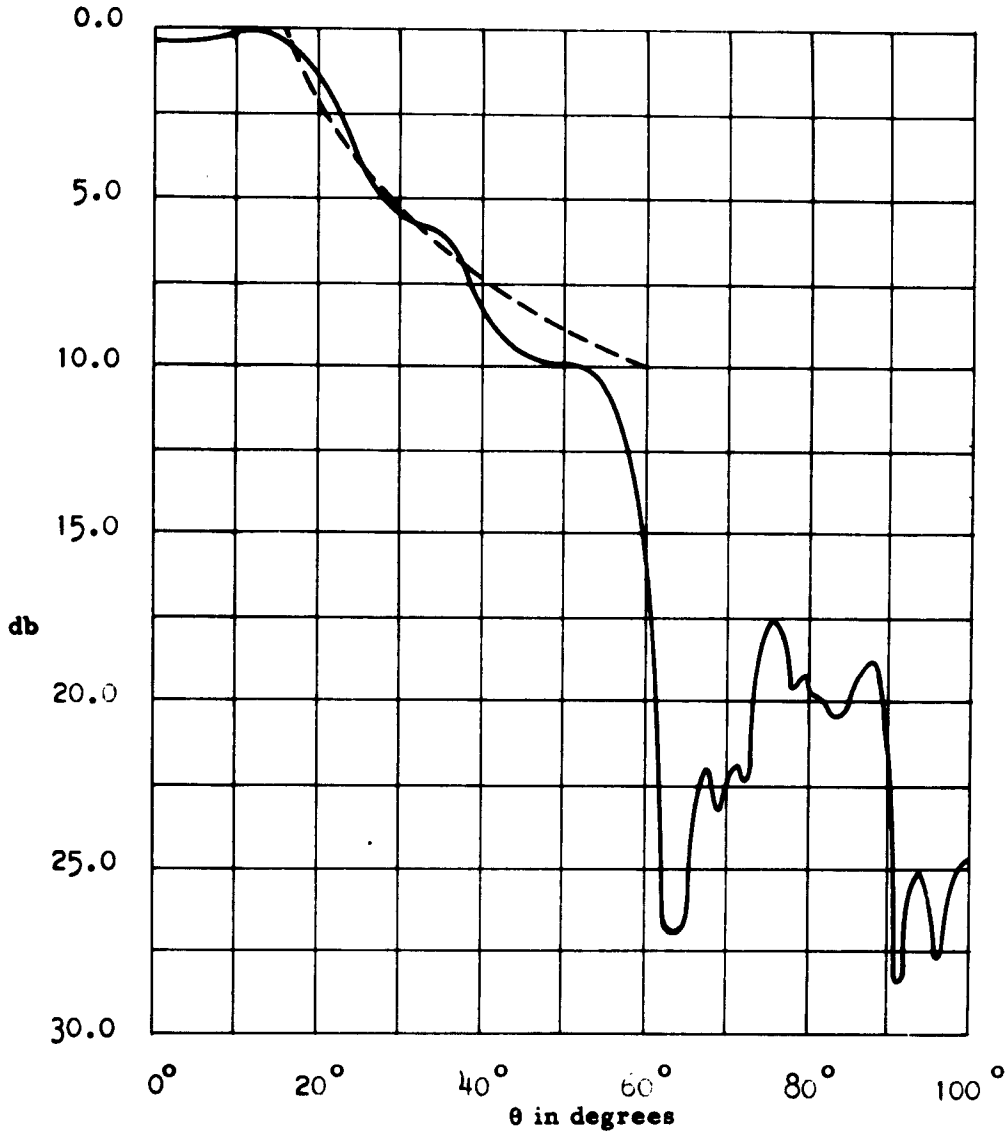

FIGURE 48. Replotted radiation pattern for array designed according to Figure 47.

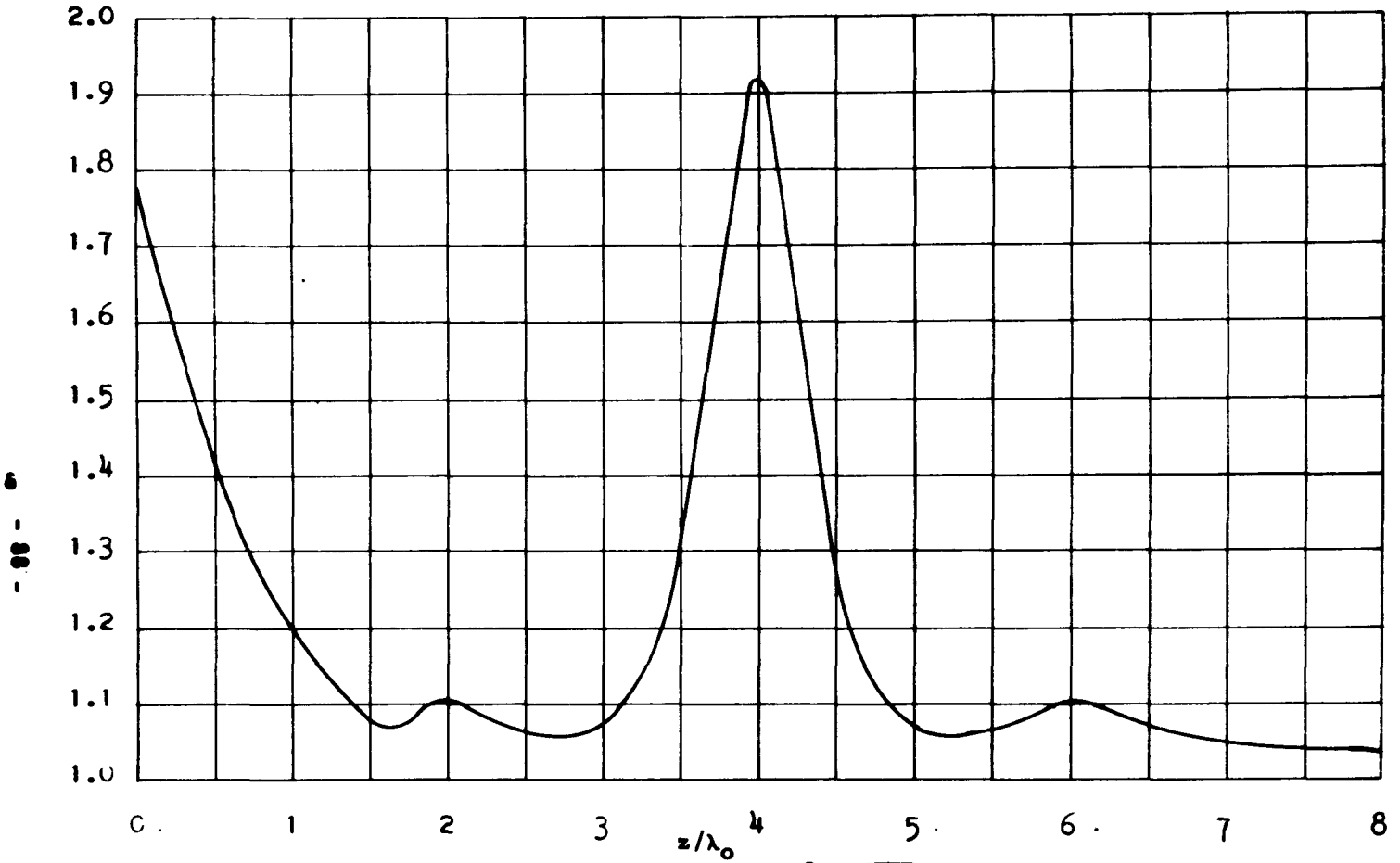

FIGURE 49. Relative wave vs distance for $8\lambda \csc^2\theta \sqrt{\cot\theta}$ array.

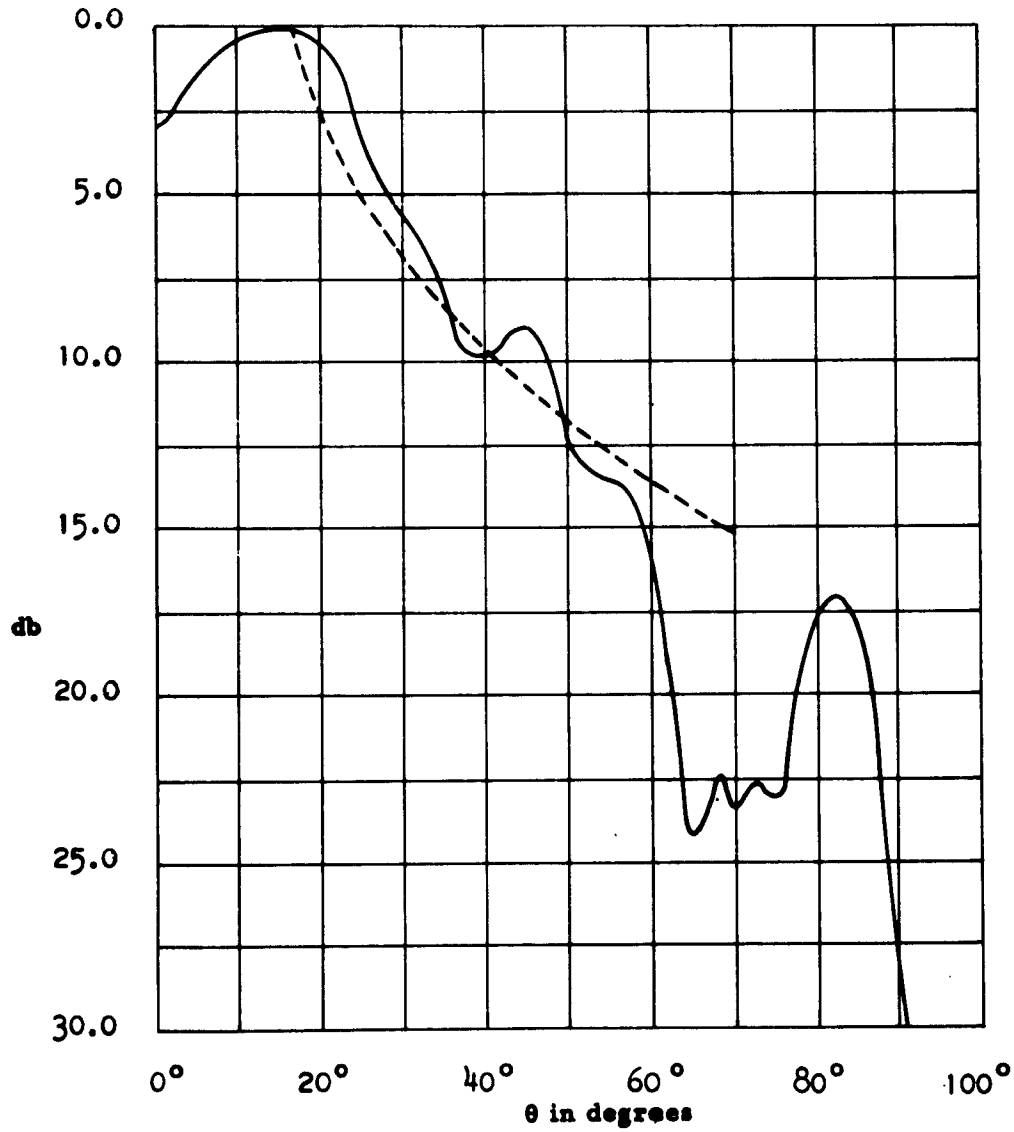

FIGURE 50. **Replotted radiation pattern for array designed according to Figure 49.**

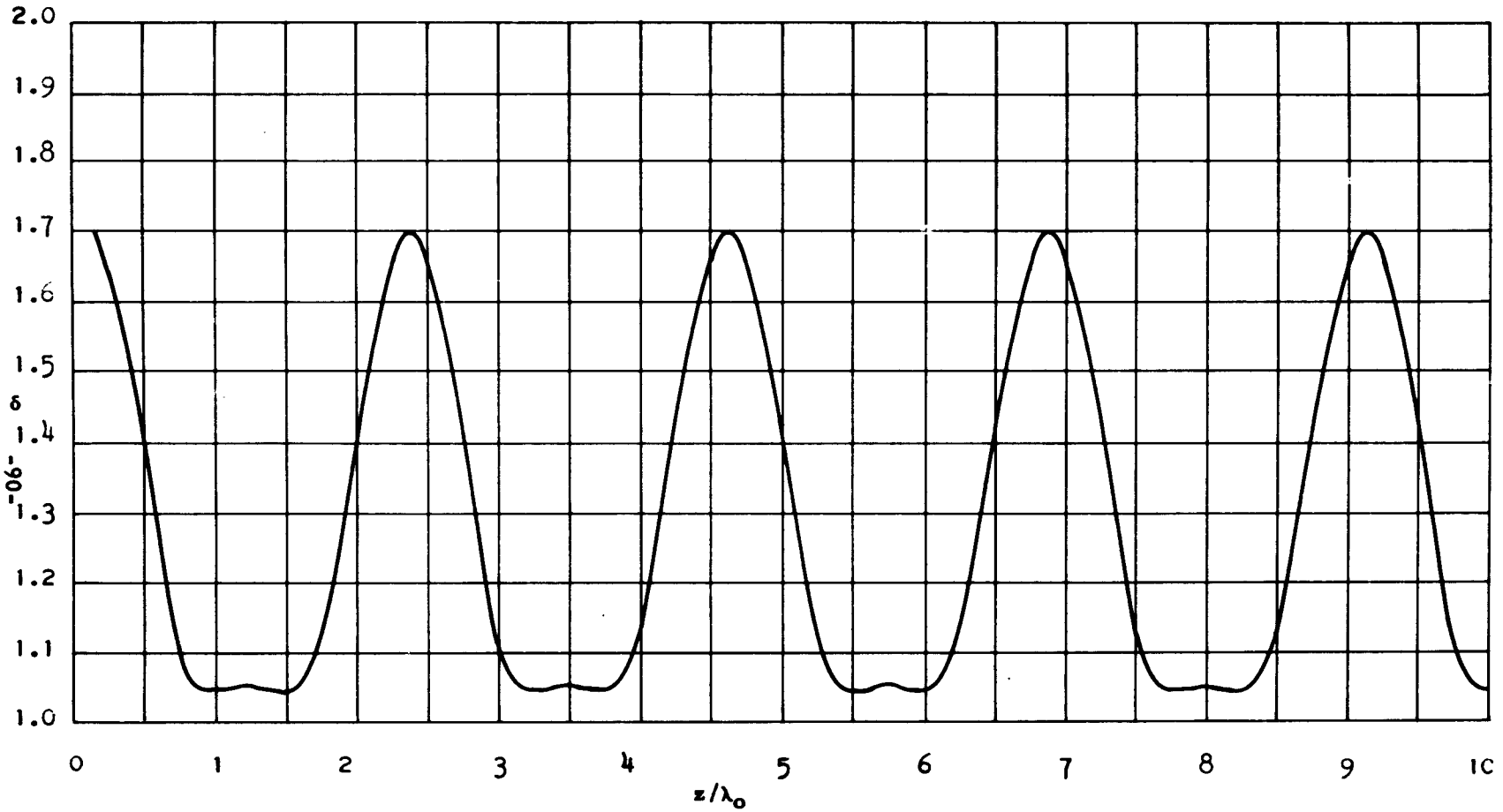

FIGURE 51. Relative wave number vs distance for 10λ array.

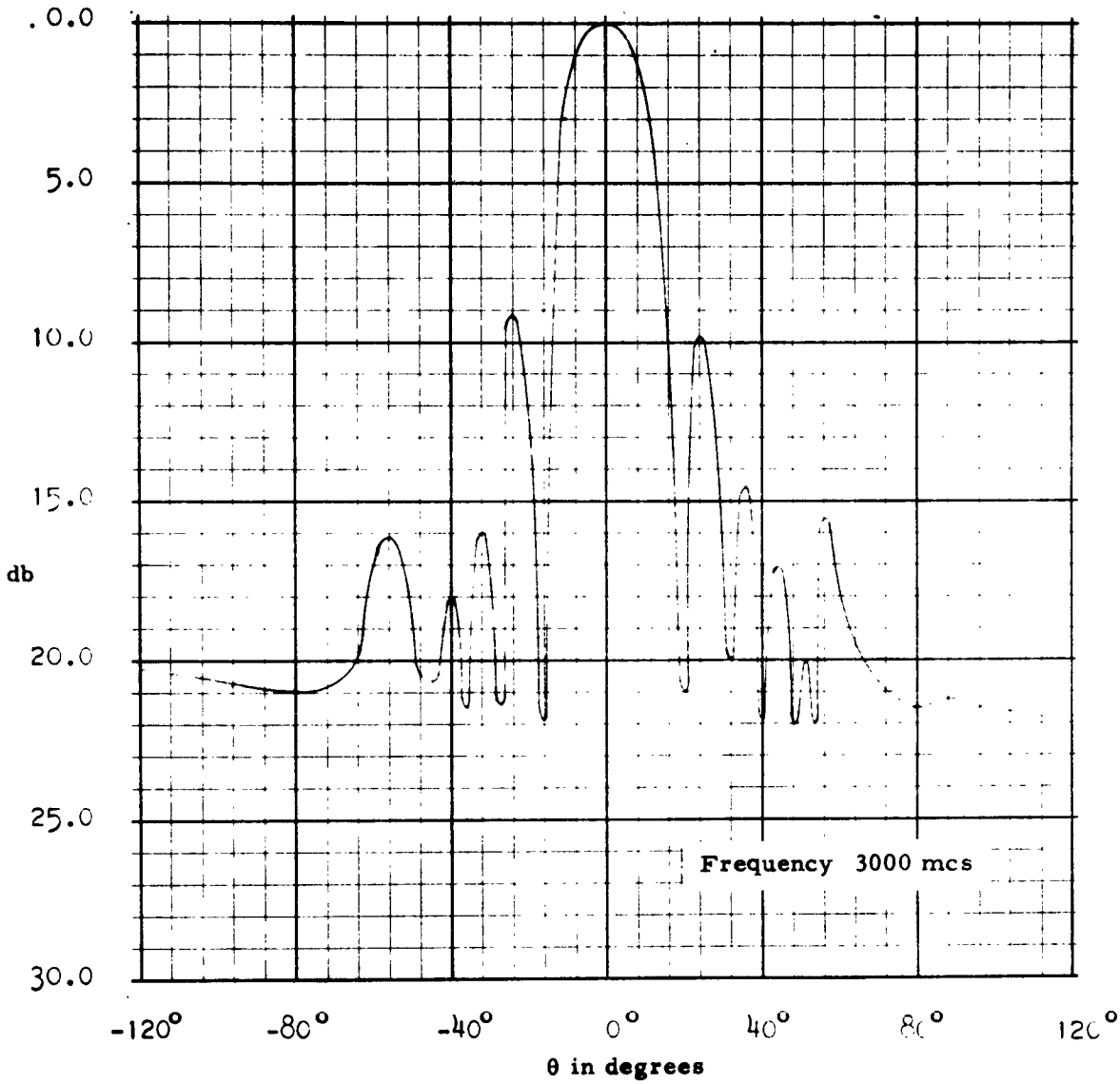

FIGURE 52. Replotted radiation pattern for distribution of Figure 51.

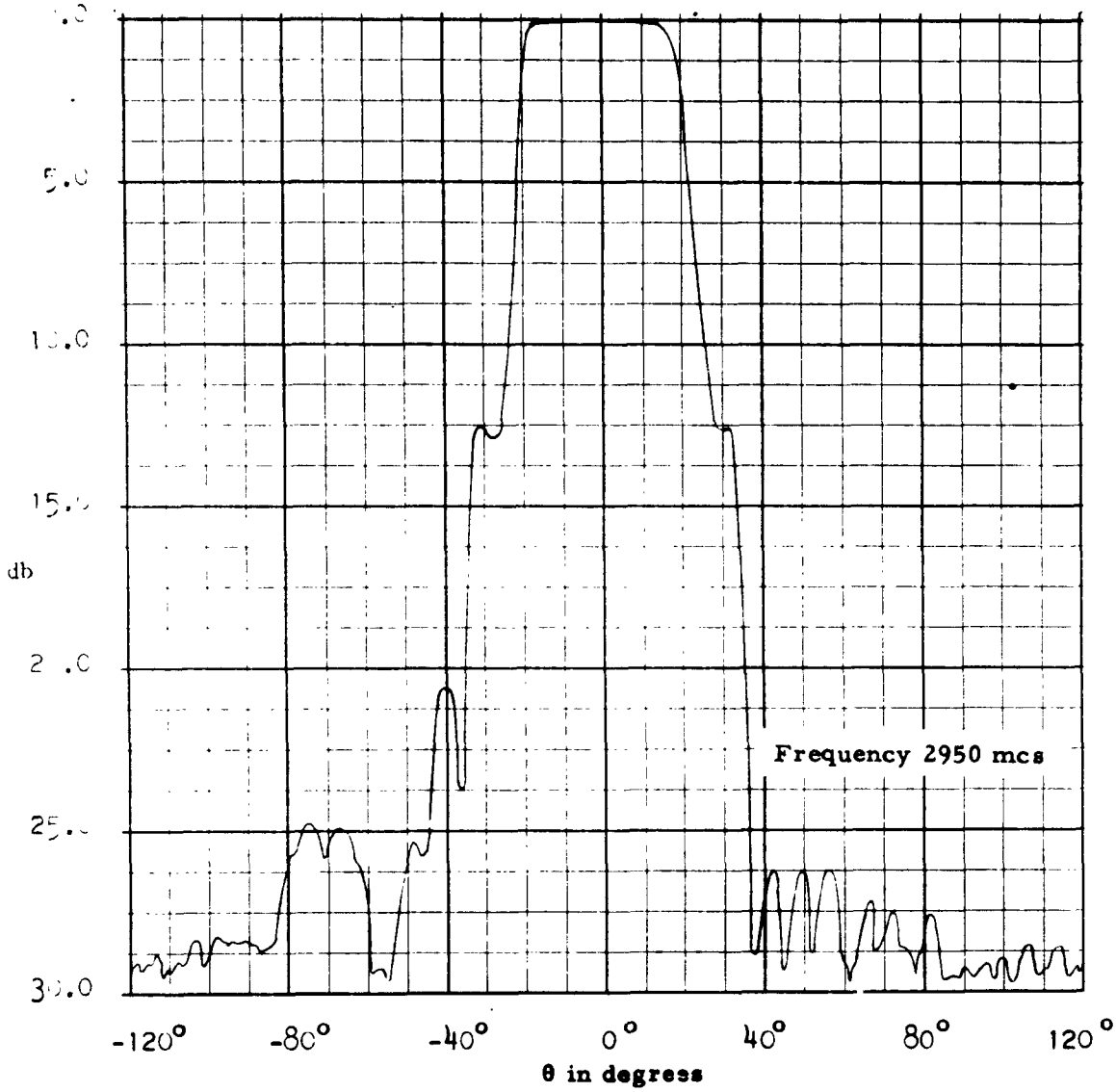

FIGURE 53. Replotted radiation pattern for distribution of Figure 51.

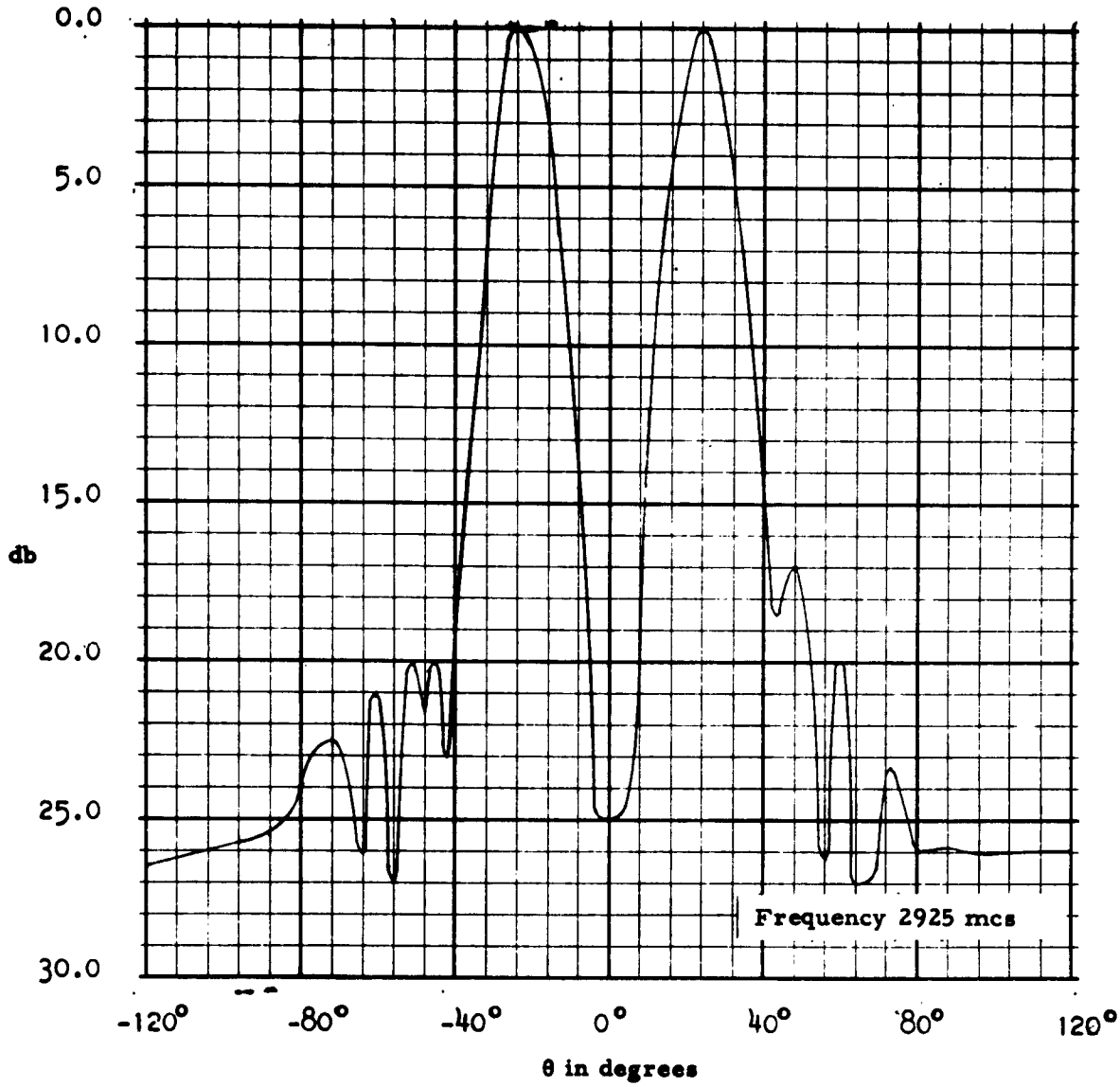

FIGURE 54. Replotted radiation pattern for distribution of Figure 51.

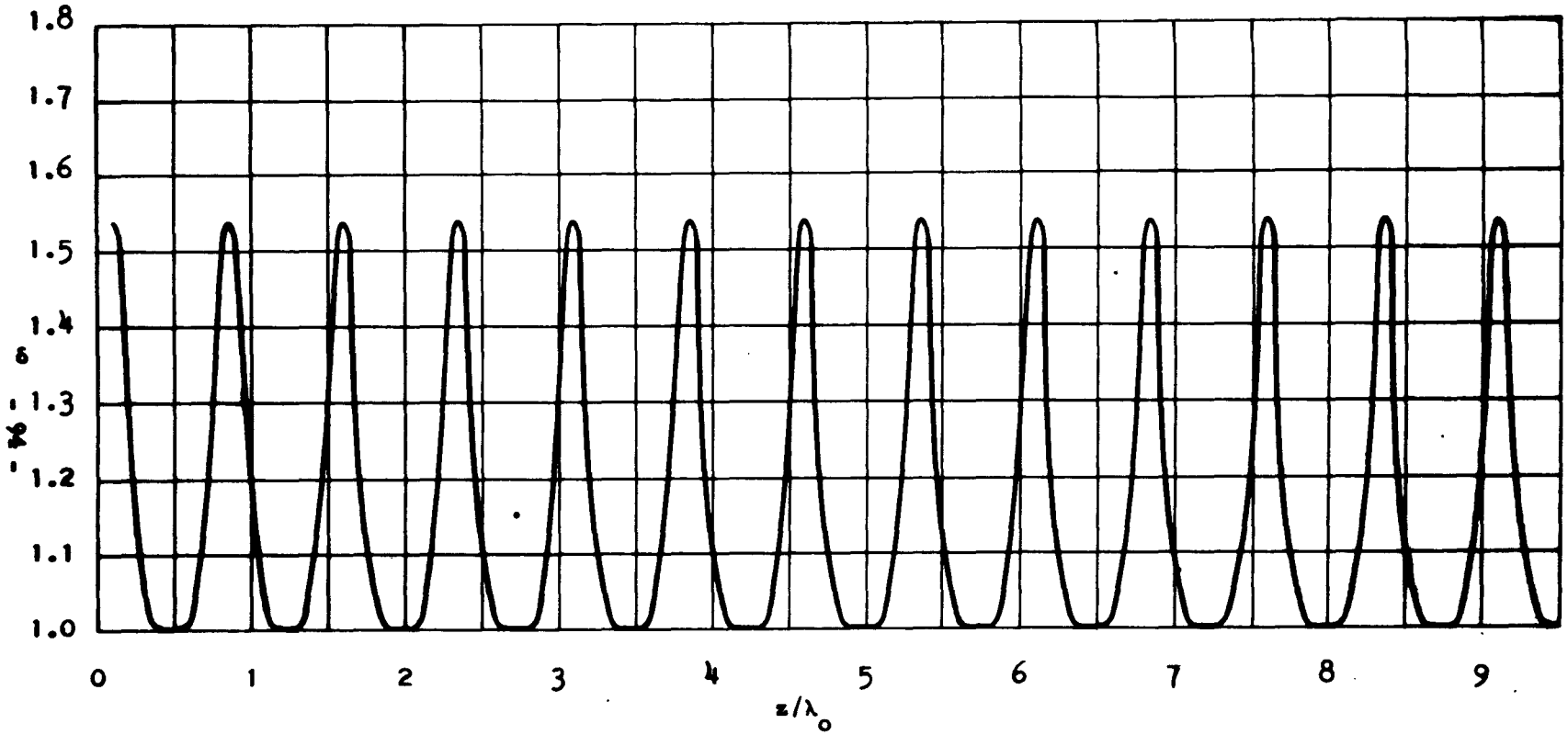

FIGURE 55. Relative wave number vs distance for beam at arbitrary angle array.

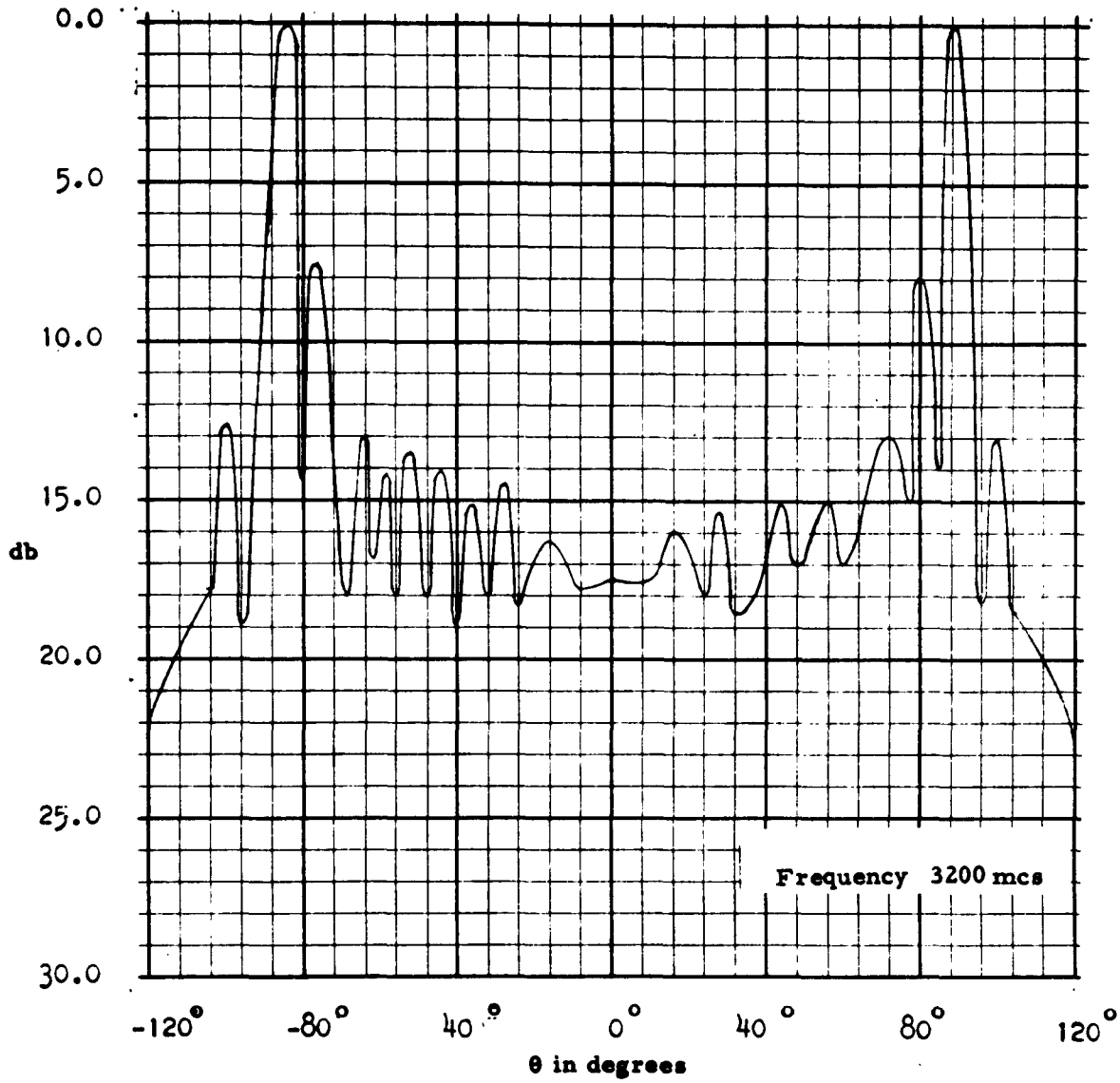

FIGURE 56. **Replotted radiation pattern for distribution of Figure 55.**

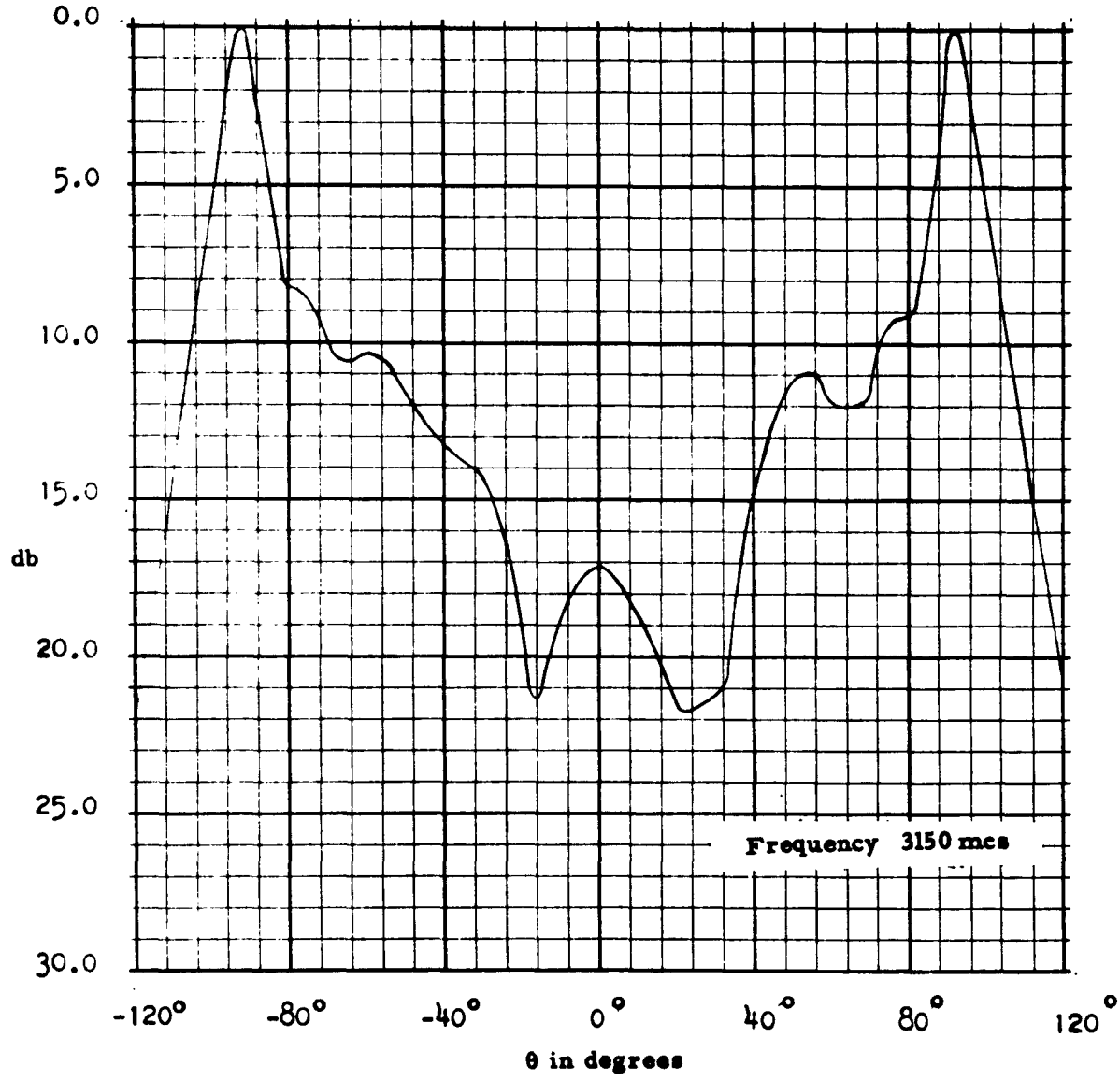

FIGURE 57. Replotted radiation pattern for distribution of Figure 55.

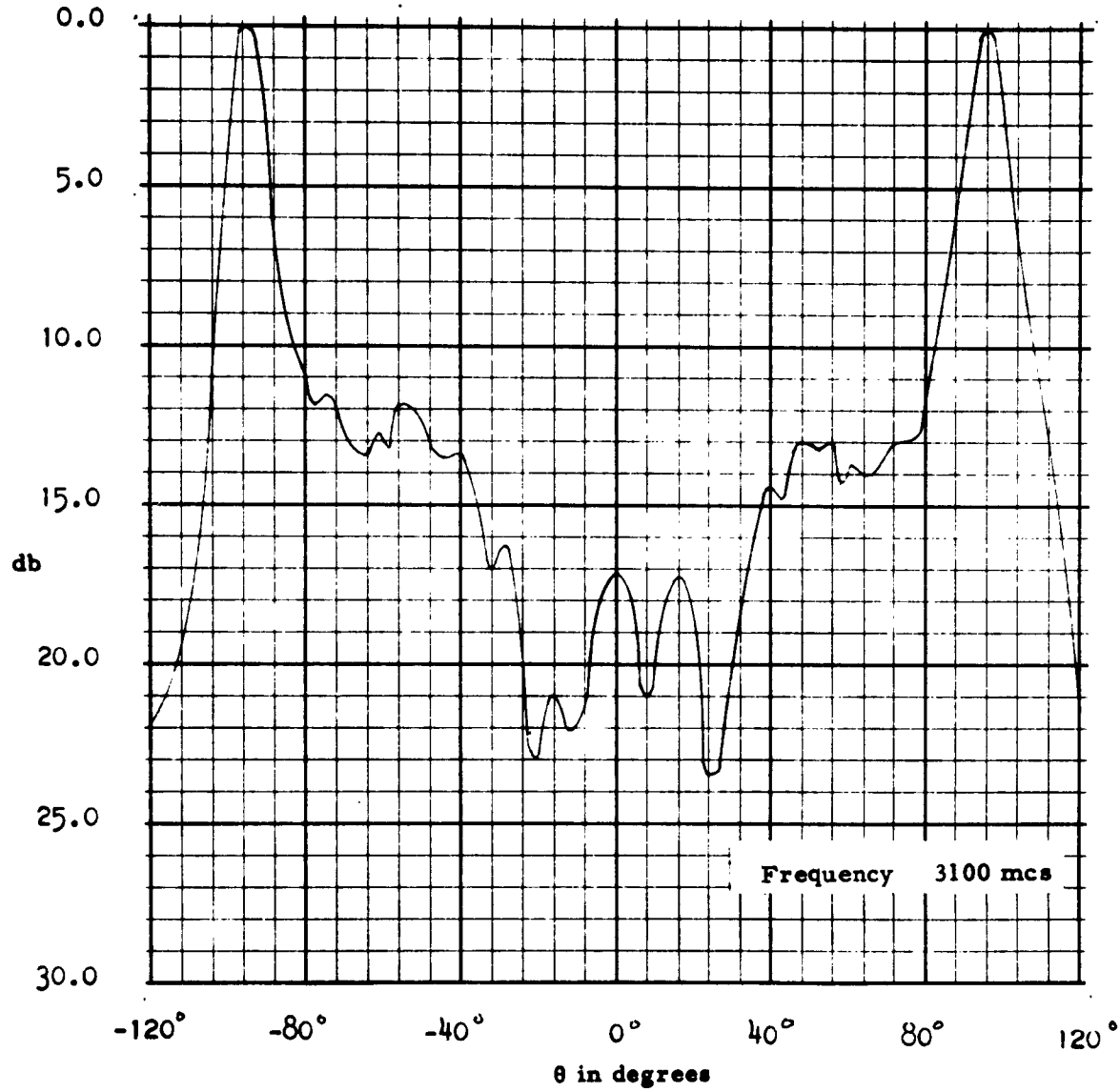

FIGURE 58. **Replotted radiation pattern for distribution of Figure 55.**

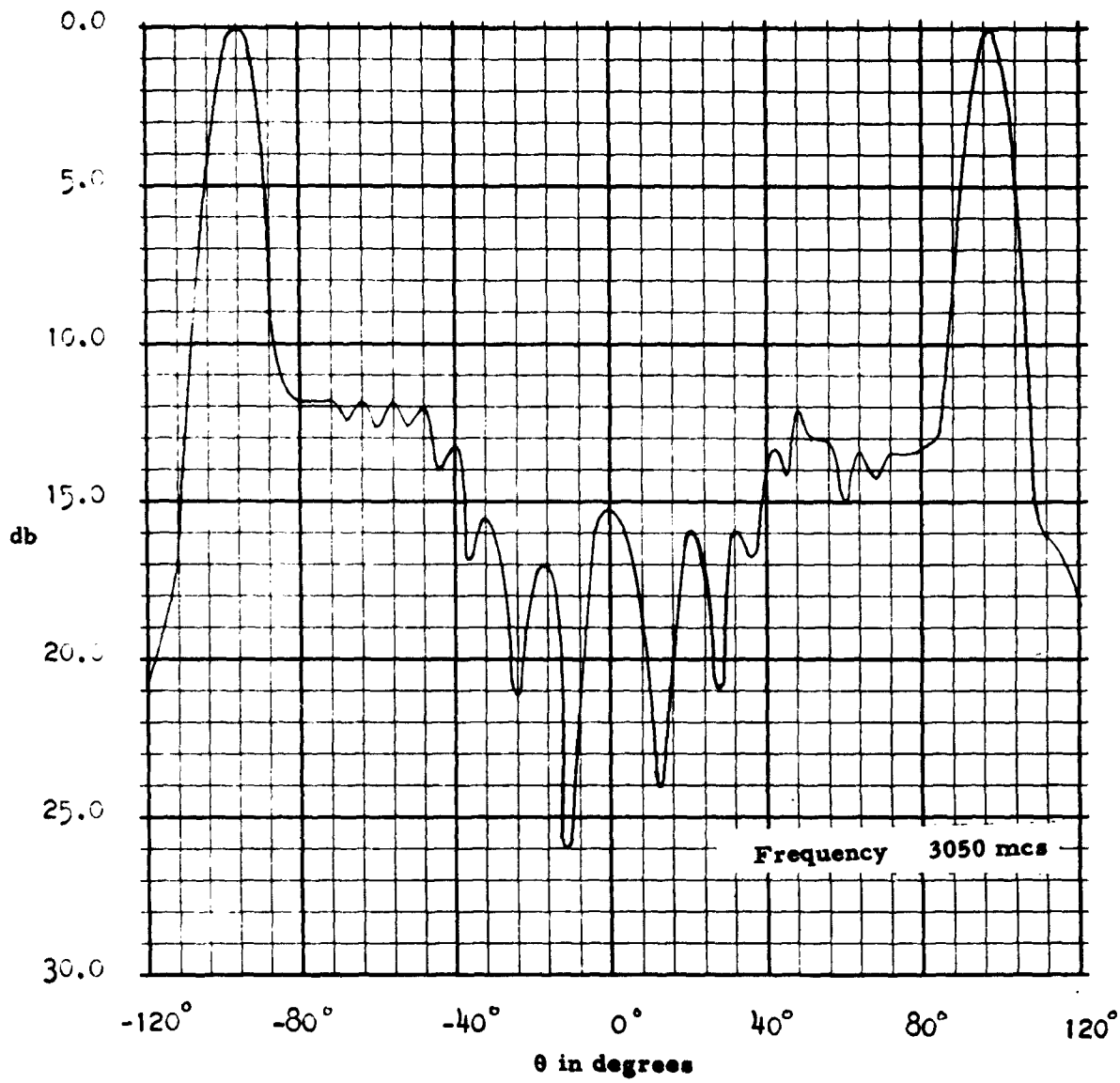

FIGURE 59. **Replotted radiation pattern for distribution of Figure 55.**

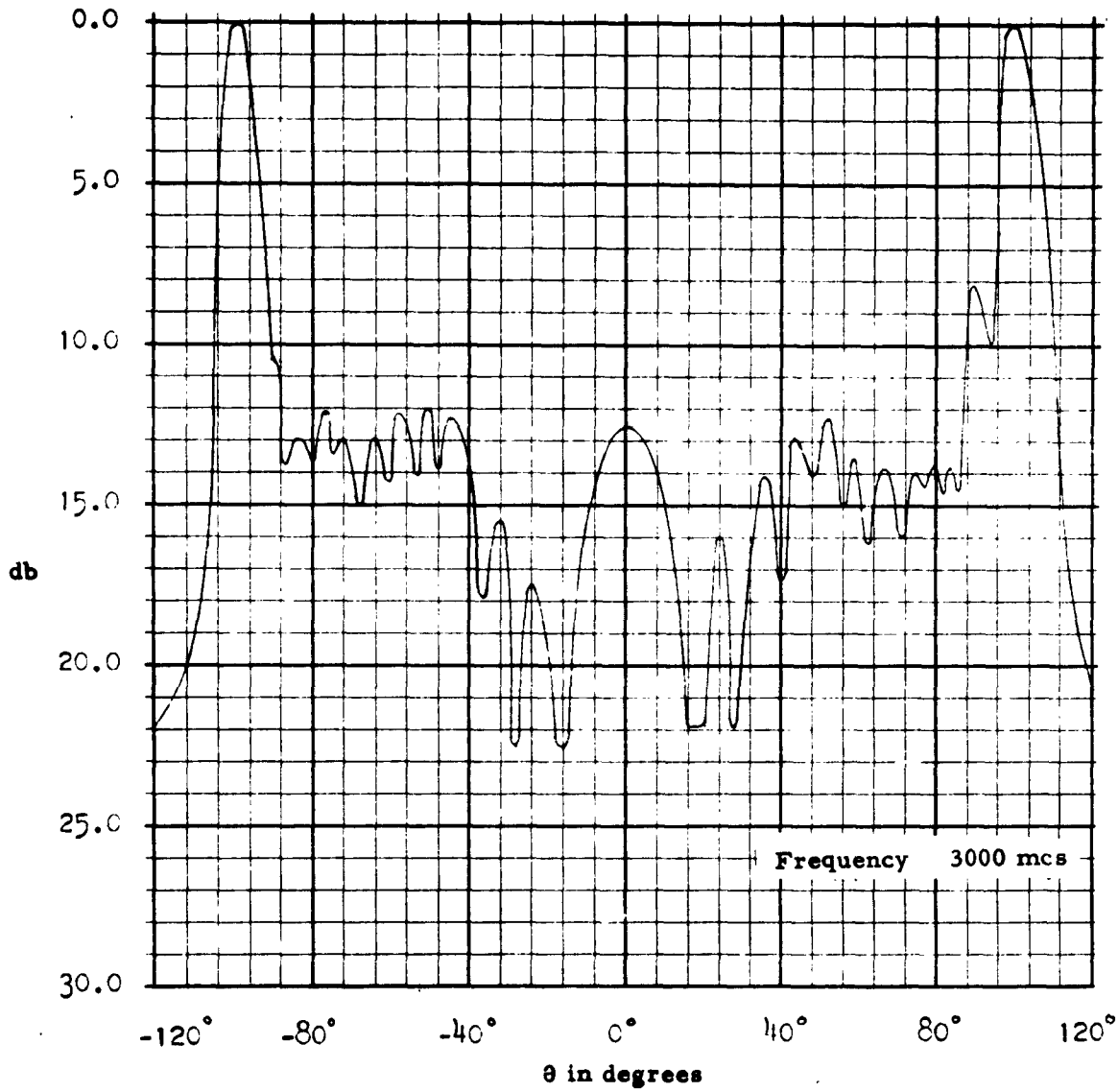

FIGURE 60. **Replotted radiation pattern for distribution of Figure 55.**

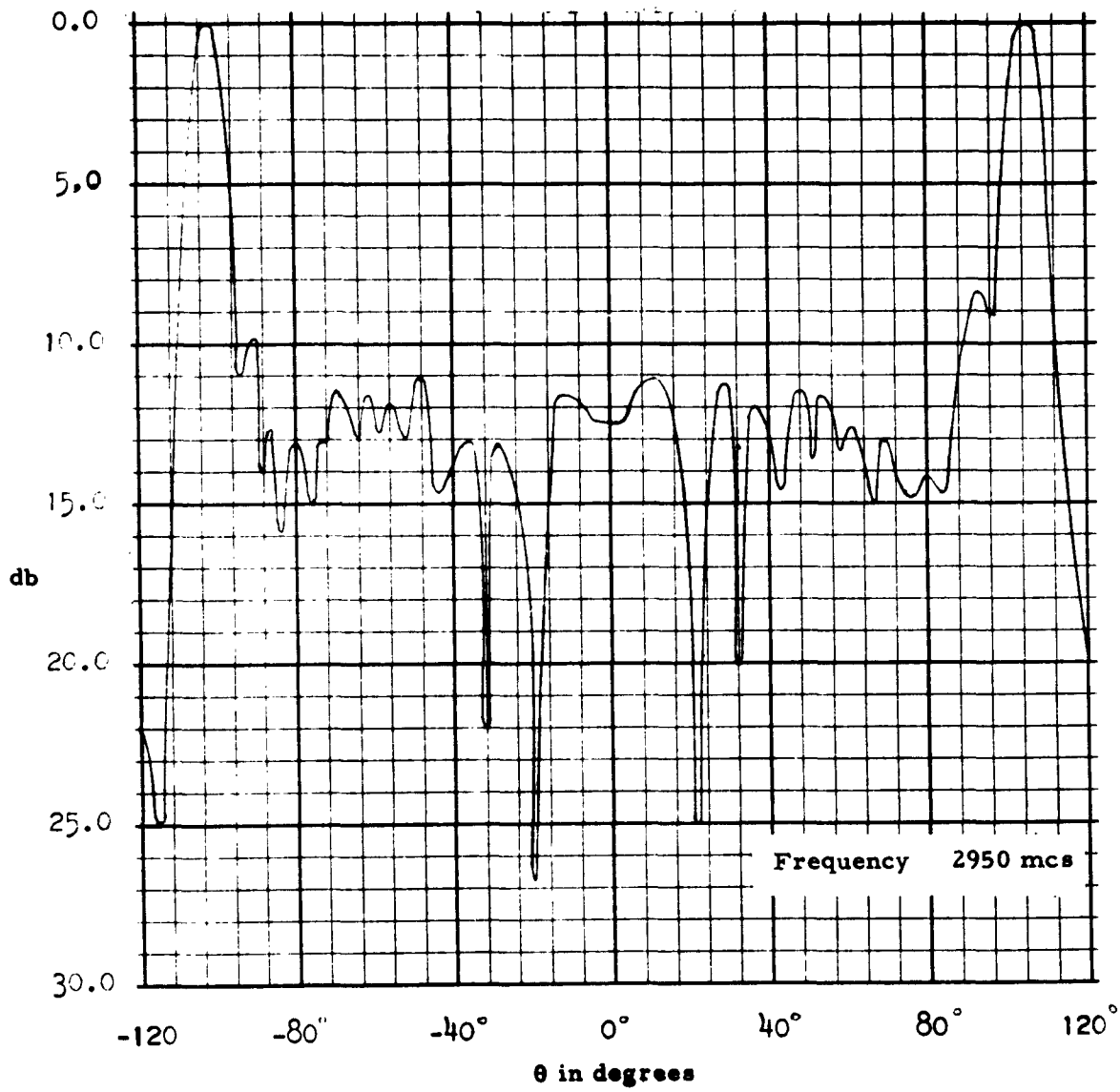

FIGURE 61. Replotted radiation pattern for distribution of Figure 55.

MASTER DISTRIBUTION LIST FOR ANTENNA LABORATORY

Note: One copy unless otherwise designated

Code	Organization
AF29	APGC (PGAPI) Eglin AFB, Florida
AF143	RADC (RCE) Attn: Dr. John S. Burgess Griffiss AFB, New York
AF69	Director of Resident Training 3380th Technical Training Grp. Keesler AFB, Mississippi Attn: OA-3011 Course
AF5	AF Missile Test Center Patrick AFB, Florida Attn: AFMTC, Tech. Library, MU-135
AF253	Technical Information Office European Office, Aerospace Res. Shell Building, 47 Cantersteen Brussels, Belgium
AF166	Hq. USAF (AFOAC-S/E) Communications-Electronics Directorate, Washington 25, D. C.
AF43	ASD (ASAPRD - Dist) Wright-Patterson AFB, Ohio
AF68	ASD (ASRNRE-3) Attn: Mr. Paul Springer Wright-Patterson AFB, Ohio
AF308	WADD (WWDRTR, Mr. A.D.Clark) Directorate of System Engr. Dyna Soar Engineering Office Wright-Patterson AFB, Ohio
Ar3	Director Evans Signal Laboratory Belmar, New Jersey Attn: Mr. O. C. Woodyard
AF124	RADC (RAALD) Attn: Documents Library Griffiss AFB, New York
AF139	AF Missile Dev. Center (MDGRT) Holloman AFB, New Mexico
AF86	SAC (Operations Analysis Office) Offutt AFB, Nebraska
AF18	AUL Maxwell AFB, Alabama
AF227	USAF Security Service (CLR) San Antonio, Texas
AF32	OAR (RROS), Col. John R. Fowler) Tempo D 4th and Independence Avenue Washington 25, D. C.
AF314	Hq. OAR (RROSP, Maj. Richard W. Nelson) Tempo D, 4th and Independence Ave. Washington 25, D. C.
AF63	WADD (WCLRSA, Mr. Portune) Wright-Patterson AFB, Ohio
AF231	Foreign Technology Division (TDEE) Wright-Patterson AFB, Ohio
AF348	Lt. Col. Jensen (SSRTW) Space Systems Division Air Force Unit Post Office Los Angeles 45, California
Ar5	Commanding General, USASRDL Ft. Monmouth, New Jersey Attn:Tech. Doc. Ctr. SIGRA/SL-ADT

Code	Organization
Ar9	Department of the Army Office of the Chief Signal Officer Washington 25, D. C. Attn: SIGRD-4a-2
Ar39	Commanding General USASRDL Fort Monmouth, New Jersey Attn: Mr. F. J. Triola
Ar42	Director U.S. Army Ordnance Ballistic Research Lab. Aberdeen Proving Ground, Md. Attn: Ballistic Measurements Lab.
Ar48	Guided Missile Fuze Library Diamond Ordnance Fuze Lab. Washington 25, D. C. Attn: R. D. Hatcher, Chief Microwave Develop. Section
Ar67	Redstone Scientific Infor. Center U.S. Army Missile Command Redstone Arsenal, Alabama (5 copies)
G2	ASTIA (TIPAA) Arlington Hall Station Arlington 12, Virginia (10 copies)
G68	Scientific and Tech. Infor. Facility Attn: NASA Representative (S-AK/DL) Post Office Box 5700 Bethesda, Maryland
Ar10	Mass. Institute of Technology Signal Corps Liaison Officer Cambridge 39, Massachusetts Attn: A. D. Bedrosian, Rm. 26-131
Ar41	Office of Chief Signal Officer Engineering + Technical Division Washington 25, D. C. Attn: SIGNET-5
Ar47	Ballistic Research Laboratories Aberdeen Proving Ground, Md. Attn: Tech. Information Branch
Ar49	Commanding General USASRDL Fort Monmouth, New Jersey Attn: SIGFM/EL-AT
Ar78	Commanding General, SIGFM/EL-PC USASRDL Fort Monmouth, New Jersey Attn: Dr. Horst H. Kedesdy Deputy Chief, Chem.-Physics Br.
G8	Library National Bureau of Standards Boulder Laboratories Boulder, Colorado (2 copies)
G27	National Bureau of Standards U.S. Department of Commerce Washington 25, D. C. Attn: Gustave Shapiro (Chief Engineering Electronics Section Electricity + Electronics Div.

Code	Organization
G31	Office of Scientific Intelligence Central Intelligence Agency 2430 E. Street, N.W. Washington 25, D. C.
G103	National Aeronautical Space Agcy. Langley Aeronautical Res. Lab. Langley, Virginia Attn: Mr. Cliff Nelson
M17	AFCRL, Office of Aerospace Research (CRRD) Attn: Contract Files L.G. Hanscom Field Bedford, Massachusetts (2 copies)
	AFCRL, Office of Aerospace Research (CRRD) Attn: Carlyle J. Sletten L.G. Hanscom Field Bedford, Massachusetts (3 copies)
M84	Hq. AFCRL, OAR (CRXR, J.R. Marple) L.G. Hanscom Field Bedford, Massachusetts
N9	Chief, Bureau of Naval Weapons Department of the Navy Washington 25, D. C. Attn: DLI-31 (2 copies)
N23	U.S. Naval Ordnance Laboratory White Oak, Silver Spring 19, Md. Attn: The Library
N27	Librarian U.S. Naval Postgraduate School Monterey, California
G75	Director National Security Agency Fort George G. Meade, Md. Attn: C3/TDL
M6	AFCRL, OAR (CRXRA-Stop 39) L.G. Hanscom Field Bedford, Massachusetts (10 copies)
M54	Hq. ESD (ESRDW, Major John J. Hobson) L.G. Hanscom Field Bedford, Massachusetts
M59	Electronic Systems Division (AFSC) Tech. Infor. Services Div. (ESAT) L.G. Hanscom Field Bedford, Massachusetts
N3	Chief, Bureau of Ships Department of the Navy Washington 25, D. C. Attn: Code 690
N16	Commander U.S. Naval Air Missile Test Center Point Mugu, California Attn: Code 366
N26	Commander U.S. Naval Ordnance Test Station China Lake, California Attn: Code 753
G9	Defense Research Member Canadian Joint Staff 2450 Mass. Avenue, N.W. Washington 8, D. C.

Code	Organization
G126	National Aeronautics and Sp. Administration Attn: Antenna Systems Br. Goddard Space Flight Center Greenbelt, Maryland
N30	Dr. J.I. Bohnert, Code 5210 U.S. Naval Research Lab. Washington 25, D. C.
N37	Chief of Naval Research Department of the Navy Washington 25, D. C. Attn: Code 427
N73	Office of Naval Research Branch Office, London Navy 100, Box 39 F.P.O. New York, N.Y. (10 copies)
N91	Commander U.S. Naval Air Test Ctr. Patuxent River, Md. Attn: ET-315, Antenna Br.
N93	Commanding Officer U.S. Naval Ordnance Lab. Corona, California Attn: Documents Lib.
N141	AFSC Scientific and Tech. Liaison Office c/o Department of the Navy Room 2305, Munitions Bldg. Washington 25, D. C.
N29	Director U.S. Naval Research Lab. Washington 25, D. C. Attn: Code 2027 (2 copies)
N35	Commanding Officer and Dir. U.S. Navy Underwater Sound Lab. Fort Trumbull, New London, Connecticut
N48	Commanding Officer U.S. Naval Air Development Ctr. Johnsville, Pennsylvania Attn: NADC Library
N85	Commanding Officer and Dir. U.S. Navy Electr. Lab., (Library) San Diego 52, California
N92	Material Laboratory, Code 932 New York Naval Shipyard Brooklyn 1, New York Attn: Mr. Douglas First
N123	Chief, Bureau of Ships Department of the Navy Washington 25, D. C. Attn: Code 817B
I601	Aero Geo Astro Corp. 1200 Duke Street Alexandria, Virginia Attn: Library

Code	Organization
I940	Aerospace Corp. Box 95085 Los Angeles 45, Calif. Attn: Library
I388	Aircom, Inc. 48 Cummington Street Boston, Massachusetts
I21	Aerospace Corp. Satellite Control Attn: Mr. R.C. Hansen Post Office Box 95085 Los Angeles 45, Calif.
I205	Battelle Memorial Institute 505 King Avenue Columbus 1, Ohio Attn: Wayne E. Rife Project Leader Elec. Engr. Div.
I469	Bell Telephone Lab. Murray Hill New Jersey
I246	Bendix Pacific Division 11600 Sherman Way North Hollywood, Calif. Attn: Engineering Library
I248	Bjorksten Res. Labs, Inc. P.O. Box 265 Madison, Wisconsin Attn: Librarian
I1	Airborne Instruments Lab., Inc. Division of Cutler Hammer Walt Whitman Road Melville, L.I. New York Attn: Library
I3	Andrew Alford, Consulting, Engr. 299 Atlantic Avenue Boston 10, Massachusetts
I374	ACF Electronics Division Bladensburg Plant 52nd Avenue + Jackson Street Bladensburg, Maryland Attn: Librarian
I8	Bell Aircraft Corporation Post Office Box One Buffalo 5, New York Attn: Eunice P. Hazelton, Librarian
I13	Bell Telephone Laboratories, Inc. Technical Information Library Whippany Laboratory Whippany, New Jersey Attn: Technical Reports Librarian
I247	Bendix Radio Division Bendix Aviation Corporation E. Joppa Road Towson 4, Maryland Attn: Dr. D.M. Allison, Jr. Director Engineering + Research
I249	Boeing Airplane Company Pilotless Aircraft Division P.O. Box 3707 Seattle 24, Washington Attn: R.R. Barber, Lib. Supervisor (2 copies)

Code	Organization	Code	Organization
I250	Boeing Company 3801 S. Oliver Street Wichita 1, Kansas Attn: Kenneth C. Knight Library Supervisor	I252	Brush Beryllium Company 4301 Perkins Avenue Cleveland 3, Ohio Attn: N.W. Bass
I253	Chance Vought Corp. 9314 W. Jefferson Blvd. Dallas, Texas Attn: A.D. Pattullo, Lib.	I986	Chance Vought Corporation Vought Electronics Div. P.O. Box 5907 Dallas 22, Texas
I470	Chu Associates P.O. Box 387 Whitcomb Avenue Littleton, Massachusetts	I918	Collins Radio Co. 855 35th Street, N.E. Cedar Rapids, Iowa Attn: Dr. R.L. McCreary
I126	Convair, A Division of General Dynamics Corp. Fort Worth, Texas Attn: K.G. Brown Division Res. Librarian	I254	Convair, A Division of General Dynamics Corp. 3165 Pacific Highway San Diego 12, California Attn: Mrs. Dora B. Burke, Engr. Lib.
I25	Cornell Aeronautical Lab, Inc 4455 Genesee Street Buffalo 21, New York Attn: Librarian	I255	Dalmo Victor Company A Division of Textron, Inc. 1515 Industrial Way Belmont, California Attn: Mary Ellen Addoms, Tech. Lib.
I28	Dorne and Margolin, Inc. 29 New York Avenue Westbury, Long Island, N.Y.	I257	Aircraft Division Douglas Aircraft Company, Inc. 3855 Lakewood Boulevard Long Beach, California (USA) Attn: Technical Library
I258	Douglas Aircraft Co., Inc. 3000 Ocean Park Blvd. Santa Monica, Calif. Attn: Peter Duyan, Jr. Chief, Elec./Electronics Section	I259	Douglas Aircraft Company, Inc. 2000 North Memorial Drive Tulsa, Oklahoma Attn: Engineering Librarian, D-250

Code	Organization
I187	Electromagnetic Res. Corp. 5001 College Avenue College Park, Maryland Attn: Mr. Martin Katzin
I299	Electronic Specialty Co. 5121 San Fernando Road Los Angeles 39, Calif. Attn: Donald L. Margerum Chief Engr. Radiating Systems Division
I262	Emerson Electric Mfg. Co. 8100 West Florissant Ave. St. Louis 21, Missouri Attn: Mr. E.R. Breslin, Librarian
I264	FAIRCHILD STRATOS CORP. Aircraft Missiles Division Hagerstown, Maryland Attn: Library
I4	Gabriel Electronics Div. Main and Pleasant Streets Millis, Massachusetts Attn: Dr. Edward Altshuler
I793	General Electric Company Missile and Space Vehicle Dept. 3198 Chestnut Street Philadelphia, Pennsylvania Attn: Documents Library
I270	General Precision Lab., Inc. 63 Bedford Road Pleasantville, New York Attn: Librarian
I415	Electronics Communication 1830 York Road Timonium, Maryland
I204	Emerson + Cuming, Inc. 59 Walpole Street Canton, Massachusetts Attn: Mr. W. Cuming
I147	Emerson Radio-Phonograph Corp. Emerson Research Laboratories 1140 Eastwest Highway Silver Spring, Maryland Attn: Mrs. R. Corbin, Librarian
I266	ITT Federal Laboratories Technical Library 500 Washington Avenue Nutley 10, New Jersey
I269	General Electric Company Building 3 - Room 143-1 Electronics Park Syracuse, New York Attn: Yolanda Burke, Doc. Library
I893	General Electric Company 3740 D. Street Philadelphia 24, Pennsylvania Attn: Mr. H.G. Lew Missile + Space Venicle Dept.
I48	Goodyear Aircraft Corp. 1210 Massillon Road Akron 15, Ohio Attn: Library, Plant G

Code	Organization
I448	Granger Associates Electronic Systems 974 Commercial Street Palo Alto, California Attn: John V.N. Granger,Pres.
I273	Hallicrafters Company 4401 West 5th Ave. Chicago 24, Illinois Attn: LaVerne LaGioia, Lib.
I274	Hoffman Electronics Corp. 3761 South Hill Street Los Angeles 7, California Attn: Engineering Library
I56	Hughes Aircraft Company Florence Ave and Teale Sts. Culver City, California Attn: Louis L. Bailin Manager, Antenna Dept.
I302	International Bus. Machines Corp. Space Guidance Center - Federal Systems Division Owego, Tioga County, N.Y. Attn: Tech. Reports Center
I265	ITT Federal Laboratories 3700 East Pontiac Street Fort Wayne 1, Indiana Attn: Technical Library
I241	Dr. Henry Jasik, Consulting Engineer 298 Shames Drive Brush Hollow Indus. Park Westbury, New York

Code	Organization
I272	Grumman Aircraft Engr. Corp. Bethpage, Long Island, N.Y. Attn: Engineering Librarian Plant No. 5
I737	The Hallicrafters Company 5th and Kostner Avenues Chicago 24, Illinois Attn: Henri Hodara, Head of Space Communication
I207	Hughes Aircraft Company Antenna Department Building 12, Mail Station 2714 Culver City, California Attn: Dr. W. H. Kummer
I981	Hughes Aircraft Company Attn: Mr. L. Stark, Microwave Dept. Radar Lab., P.O. Box 2097 Building 600, Mail Station C-152 Fullerton, California
I414	International Resistance Company 401 N. Broad Street Philadelphia 8, Pennsylvania Attn: Research Library
I230	Atlantic Research Corporation Shirley Highway at Edsall Road Alexandria, Virginia Attn: Delmer C. Ports
I279	Lockheed Aircraft Corporation 2555 N. Hollywood Way California Div. Engr. Library Dept. 72-25, Plant A-1, Bldg. 63-1 Burbank, California Attn: N.C. Harnois

Code	Organization
I468	Lockheed Aircraft Corp. Missiles and Space Div. Technical Information Ctr. 3251 Hanover Street Palo Alto, California (2 copies)
I280	The Martin Company Baltimore 3, Maryland Attn: Engineering Library Antenna Design Group
I66	The W. L. Maxson Corp. 475 10th Avenue New York, New York Attn: Miss Dorothy Clark
I283	McMillan Laboratory, Inc. Brownville Avenue Ipswich, Massachusetts Attn: Security Officer, Document Room
I471	Microwave Associates, Inc. South Avenue Burlington, Massachusetts
I648	The Mitre Corporation 244 Wood Street Lexington 73, Massachusetts Attn: Mrs. Jean E. Claflin, Librarian
I934	Motorola, Inc. Phoenix Research Lab. 3102 N. 56th Street Phoenix, Arizona Attn: Dr. A. L. Aden
I136	Martin-Marietta Corp. 12250 S. State Highway 65, Jefferson County, Colorado Attn: Mr. Jack McCormick
I63	Mathematical Reviews 190 Hope Street Providence 6, Rhode Island
I282	McDonnell Aircraft Corp., Dept. 644 Box 516, St. Louis 66, Missouri Attn: C.E. Zoller Engineering Library
I116	Melpar, Inc. 3000 Arlington Boulevard Falls Church, Virginia Attn: Engineering Technical Library
I390	Microwave Develop. Lab., Inc. 92 Broad Street Wellesley 57, Massachusetts Attn: N. Tucker, General Manager
I85	Motorola, Inc. 8201 East McDowell Road Phoenix, Arizona Attn: Dr. Thomas E. Tice
I641	National Research Council Radio + Electrical Engr. Div. Ottawa, Ontario, Canada Attn: Dr. G.A. Miller, Head Microwave Section

Code	Organization
I284	North American Aviation, Inc. 12214 Lakewood Boulevard Downey, California Attn: Tech. Infor. Ctr. (495-12) Space + Infor. Systems Div.
I286	Page Communications Engr., Inc. 2001 Wisconsin Avenue, N.W. Washington 7, D. C. Attn: (Mrs.)Ruth Temple, Librarian
I287	Philco Corporation Research Division Union Meeting Pond Blue Bell, Pa. Attn: Research Librarian
I288	Polytechnic Research + Develop. Co., Inc. 202 Tillary Street Brooklyn 1, New York Attn: Technical Library
I914	Radiation Systems, Inc. 440 Swann Avenue Alexandria, Virginia Attn: Library
I291	Radio Corporation of America Defense Elec. Products Building 10, Floor 7 Camden 2, New Jersey Attn: Mr. Harold J. Schrader Staff Engineer, Organ. of Chief Tech. Administrator
I285	North American Aviation, Inc. Los Angeles International Airport Los Angeles 45, California Attn: Engineering Tec. File
I82	Northrop Corporation Norair Division 1001 East Broadway Hawthorne, California Attn: Technical Information 3924-31
I225	Pickard + Burns, Inc. 103 Fourth Avenue Waltham 54, Massachusetts Attn: Dr. Richard H. Woodward
I289	Radiation, Inc. Melbourne, Florida Attn: RF Systems Division Technical Information Center
I290	RCA Laboratories David Sarnoff Research Center Princeton, New Jersey Attn: Miss Fern Cloak, Librarian
I473	Radio Corporation of America Missile Control + Elec. Division Bedford Street, Burlington, Mass. Attn: Librarian

Code	Organization
I757	Radio Corporation of America Surface Comm. Systems Lab. 75 Varick Street New York 13, N.Y. Attn: Mr. S. Krevsky
I930	Radio Corp. of America Defense Elec. Products Adv. Military Systems Princeton, New Jersey Attn: Mr. David Shore
I547	The Rand Corporation 1700 Main Street Santa Monica, Calif. Attn: Tech. Library
I293	Raytheon Company Boston Post Road Wayland, Mass. Attn: Mr. Robert Borts
I472	Raytheon Company Missile Systems Div. Hartwell Road, Bedford, Mass. Attn: Donald H. Archer
I295	Republic Aviation Corp. Farmingdale, L.I., N.Y. Attn: Engr. Library Thru: AF Plant Repr. Republic Aviation Corp. Farmingdale, L.I., N.Y.
I391	Sage Laboratories, Inc. 3 Huron Drive Natick, Massachusetts
I789	Radio Corporation of America West Coast Missile + Surface Radar Division Engineering Library, Bldg. 306/2 Attn: L.R. Hund, Librarian 8500 Balboa Blvd, Van Nuys, California
I292	Director, USAF Project RAND Via: AF Liaison Office The Rand Corporation 1700 Main Street Santa Monica, California
I373	Rantec Corporation 23999 Ventura Boulevard Calabasas, California Attn: Grace Keener, Office Manager
I294	Raytheon Company Wayland Laboratory Wayland, Massachusetts Attn: Miss Alice G. Anderson, Lib.
I510	Remington Rand UNIVAC Div. of Sperry Rand Corp. P.O. Box 500 Blue Bell, Pennsylvania Attn: Engineering Library
I184	Ryan Aeronautical Company 2701 Harbor Drive Lindbergh Field San Diego 12, California Attn: Library
I142	Sanders Associates, Inc. 95 Canal Street Nashua, New Hampshire Attn: Mr. Norman R. Wild

Code	Organization
I96	Sandia Corporation P.O. Box 5800 Albuquerque, New Mexico Attn: Records Management and Services Department
I312	STL Technical Library Document Acquisitions Space Tech. Lab., Inc. P.O. Box 95001 Los Angeles 45, Calif.
I367	Stanford Research Institute Documents Center Menlo Park, California Attn: Acquisitions
I260	Sylvania Elec. Prod. Inc. Electronic Defense Lab. P.O. Box 205 Mountain View, Calif. Attn: Library
I240	TRG, Inc. 400 Border Street, East Boston, Mass. Attn: Dr. Alan F. Kay
I139	Westinghouse Electric Corp. Electronics Division Friendship Int'l Airport Box 1897 Baltimore 3, Maryland Attn: Engineering Library
I338	A. S. Thomas, Inc. 355 Providence Highway Westwood, Mass. Attn: A. S. Thomas, Pres.
I682	Scanwell Laboratories, Inc. 6601 Scanwell Lane Springfield, Va.
I297	Sperry Gyroscope Company Great Neck, Long Island, New York Attn: Florence W. Turnbull Engineering Librarian
I104	Sylvania Electric Products, Inc. 100 First Avenue, Waltham 54, Mass. Attn: Charles A. Thornhill, Rpt. Lib. Waltham Lab. Library
I818	Sylvania Reconnaissance Systems Lab. Box 188, Mountain View, California Attn: Marvin D. Waldman
I708	Texas Instruments, Inc. 6000 Lemmon Avenue Dallas 9, Texas Attn: John B. Travis Systems Planning Branch
U1	Library Geophysical Institute of the University of Alaska College, Alaska
U61	Brown University Department of Elec. Engineering Providence, Rhode Island Attn: Dr. C.M. Angulo

Code	Organization
U157	California Institute of Tech. Jet Propulsion Laboratory 4800 Oak Grove Drive Pasadena, California Attn: Mr. I.E. Newlan
U3	Space Sciences Laboratory Leuschner Observatory University of California Berkeley 4, California Attn: Dr. Samuel Silver, Professor of Engr. Science and Dir., Space Sciences Lab.
U289	University of Southern Calif. University Park Los Angeles, California Attn: Dr. Raymond L. Chuan Director, Engineering Center
U183	Columbia University Department of Electrical Engr. Morningside Heights, N. Y., N. Y. Attn: Dr. Schlesinger
U10	Cornell University School of Electrical Engr. Ithaca, New York Attn: Prof. G.C. Dalman
U59	Library Georgia Technology Res. Inst. Engr. Experiment Station 722 Cherry Street, N.W. Atlanta, Georgia Attn: Mrs. J.H. Crosland, Lib.
U54	Harvard College Observatory 60 Garden Street Cambridge 39, Mass. Attn: Dr. Fred L. Whipple
U99	California Institute of Tech. 1201 E. California Drive Pasadena, California Attn: Dr. C. Papas
U100	University of California Electronics Research Lab. 332 Cory Hall, Berkeley 4, Calif. Attn: J.R. Whinnery
U239	Case Institute of Technology Electrical Engineering Dept. 10900 Euclid Avenue Cleveland, Ohio Attn: Professor Robert Plonsey
U238	University of Southern Calif., Engineering Center University Park Los Angeles 7, California Attn: Z.A. Kaprielian Assoc. Professor of Elec. Engr.
U86	University of Florida Department of Electrical Engr. Gainesville, Florida Attn: Prof. M.H. Latour, Library
U102	Harvard University Technical Reports Collection Gordon McKay Library 303 Pierce Hall Oxford Street, Cambridge 38, Mass. Attn: Librarian
U103	University of Illinois Documents Division Library Urbana, Illinois

Code	Organization
U104	University of Illinois College of Engineering Urbana, Illinois Attn: Dr. P.E. Mayes, Dept. of Electrical Engr.
U105	The John Hopkins University Applied Physics Laboratory 8621 Georgia Avenue Silver Spring, Maryland Attn: Mr. George L. Seielstad
U68	Lowell Technological Institute Research Foundation P.O. Box 709 Lowell, Massachusetts Attn: Dr. Charles R. Mingins
U26	Mass. Institutute of Technology Lincoln Laboratory P.O. Box 73 Lexington 73, Mass. Attn: Mary A. Granese, Lib.
U107	University of Michigan Electronic Defense Group Inst. of Science + Technology Ann Arbor, Michigan Attn: J.A. Boyd, Supervisor
U37	University of Michigan Engineering Res. Institute Willow Run Laboratories, Willow Run Airport Ypsilanti, Michigan Attn: Librarian
U194	Physical Science Laboratory New Mexico State University University Park, New Mexico Attn: Mr. H.W. Haas
U22	The John Hopkins University Homewood Campus Baltimore 18, Maryland Attn: Dr. Donald E. Kerr, Dept. of Physics
U228	University of Kansas Electrical Engineering Dept. Lawrence, Kansas Attn: Dr. H. Unz
U32	Mass. Institute of Technology Research Lab. of Electronics Building 26, Room 327 Cambridge 39, Massachusetts Attn: John H. Hewitt
U34	McGill University Dept. of Electrical Engineering Montreal, Canada Attn: Dr. T. Pavlasek
U79	University of Michigan Office of Research Administration Radiation Laboratory 912 N. Main Street Ann Arbor, Michigan Attn: Mr. Ralph E. Hiatt
U108	University of Minnesota Minneapolis 14, Minnesota Attn: Mr. Robert H. Stumm, Lib.
U39	New York University Institute of Mathematical Sciences Room 802, 25 Waverly Place New York 3, New York Attn: Morris Kline, Dr.

Code	Organization
U96	Northwestern University Microwave Laboratories Evanston, Illinois Attn: R.E. Beam
U109	The University of Oklahoma Research Institute Norman, Oklahoma Attn: Prof. C.L. Farrar, Chairman Electrical Engineering
U48	Polytechnic Institute of Brooklyn Microwave Research Institute 55 Johnson Street Brooklyn, New York Attn: Dr. Arthur A. Oliner
U361	The Pennsylvania State Univ. 223 Electrical Engineering University Park, Pa. Attn: A.H. Waynick, Director Inosphere Research Lab.
U176	Library W.W. Hansen Lab. of Physics Stanford University Stanford, California
U309	Technical University Oestervoldgade 10 G Copenhagen, Denmark Attn: Prof. Hans Lottrup Knudsen
U111	The University of Texas Electrical Engr. Research Lab. P.O. Box 8026, Univ. Station Austin 12, Texas Attn: Mr. John R. Gerhardt Assistant Director
U43	Antenna Laboratory Dept. of Electrical Engineering The Ohio State University 2024 Neil Avenue Columbus 10, Ohio Attn: Reports Librarian
U185	University of Pennsylvania Inst. of Cooperative Research 3400 Walnut Street Philadelphia, Pennsylvania Attn: Dept. of Elec. Engineering
U97	Polytechnic Institute of Brooklyn Microwave Research Institute 55 Johnson Street Brooklyn, New York Attn: Mr. A.E. Laemmel
U184	Purdue University Dept. of Electrical Engineering Lafayette, Indiana Attn: Dr. Schultz
U110	Syracuse University Research Inst. Collendale Campus Syracuse 10, New York Attn: Dr. C.S. Grove, Jr., Director of Engineering Research
U186	University of Tennessee Ferris Hall W. Cumberland Avenue Knoxville 16, Tennessee
U51	The University of Texas Defense Research Laboratory Austin, Texas Attn: Claude W. Horton, Physics Library

Code	Organization
U132	University of Toronto Dept. of Electrical Engr. Toronto, Canada Attn: Prof. G. Sinclair
U187	University of Wisconsin Dept. of Electrical Engr. Madison, Wisconsin Attn: Dr. Scheibe
U133	University of Washington Dept. of Electrical Engineering Seattle 5, Washington Attn: D.K. Reynolds
AF33	AFOSR, OAR (SRYP) Tempo D 4th and Independence Avenue Washington 25, D. C.

AD AFCRL 63-102

A. S. Thomas, Inc., 355 Providence Highway, Westwood, Mass.
NEW TECHNIQUES OF PATTERN SHAPING FOR LOW SILHOUETTE ANTENNAS by A. S. Thomas. Final Report December 1962

The infinite modulated reactance sheet is studied with the phase and amplitude contours of the near field presented. It is shown that the infinite reactance sheet is an excellent description of the modulated Yagi. Experimental radiation patterns of low sidelobe endfire arrays are given together with radiation patterns of Yagi arrays giving cosecant type radiations, flat top flared beams, and beams at an arbitrary angle. The beams at an arbitrary angle are obtained from a cosine to the even power modulation of the relative wave number.

UNCLASSIFIED

1. Antenna
2. Surface Wave Structures
3. Phase Modulation
4. Yagi
I. Thomas, A. S.
II. Electronic Systems Division
Air Force Systems Command
Office of Aerospace Research
Laurence G. Hanscom Field
Bedford, Massachusetts
III. Contract AF19(604)-4983

Armed Services Technical Information Agency

UNCLASSIFIED

AD AFCRL 63-102

A. S. Thomas, Inc., 355 Providence Highway, Westwood, Mass.
NEW TECHNIQUES OF PATTERN SHAPING FOR LOW SILHOUETTE ANTENNAS by A. S. Thomas. Final Report December 1962

The infinite modulated reactance sheet is studied with the phase and amplitude contours of the near field presented. It is shown that the infinite reactance sheet is an excellent description of the modulated Yagi. Experimental radiation patterns of low sidelobe endfire arrays are given together with radiation patterns of Yagi arrays giving cosecant type radiations, flat top flared beams, and beams at an arbitrary angle. The beams at an arbitrary angle are obtained from a cosine to the even power modulation of the relative wave number.

UNCLASSIFIED

1. Antenna
2. Surface Wave Structures
3. Phase Modulation
4. Yagi
I. Thomas, A. S.
II. Electronic Systems Division
Air Force Systems Command
Office of Aerospace Research
Laurence G. Hanscom Field
Bedford, Massachusetts
III. Contract AF19(604)-4983

Armed Services Technical Information Agency

UNCLASSIFIED

AD AFCRL 63-102

A. S. Thomas, Inc., 355 Providence Highway, Westwood, Mass.
NEW TECHNIQUES OF PATTERN SHAPING FOR LOW SILHOUETTE ANTENNAS by A. S. Thomas. Final Report December 1962

The infinite modulated reactance sheet is studied with the phase and amplitude contours of the near field presented. It is shown that the infinite reactance sheet is an excellent description of the modulated Yagi. Experimental radiation patterns of low sidelobe endfire arrays are given together with radiation patterns of Yagi arrays giving cosecant type radiations, flat top flared beams, and beams at an arbitrary angle. The beams at an arbitrary angle are obtained from a cosine to the even power modulation of the relative wave number.

UNCLASSIFIED

1. Antenna
2. Surface Wave Structures
3. Phase Modulation
4. Yagi
I. Thomas, A. S.
II. Electronic Systems Division
Air Force Systems Command
Office of Aerospace Research
Laurence G. Hanscom Field
Bedford, Massachusetts
III. Contract AF19(604)-4983

Armed Services Technical Information Agency

UNCLASSIFIED

AD AFCRL 63-102

A. S. Thomas, Inc., 355 Providence Highway, Westwood, Mass.
NEW TECHNIQUES OF PATTERN SHAPING FOR LOW SILHOUETTE ANTENNAS by A. S. Thomas. Final Report December 1962

The infinite modulated reactance sheet is studied with the phase and amplitude contours of the near field presented. It is shown that the infinite reactance sheet is an excellent description of the modulated Yagi. Experimental radiation patterns of low sidelobe endfire arrays are given together with radiation patterns of Yagi arrays giving cosecant type radiations, flat top flared beams, and beams at an arbitrary angle. The beams at an arbitrary angle are obtained from a cosine to the even power modulation of the relative wave number.

UNCLASSIFIED

1. Antenna
2. Surface Wave Structures
3. Phase Modulation
4. Yagi
I. Thomas, A. S.
II. Electronic Systems Division
Air Force Systems Command
Office of Aerospace Research
Laurence G. Hanscom Field
Bedford, Massachusetts
III. Contract AF19(604)-4983

Armed Services Technical Information Agency

UNCLASSIFIED